TECHNICAL TRANSACTIONS

CZASOPISMO TECHNICZNE

MECHANICS

MECHANIKA

ISSUE 3-M (10)

ZESZYT 3-M (10)

YEAR 2016 (113)

ROK 2016 (113)

WYDAWNICTWO POLITECHNIKI KRAKOWSKIEJ

TECHNICAL TRANSACTIONS | CZASOPISMO TECHNICZNE

MECHANICS | MECHANIKA

ISSUE 3-M (10) | ZESZYT 3-M (10)
YEAR 2016 (113) | ROK 2016 (113)

Basic version of each Technical Transactions magazine is its online version
Pierwotną wersją każdego zeszytu Czasopisma Technicznego jest jego wersja online
www.ejournals.eu/Czasopismo-Techniczne www.technicaltransactions.com www.czasopismotechniczne.pl

TECHNICAL TRANSACTIONS | **CZASOPISMO TECHNICZNE**
MECHANICS | MECHANIKA
3-M/2016

BOGDAN ANTOSZEWSKI*, MONIKA KRZYWICKA**, SZYMON TOFIL*

LASER SURFACE TEXTURING OF TITANIUM ALLOYS FOR BIOMEDICAL APPLICATIONS

LASEROWE TEKSTUROWANIE ELEMENTÓW ZE STOPÓW TYTANU DO ZASTOSOWAŃ BIOMEDYCZNYCH

A b s t r a c t

The article presents the methodology and results of laser surface texturing of the Ti6Al7Nb alloy. Laser treatment was carried out by means of a laser TruMicro 5325c Trumpf with a wavelength of 343 nm and a pulse duration of 6.2 ps. The impact of pulse frequency, scanning speed of a laser beam and laser power on the shape and dimensions of texture was studied. By selecting a suitable shape, size and density of laser texture for the surface of titanium alloys applied in knee replacement it is possible to reduce the coefficient of friction and wear of polyethylene to increase the osseointegration and adhesion of the coatings.

Keywords: laser micromachining, *texturing*, *titanium alloys*

S t r e s z c z e n i e

W artykule przedstawiono metodykę oraz wyniki badań laserowego teksturowania powierzchni elementów ze stopu Ti6Al7Nb. Obróbkę laserową wykonano z zastosowaniem lasera TruMicro 5325c Trumpf o długości fali 343 nm i czasie trwania impulsu 6,2 ps. Badano wpływ częstotliwości, prędkości skanowania oraz mocy wiązki laserowej na kształt i wymiary elementu tekstury. Poprzez wybór odpowiedniego kształtu, wymiarów oraz zagęszczenia elementów tekstury możliwe jest zmniejszenie współczynnika tarcia oraz zużycia panewki polietylenowej w protezie stawu kolanowego, w ten sposób można też poprawić osteointegrację i przyczepności powłok.

Słowa kluczowe: mikroobróbka laserowa, *teksturowanie*, *stopy tytanu*

DOI: 10.4467/2353737XCT.16.113.5724

* Prof. D.Sc. Ph.D. Eng. Bogdan Antoszewski, M.Sc. Eng. Szymon Tofil, Centre for Laser of Metals, Faculty of Mechatronics and Machine Design, Kielce University of Technology.

** M.Sc. Eng. Monika Krzywicka, Fundamentals of Technology Chair, Faculty of Production Engineering, University of Life Sciences in Lublin.

1. Introduction

The knee joint is one of the most loaded biobearing in the human body, which is prone to injuries. In order to treat rheumatoid arthritis, osteoarthritis, high distortion and post--traumatic conditions, total knee arthroplasty is performed. The use of implants reduces pain and improves the quality of life of patients suffering from the described health problems.

In the metal-polymer friction pair, mainly the polymer component is destroyed. Typical kinds of destruction of an element made of UHMWPE include: abrasive friction, plastic deformation and creep, pitting, change of chemical composition, color and structure, loosening and cracking [1–3].

Laser micromachining has a huge potential for functionalizing the surface of biomaterials. Application of a laser surface texturing enables the use of a wide range of materials for which different shapes and sizes of textures can be produced on the surface in a reproducible, rapid and economical way. In addition, it allows avoiding the formation of impurities, it is easier in control and more precise; there is a reduced heat-affected zone and only minor adverse concentric zones of deposition of evaporated material are formed around the elements of texture [4, 5].

Laser surface texturing greatly reduces friction and wear of titanium and its alloys. In the generated textures there are accumulated impurities, which have a positive effect on reducing the abrasive friction of prostheses. Qin et al. [6] compared round, square and triangular textures of different sizes. Round textures had the most stable and the most favourable tribological parameters, but for all of the samples the reduction of the coefficient of friction and wear was reported to be comparable with the non-textured ones. Tianchang et al. [7] compared textures in the form of holes with a diameter of 150 microns, a depth of 40 microns and a density of 13%, 23%, 44%. It was observed that the friction coefficient was lower and more stable for textures with the highest density. Density and the shape of texture are the most important factors affecting tribological properties [7, 8].

Laser micromachining has also a beneficial effect on cell adhesion, biological fluids spreading, osseointegration and the strength of the implant-bone joint. Mirhosseini et al. [8] observed a better adhesion of osteoblasts and their more even distribution on the laser surface texturing of titanium alloys. The cells on the texturing surface had a tendency to cluster [8]. Chem et al. [9] report that bioactivity is a function of surface chemistry and surface topography. The study shows that surfaces undergoing laser texturing have a better osseointegration, because the cells grow into the prosthesis [9]. Götz et al. [10] indicated that in order to improve osseointegration, the optimal diameter of textures for alloy Ti6Al4V is 200 microns. Bobyn et al. [11] studied prosthesis of different sizes and textures and they indicated the values of 100–400 microns as the optimal diameter. Other studies confirm that the minimum diameter of textures should be about 140–200 microns.

Wettability is an important factor determining biocompatibility. Cell adhesion is increased on hydrophilic surfaces [4, 12–14]. The oxidised surfaces of titanium alloys are considered to be hydrophilic [4]. The laser surface modification of titanium improves wettability. Dahotre al. [15] observed improvement in wettability for all the tested textures (in the form of columns and grooves). Hao et al. [16] compared the properties of the samples after texturing to the non-textured ones by means of a high power diode laser

(HPDL). They noted improvement in wettability, which indicates a better integration with biological fluids.

Obtaining fully functional biomaterials is possible by modifying their surface. Among methods of surface engineering, surface laser texturing has an enormous potential. Laser surface texturing has a beneficial effect on cell adhesion, osseointegration, distribution of biological fluids and improves tribological properties. Many authors present the results of experiments in which spherical textures provide improvement in tribological properties. As shown in the literature, there are divergent results of studies on the impact of the density and dimensions of textures on the improvement of wear resistance. The dimensions of the textures produced on the surface of titanium alloys should be the subject of further research.

The purpose of this study is to choose operating parameters of the laser to produce spherical textures of different depths in the titanium alloy.

2. Materials and methods

The study covered samples which were made of titanium alloy Ti6Al7Nb. The chemical composition of the alloy was in accordance with ISO 5832-11: Fe max. 0.25%, max. 0.2%, N max 0.05% C max. 0.08% H max. 0.009% Al 5.5-6.5% 6.5-7.5 Nb, Ta max. 0.5%, remainder Ti.

Laser surface texturing of Ti6Al7Nb alloy was carried out at the station equipped with a laser TRUMPF TruMicro 5325c with the following characteristics:

- laser type: diode-pumped disk laser pulse with harmonic generation 3,
- wavelength: 343 nm,
- average power: 5 W,
- pulse duration of 6.2 ps,
- pulse frequency of 400 kHz can be divided by a natural number from 1 to 10,000,
- the maximum pulse energy of 12.6 μJ,
- mod TEM_{00},
- $M^2 = 1.3$,
- fluence 4.8 J/cm^2.

At such short laser pulses of a few picoseconds, the “cold ablation” takes place. The shape and diameter of the textures were chosen based on literature review. In order to select the depth of textures, a plan of experience was prepared – a static determined poly--selective rotatable PS/DS-P: λ. On the samples surface, spherical texturing with a diameter of 250 microns was made. For this purpose, software provided with the above-described laser device was used, which allows, inter alia, drilling holes. This is a standard procedure in which we can ask specific dimension values expected for texture.

3. Results

Laser micromachining was carried out in argon. In selecting parameters for laser texturing two parameters were changed: the power and speed of the scanning beam. Figure 1 shows 4 rows of textures produced with the following laser parameters:

– row 1: power 50%, the laser beam scanning speed of 50 mm/s,
– row 2: power 50%, the laser beam scanning speed of 100 mm/s,
– row 3: power 100%, the laser beam scanning speed of 50 mm/s,
– row 4: power 100%, the laser beam scanning speed of 100 mm/s.

The analysis of microscopic research showed that the smallest heat-affected zone, with the most regular edges and the lowest deposition of the vaporized material are the hollows formed at a laser power of 100% and a laser beam scanning speed of 50 mm/s (row 3). In order to assess the quality of the texture, the profile of the hole was analysed (Fig. 1).

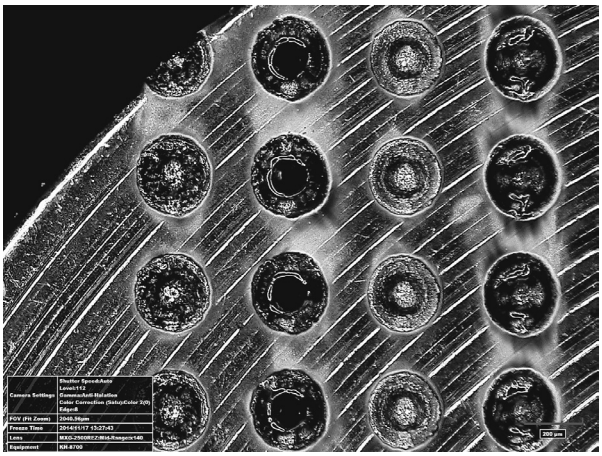

Fig. 1. General view of the textured surface (from left 1, 2, 3, 4 row)

After selecting the correct scanning speed of the laser beam and the power of laser, the impact of pulse frequency on the change of the depth of textures was analyzed. After scanning the surface by laser beam with a pulse frequency of 400 kHz, the texture with a depth of 40 microns was obtained. After double-scanning of the surface by a laser beam with a pulse frequency of 400 kHz, the texture with a depth of 79 microns was obtained (Fig. 2).

After scanning the surface by a laser beam with a pulse frequency of 400 kHz and then scanning the surface by alternate pulse, a texture with a depth of 63 microns was obtained. When choosing the pulse frequency of 133 kHz, the textures of 16 microns depth was obtained. When choosing the pulse frequency of 80 kHz, the textures of 10 microns depth was obtained.

Microscopic analysis showed that the use of argon allows reducing oxidation of the surface. In the literature, there is divergent data on the effects of cover gases on the surface oxidation of titanium alloys. Laser micromachining which was carried out without a cover

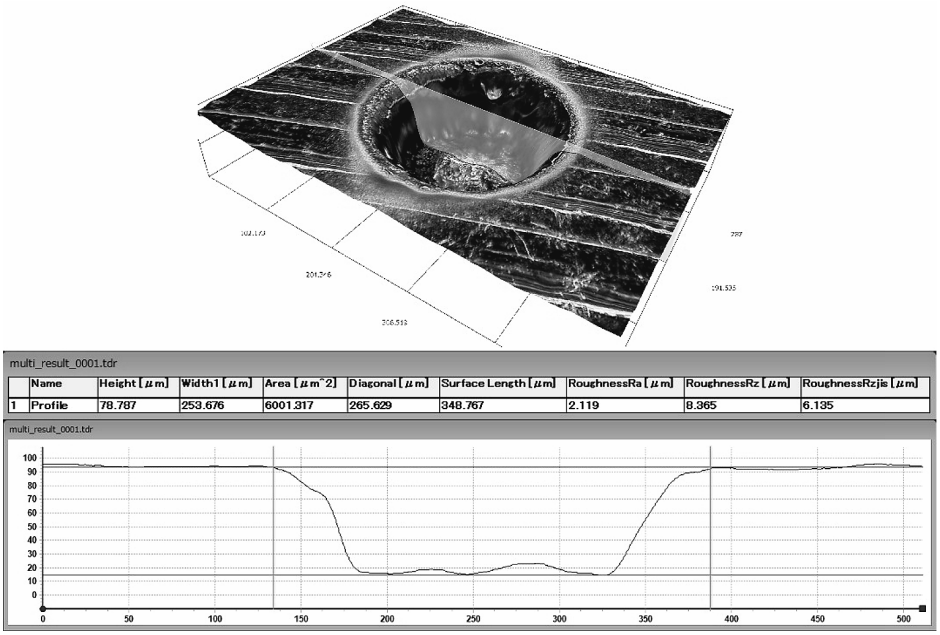

Fig. 2. The profile of a spherical texture with a diameter of 254 microns and a depth of 79 microns

gas leads to oxidation of the surface of Ti6Al4V alloy. The increase in the oxygen content improves wettability. Anselme [17] pointed out that surface texturing by laser reduces surface energy and makes the surface hydrophobic, and only the use of anodization causes hydrophilic properties.

4. Conclusions

The results show that with properly chosen laser parameters and by means of a suitable automatic control, it is possible to produce textures of selected shapes and repeating geometrical dimensions on the surface of the titanium alloy. The change of pulse frequency influenced in direct proportion the change in the depth of textures. The use of argon leads to reduction of surface oxidation. The best texture quality was obtained at the maximum power of the laser and at the scan speed of laser beam of 50 mm/s.

The aim of further research will be to determine the influence of textures density on the properties of titanium alloys used in knee replacement.

References

[1] Widuchowski J., *Kolano. Endoprotezoplastyka – całkowita wymiana stawu*, Sport&Med, Katowice 2001 [in Polish].

[2] Gierzyńska-Dolna M., Nabrdalik M., *Procesy zużycia endoprotez stawu kolanowego*, Inżynieria Materiałowa, **5**, 2005, 661-663 [in Polish].

[3] Cunha A., Serro A.P., Oliveira V., Almeida A., Vilar R., Durrieu M.Ch., *Wetting behaviour of femtosecond laser textured Ti-6Al-4V surfaces*, Applied Surface Science, **265**, 2013, 688-696.

[4] Antoszewski B., Radek N., *Ocena wpływu zwilżalności na właściwości tribologiczne powierzchni z teksturą*, Tribologia, **3**, 2012, 13-20.

[5] Bereznai M., Pelsoczi I., Toth Z., Turzo K., Radnai M., Bor Z., Fazekas A., *Surface modifications induced by ns and sub-ps excimer laser pulses on titanium implant material*, Biomaterials, **24**, 2003, 4197-4203.

[6] Qin L., Lin P., Zhang Y., Dong G., Zeng Q., *Influence of surface wettability on the tribological properties of laser textured Co–Cr–Mo alloy in aqueous bovine serum albumin solution*, Applied Surface Science, **268**, 2013, 79-86.

[7] Tianchang H., Litian H., Qi D., *Effective solution for the tribological problems of Ti6Al-4V: Combination of laser surface texturing and solid lubricant film*, Surface&Coatings Technology, **206**, 2012, 5060-5066.

[8] Mirhosseini N., Crouse P.L., Schmidth M.J.J., Lia L., Garrod D., *Laser surface micro-texturing of Ti-6Al-4V substrates for improved cell integration*, Applied Surface Science, **19**, 2007, 7738--7743.

[9] Chen J., Bly R.A., Saad M.M., AlKhodary M.M., El-Backly R.M., Cohen D.J., Kattamis N., Fatta M.M., Moore W.A., Arnold C.B., Marei M.K., Soboyejo W.O., *In-vivo study of adhesion and bone growth around implanted laser groove/RGD-functionalized Ti-6Al-4V pins in rabbit femurs*, Materials Science and Engineering, **31**, 2011, 826-832.

[10] Götz H.E., Müller M., Emmel A., Holzwarth U., Erben R.G., Stangl R., *Effect of surface finish on the osseointegration of laser-treated titanium alloy implants*, Biomaterials, **25**, 2004, 4057-4064.

[11] Bobyn J.D., Pilliar R.M., Cameron H.U., Weatherly G.C., *The optimum pore size for the fixation of porous-surfaced metal implants by the ingrowth of bone*, Clinical Orthopaedics and Related Research, **150**, 1980, 263-70.

[12] Radek N., Antoszewski B., *The influence of laser treatment on the properties of electro-spark deposited coatings*, Kovove Materialy-Metallic Materials, **47**(1), 2009, 31-38.

[13] Li J., Liao H., Fartash B., Hermansson L., Johnsson T., *Surfacedimpled commercially pure titanium implant and bone ingrowth*, Biomaterials, **18**, 1997, 691-696.

[14] Ahuir-Torres J.I., Hernández-López J.M., Arenas M.A., Conde A., de Damborenea J., *Synthesis of TiO2 nanopore arrays by pulsed laser treatment and anodic oxidation*, Surface and Coatings Technology, **25**, 2014, 408-414.

[15] Dahotre N.B., Paital S.R., Samant A.N., Daniel C., *Wetting behaviour of laser synthetic surface microtextures on Ti-6Al-4V for bioapplication*, Philosophical Transactions of the Royal Society, A **368**, 2010, 1863-1889.

[16] Hao L., Lawrence J., Li L., *Manipulation of the osteoblast response to a Ti-6Al-4V titanium alloy using a high power diode laser*, Applied Surface Science, **247** (1-4), 2005, 602-606.

[17] Anselme K., *Osteoblast adhesion on biomaterials*, Biomaterials, **7**, 2000, 667-681.

TECHNICAL TRANSACTIONS | **CZASOPISMO TECHNICZNE**
MECHANICS | MECHANIKA
3-M/2016

ROBERT ULEWICZ*

INFLUENCE OF SELECTED TECHNOLOGICAL FACTORS ON FATIGUE STRENGTH

WPŁYW WYBRANYCH CZYNNIKÓW TECHNOLOGICZNYCH NA WŁASNOŚCI ZMĘCZENIOWE

A b s t r a c t

The determination of the material fatigue limit is important with regard to the determination of safe service life of structural materials. Depending on the type of treatment and the type and size of introduced stresses, technological procedures can affect negatively or positively the fatigue properties of steel. Based on literature research and our own research, the article presents the influence of selected technological factors on fatigue properties. Our own studies were performed with the use of load high frequencies of 20 kHz in the ultra-high-cyclic area.

Keywords: fatigue, *S–N curve*, *coatings*, *shot peening*

S t r e s z c z e n i e

Wyznaczenie granicy zmęczenia materiału jest istotne ze względu na określenie bezpiecznego resursu. W zależności od rodzaju zabezpieczeń antykorozyjnych i typu obróbki oraz wielkości wprowadzonych naprężeń zabiegi technologiczne mogą wpływać negatywnie lub pozytywnie na własności zmęczeniowe stali. W artykule przedstawiono na podstawie badań literatury oraz własnych, wpływ wybranych czynników technologicznych na własności zmęczeniowe. Badania własne przeprowadzono z zastosowaniem wysokich częstotliwości obciążenia 20 kHz w obszarze ultra wysokocyklowym.

Słowa kluczowe: zmęczemie, *S–N krzywa*, *powłoka*, *kuleczkowanie*

DOI: 10.4467/2353737XCT.16.114.5725

* Assoc. Prof. D.Sc. Ph.D. Eng. Robert Ulewicz, Institute of Production Engineering, Faculty of Management, Czestochowa University of Technology.

1. Introduction

Contemporary trends to reduce the consumption of materials in the construction of machines and devices require the use of high-strength, and therefore materials which are generally more fragile and susceptible to fatigue. The analysis of the causes of machines and equipment elements failures shows that about 90% of all reported cases of cracking is caused by the process of fatigue. Using anticorrosion coverings, and, in particular, coverings of galvanic-technical coatings, does not have a beneficial effect on the fatigue properties of structural steel. In the case of fatigue cracking, the cracking is caused by periodically--variable stresses of a much smaller value than their tensile strength specified in the static tensile test, but also with a sufficiently high number of cycles of load changes in the range of 10^5–10^8.

The analysis of fatigue cracking confirms that the nucleation and propagation of fatigue cracks are controlled by local processes in micro areas of the material [1, 2].

2. Influence of selected factors on fatigue characteristics of materials

The fatigue process is influenced by many factors which can significantly delay or accelerate the process of fatigue. These factors can be divided into internal and external. Internal factors include material structure, chemical composition, grain size, sample size as well as shape and distribution of non-metallic inclusions, while external factors include frequency, asymmetry of the cycle, the size of mean stress and the stress state. In practice, one cannot be limited to a single factor (Table 1), in the operational and research assumptions one should respect a current impact of several factors [13].

Table 1

Effect of selected factors on fatigue curve characteristic

Role of the factor	K_{th} [MPa·m$^{1/2}$]	$V_p = da/dN$ [m/cycle]	σ_c [MPa]
Asymmetry of the cycle	↓	↑	↓
Frequency	↑	↑↓	↑
Temperature	↓	↑↓	↑↓
Aggressive environment	↓	↑	↓
Grain size	↑↓	↑	↓
R_e	↓	↓	↑
R_m	↓	↓	↑

↑ – high impact, ↓ – small impact, ↑↓ – no information

In order to increase the low yield strength on fatigue, in practice, many methods of technological treatments are applied, which is particularly useful for parts which have a sharp undercut construction. Since fatigue cracks are generally formed on the element surface or just under the surface, mechanical properties of surface layers should primarily

be improved [5, 6]. This condition can be achieved by surface treatment of the element, inter alia: mechanical treatment: shot peening or surface rolling, thermal treatment: surface hardening, thermal-chemical treatment: carburizing, nitriding.

As a result of a mechanical or thermo-chemical treatment, the strength of the surface layer of metal increases, as well as, even though usually prohibitively, the fatigue strength limit. At the same time their own stresses are formed, which are compensated by stress resulting from the tensile force of the core [3, 4, 8]. However, the decision about which of the two operations is more important will depend on the type of used treatment and occurring stress.

Despite the fact that in recent decades this problem has been considered utterly important and investigated very intensively (a lot of experimental research results have been published), it failed to draw up comprehensive and theoretically justified guidelines that are likely to allow for determining the effects of a chosen method of treatment in a given specific case. However, given a large number of factors that affect the final results (type of treatment, type of material, shape of the body element, dimensions, type of stress, loading, etc.) results obtained on samples during research cannot be used for actual elements, which are normally of larger dimensions; they can be used only as documents that form the basis for drawing up qualitative, and possibly partly quantitative opinions, in order to give opinions on the impact of type of treatment of a surface layer on the fatigue strength limit.

A positive effect in the form of the introduction into the surface of a layer of high compressive stress is obtained in the process of shot peening.

Stresses forces in the curved surface have a positive impact not only on slowing down of the process of initiation of the first fatigue cracks, but also on the expansion of the already formed ones and lead to a significant inhibition of the growth of the existing cracks [9]. The degree of stresses in shot peening process is visibly associated with the type of surface coverage, where this factor is readable as well at this stage of fatigue damages.

The increase of the limit of fatigue strength is typically less than 20%, and in some cases, this limit was lower than the limit of fatigue strength of the polished samples. In this case, on the one hand, there is a positive effect on the increase of durability of the surface layer, on the other hand, the negative action arises as a result of irregularities in the surface of the

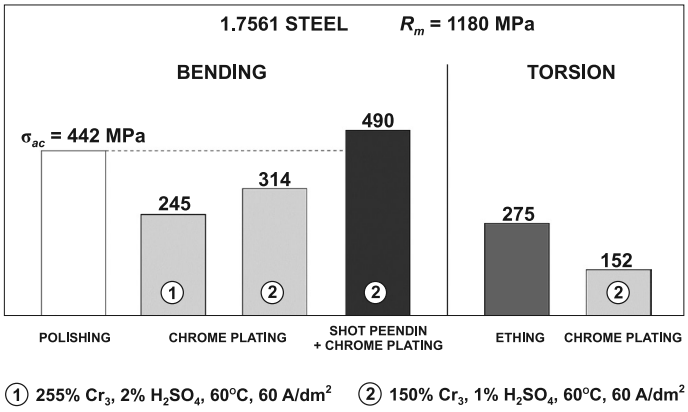

Fig. 1. Scheme of the residual stresses in the surface layer of the material after shot peening [9]

element. Shot peening is desirable for elements with a rough surface, and it particularly finds application in forgings and elements which are not further subjected to subsequent treatments after heat treatment.

The application of a product galvanized coating on the surface in order to prevent corrosion or to increase abrasion resistance, usually produces considerable tensile stresses in the coated-parental material, thereby reducing resistance to fatigue. During the chrome plating, but also during other galvanic treatments, the negative effect of treatment increases with the increase of material strength (R_m). We observe the increase in adverse effects with the increase in thickness of the applied layer (coating). The described adverse effect can be corrected to some extent by precipitation conditions (temperature of the electrolyte). Other possibilities for the removal of adverse actions of galvanic treatment are provided by the method of shot peening of a part of the elements prior to processing, Fig. 1 [9, 10, 14, 15].

3. Experimental material and procedure

The 1.0117 steel was used for this research. The first series of samples was coated with chromium coating. There, the CHEMOCHROM 3 S bath was used. The second series of samples was coated with nickel coating in the SUPRAGAL bath. The third series of samples was subjected to the shot peening process (shot peening parameters: shot diameter 0.45 mm, angle of the attack 75°, speed v_T = 78.1 m·s^{-1}, amount of shot q_n = 45 kg·m^{-2}). The fourth series of samples was the parental material. Fatigue tests were carried out on a high-frequency fatigue machine KAUP-ZU in the ultra-high-cyclic area at the load frequency of 20 kHz. The samples for fatigue tests were made in accordance with the assumptions described by Salam and Lamerand.

4. Results and discussion

Fatigue research in the area of very high load cycles ($N \approx 6 \cdot 10^6 - N \approx 1 \cdot 10^{10}$ cycles) was made at high-frequency loads of stretching-compressing type with sinusoidal course (f = 20 kHz, R = –1, T = 20 ± 10°C with cooling the samples in distilled water with anticorrosive inhibitor). The research results are shown in Fig. 2.

For the parent material, the applied stress of amplitude σ_a decreased from σ_a = 270 MPa (for $N_f = 5.7 \cdot 10^7$ cycles) to σ_a = 160 MPa (for $N_f = 1.3 \cdot 10^{10}$ cycles), which gives the amplitude difference of $\Delta\sigma_a$ = 110 MPa. In general, we can say that the amplitude of pressure continues to decline with the growing number of cycles to the growing damage beyond conventional border of cycles ($N_C = 1 \cdot 10^6 - N_C = 1 \cdot 10^7$ of cycles – typically used range of cycles to demarcate the fatigue limit σ_C) [11, 12]. This fact is vital because of the reliability and safety of machinery and equipment [7]. For the steel with a nickel coating, the applied stress of amplitude σ_a decreased from σ_a = 260 MPa (for $N_f = 0.2 \cdot 10^7$ cycles) to σ_a = 170 MPa (for $N_f = 0.9 \cdot 10^{10}$ cycles), which gives the amplitude difference of $\Delta\sigma_a$ = 90 MPa. In the case of the chromium coating, the applied stress of amplitude σ_a decreased from σ_a = 260 MPa (for $N_f = 0.3 \cdot 10^7$ cycles) to σ_a = 170 MPa (for $N_f = 0.8 \cdot 10^{10}$

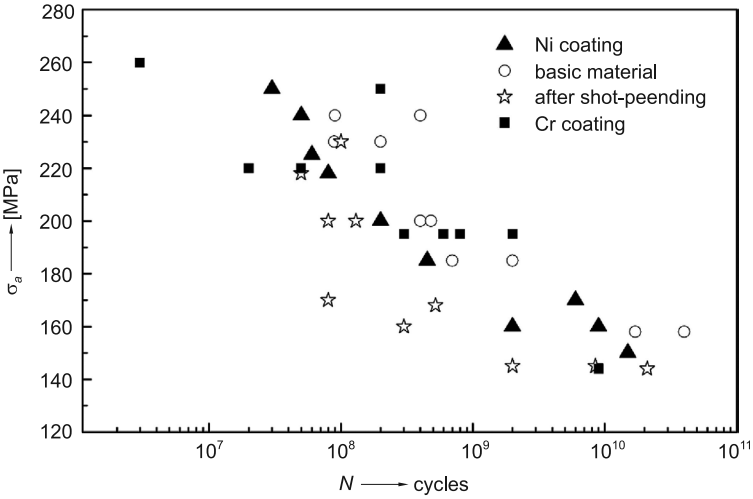

Fig. 2. The dependence of stress amplitude σ_a on number of cycles N (f = 20 kHz, $T = 20 \pm 10$°C, $R = -1$)

cycles), which gives the amplitude difference of $\Delta\sigma_a$ = 90 MPa. In the fatigue life test results for 1.0117 steel after the process of ball peening, the applied stress of amplitude σ_a decreased from σ_a = 225 MPa (for $N_f = 5.3 \cdot 10^7$ cycles) to σ_a = 145 MPa (for $N_f = 1.7 \cdot 10^{10}$ cycles), which gives the amplitude difference of $\Delta\sigma_a$ = 80 MPa.

5. Summary

The optimization of structural material selection plays an important role in the processes of exploitation, which tends to carry out research activities related to the material resistance on working conditions, especially in the field of variable loads. In order to achieve more durable parts of machines, it is necessary to develop research on the impact of technological and structural factors as well as surface conditions. Anticorrosive protections, technical coatings or decorative coatings can significantly affect the fatigue strength of machine parts. The fatigue tests f = 20 kHz, T = 20°C, R = –1, $N_c > 10^7$ at high-frequency loading cycle were carried out for all the series of samples. There were experimentally determined dependencies $\sigma_a = f(N_f)$ in the areas of high and giga-cyclic range from $N_f = 0.2 \cdot 10^7 - 3.3 \cdot 10^{10}$ cycles. The results of all samples of 1.0117 steel with coatings in the area over a conventional fatigue limit, with stress amplitude decrease σ_a increases the number of cycles to fatigue crack, for steels with coating Ni $\Delta\sigma_a$ = 170 MPa, for steel with coating Cr_3 $\Delta\sigma_a$ = 90 MPa. For samples after shot peening in the area over the conventional fatigue limit with a decrease in the amplitude of the stress σ_a increases the number of cycles to fatigue crack, $\Delta\sigma_a$ = 80 MPa.

The obtained fatigue results in the giga-cyclic range with the use of the high frequencies of load demonstrated that the coatings to a much lesser extent affect the reduction in the

fatigue properties with the use of load high-frequency, in comparison with the results obtained when the low frequencies of loading were used [11, 12]. However, considering the studies performed we can conclude that the shot peening treatment had the greatest impact of surface treatment on material fatigue. As a result of the performed tests, the new information was obtained on fatigue properties of steel with galvanic coatings in the area of very high load cycles and with surface treatment in the area of very high load cycles. It was also determined how the process of removing unnecessary, undesirable coatings by shot peening affects fatigue properties.

References

[1] Lipinski T., Wach A., *The effect of fine non-metallic inclusions on the fatigue strength of structural steel*, Archives of Metallurgy and Materials, 60, 2015, 65-69.

[2] Lipinski T., Wach A., *Influence of outside furnace treatment on purity medium carbon steel*, Proc. of 23rd International Conference on Metallurgy and Materials, Brno 2014, 738-743.

[3] Dudek A., Adamczyk L., *Properties of hydroxyapatite layers used for implant coatings*, Optica Applicata, 43, 2013, 143-151.

[4] Guidoni G., Dudek A., Patsias S., Anglada M., *Fracture behaviour of thermal barrier coatings after high temperature exposure in air*, Materials Science and Engineering A – Structural Materials Properties Microstructure and Processing, 397, 2005, 209-214.

[5] Radek N., Pietraszek J., Antoszewski B., *The Average Friction Coefficient of Laser Textured Surfaces of Silicon Carbide Identified by RSM Methodology*, Advanced Materials Research, 874, 2014, 29-34.

[6] Radek N, Bartkowiak K., *Laser treatment of electro-spark coatings deposited in the carbon steel substrate with using nanostructured WC-Cu electrodes*, Physics Procedia, 39, 2012, 295-301.

[7] Ulewicz R., Novy F., Selejdak J., *Fatigue Strength of Ductile Iron in Ultra-High Cycle Regime*, Advanced Materials Research, 874, 2014, 43-48.

[8] Major I., Major M., *Modeling of Wave Propagation in the ADINA Software for Simple Elastic Structures*, Advanced Materials Research, 1020, 2014, 171-176.

[9] Linhart V., *Vliv technologických úprav na únavove vlasnosti castr*, [in:] Letná škola únavy materiálov, Žilina, 1992, 55-68 [in Slovak].

[10] Mikova K., Bagherifard S., Bokuvka O., Guagliano M., Trsko L., *Fatigue behavior of X70 microalloyed steel after severe shot peening*, International Journal of Fatigue, **55**, 2013, 33-42.

[11] Mikova K., Bagherifard S., Bokuvka O., Guagliano M., Trsko L., *Fatigue behavior of X70 microalloyed steel after severe shot peening*, International Journal of Fatigue, 55, 2013, 33-42.

[12] Hracek S., Trsko L., Bokuvka O., *Comparison of structural design in high and ultra-high cycle fatigue regions*, Transactions of Famena, 38, 2014, 1-12.

[13] Ulewicz R., Mazur M., *Fatigue testing structural steel as a factor of safety of technical facilities maintenance*, Production Engineering Archives, 1 (1), 2013, 32-34.

[14] Shiozawa K., Morii Y., Nishino S., Lu L., *Subsurface Crack Initiation and Propagation Mechanism in High-Strength Steel in a Very High Cycle Fatigue Regime*, International Journal of Fatigue, 28, 2006, 1521-1532.

[15] Klimecka-Tatar D., Pawlowska G., Orlicki R., Zaikov G.E., *Corrosion Characteristics in Alkaline and Ringer Solution of Fe68-xCoxZr10Mo5W2B15 Metalic Glasses*, Journal of the Balkan Tribological Association, 20, 2014, 124-130.

TECHNICAL TRANSACTIONS | **CZASOPISMO TECHNICZNE**
MECHANICS | MECHANIKA
3-M/2016

AGNIESZKA SZCZOTOK*

GUIDANCE AND ADVICE TO IMAGE ANALYSIS APPLIED IN MATERIALS SCIENCE

PRAKTYCZNE WSKAZÓWKI DO ANALIZY OBRAZU W BADANIACH MATERIAŁÓW INŻYNIERSKICH

A b s t r a c t

The paper summarizes selected examples from quantitative metallography of engineering materials and indicates potential errors which should be avoided. Problems in the areas of sample preparation (cutting, grinding, polishing and etching), microscopic observation, image collection, image processing, quantitative image analysis together with the interpretation of the results were shortly characterized.

Keywords: *metallography*, *sample preparation*, *image analysis*, *microstructure*

S t r e s z c z e n i e

W artykule przedstawiono zestawienie wybranych przykładów z praktyki metalografii ilościowej materiałów inżynierskich wraz ze wskazaniami potencjalnych błędów, jakie można popełnić i jakich warto unikać. Scharakteryzowano pokrótce problemy, na które warto zwrócić uwagę podczas preparatyki próbek, akwizycji obrazu makro- i mikrostruktury, procedury przetwarzania obrazu, ilościowej analizy obrazu i interpretacji wyników.

Słowa kluczowe: *metalografia*, *preparatyka*, *analiza obrazu*, *mikrostruktura*

DOI: 10.4467/2353737XCT.16.115.5726

* Ph.D. Eng. Agnieszka Szczotok, Institute of Materials Science, Faculty of Materials Science and Metallurgy, Silesian University of Technology.

1. Introduction

It is well known that the properties of materials are directly dependent on their structure. That is why it is reasonable to create a quantitative characterization of a structure which possesses desirable parameters. Microstructure generally consists of two or more phases with fundamentally different properties. The description of a material structure at the micro- and macro scale consists of size, shape and elongation of grains in the case of one-phase materials. The characterization of multiphase materials involves, besides grains description, a kind of phases, their volume fraction, distribution and position of each one in relation to others. In the case of both one- and multiphase materials, the depiction of their microstructure can also involve possible defects present in the materials, like nonmetallic inclusions, pores, cracks, etc.

Scientists can usually use only a part of a section taken through the sample of a given microstructure and then evaluate the measurable properties of the material (volume fractions, object number, etc.). This process is repeated on many sections in order to determine average values or other characteristics.

A typical analysis of a material structure requires the following stages [1]: preparation of the surface of the material (cutting, grinding, polishing and etching), microscopic observation and image collection, image processing, quantitative image analysis and interpretation of results.

Optical microscopes, scanning electron microscopes, transmission electron microscopes, computed tomography (CT) and magnetic resonance (MR) imaging are just some of possible methods applied to research of macro- and microstructure of materials. They enable to obtain 2D (two-dimensional) and 3D (three-dimensional) digital images of material microstructure [2]. The new diagnostic imaging methods (CT, MR, etc.) seem to be a real challenge for image analysis specialists. Obviously, results of image analysis are strongly dependent on the knowledge and experience of people carrying out the analysis.

Quantitative characterization with image analysis techniques is an important ingredient in predicting microstructure-property relations for heterogeneous materials.

2. Sample preparation

Proper preparation of metallographic specimens to determine microstructure and content requires that a rigid step-by-step process be followed. The final stages of metallographic sample preparation should produce a polished surface which will reveal the true microstructure. Each stage of metallographic preparation (sectioning, rough grinding, mounting, fine grinding, rough polishing and final polishing) is vital to the final result. Incorrect preparation can lead to an erroneous interpretation with potentially serious consequences. Mechanical polishing will always leave a layer of disturbed material on the surface of a specimen if the specimen is particularly susceptible to mechanical damage (or excessive force is used in the grinding and polishing stages) debris can become embedded in the surface and plastic deformation may exist below the surface. Ideally, there should be no scratches after polishing, but it is often hard to completely remove them all.

Electropolishing or chemical polishing can be used to remove this, leaving an undisturbed surface.

Microscopic examination and evaluation of the final surface of metallographic samples should be done before the next step of research activities. The presence of artifacts on the sample surface would lead to an incorrect interpretation of the image of analyzed particles after binarization (detection of carbides and partly scratches in Fig. 1b).

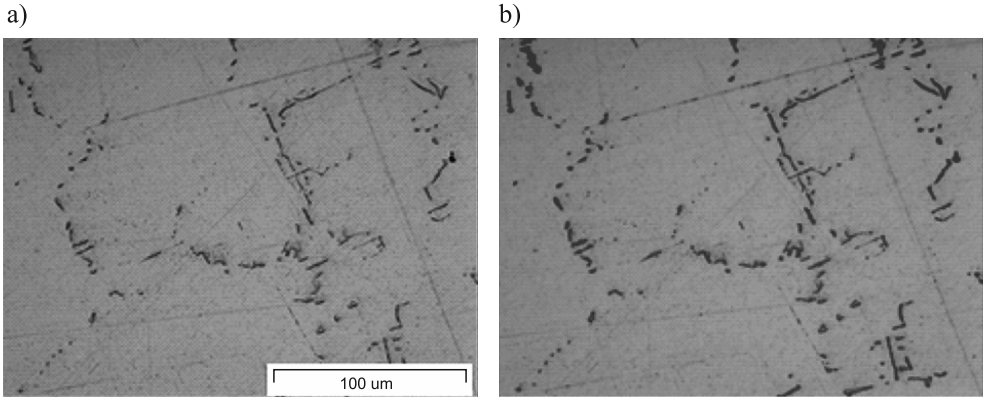

Fig. 1. Microstructure of Ni-based superalloy with carbides and visible scratches (preparation artifacts): a, b) LM, BF; c) LM, DF

To highlight surface defects, scratches or engraving a dark field illumination is mainly used. Examples of the microstructure image with scratches which are grooves in the surface of a sample, produced by the points of abrasive particles are presented in Figs. 1a, b. To enhance the contrast between the phases, different etchants and different etching methods can be used consecutively.

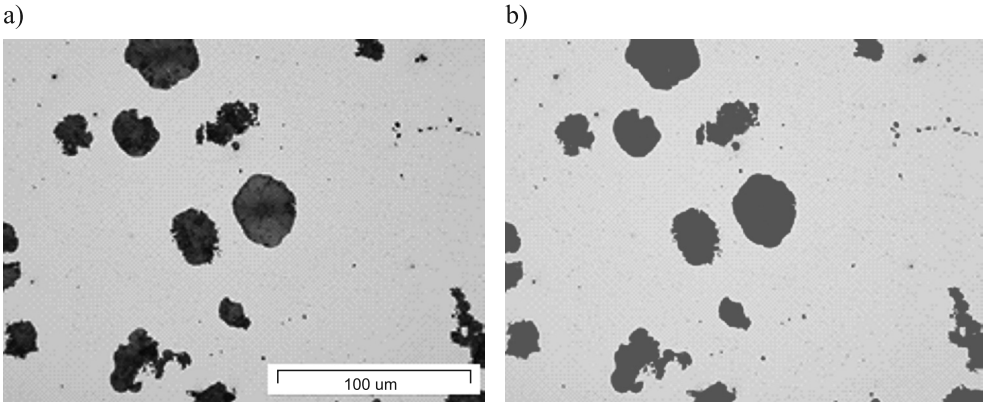

Fig. 2. Differences in the grey level of particles and background in a spheroidal grey cast iron: grey initial image, LM, BF (a) and binarization of graphite (b)

Polishing and etching of the investigated material often leads to significant differences in the intensity of light reflected from the parts of the area studied that are occupied by different phases. As a result, particles revealed on a cross-section appear to have a grey level distinguishing them from the background. Differences in the grey level of various phase constituents can be used to detect particles and conduct simple measurements on their geometrical features. An example is presented in Fig. 2.

Microscopic examination of a properly polished, unetched specimen will reveal only a few structural features such as pores, inclusions and cracks or other physical imperfections. Etching is used to highlight, and sometimes identify, microstructural features or phases present. Sometimes etching of a metallographic sample surface is not indispensable, because polishing of the sample surface makes it possible to obtain sufficient contrast required to perform selective detection of the investigated particles (example of pores in Fig. 3a, b). Some significant information about the position of each analyzed precipitate in relation to the others, and distribution of the precipitates in the microstructure could be missed exclusive of etching (Fig. 3c, d). Nevertheless, without etching the selective detection of some particles is possible (example of carbides in the Ni-based superalloy in Fig. 4).

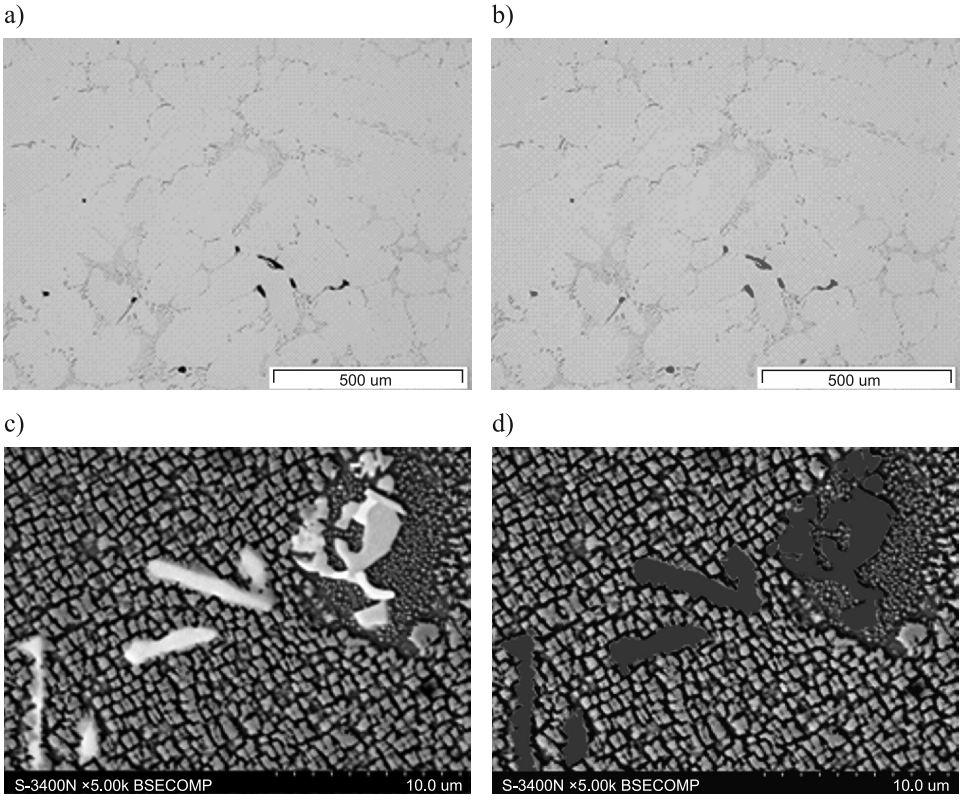

Fig. 3. Detection of pores on the unetched sample (a, b – LM, BF) and carbides on the etched sample (c, d – SEM, BSE) in Ni-based superalloy

3. Microscopic observation

Techniques of light (optical) microscopy (LM) and scanning electron microscopy (SEM) are mostly applied for the visualization of microstructures. Correct sample preparation process is not the only factor that can influence the measurement results of particles occurring in a material. The applied technique of observation and conditions of acquisition are significant for easier and less time-consuming image threshold and mathematical morphological operations (Fig. 4).

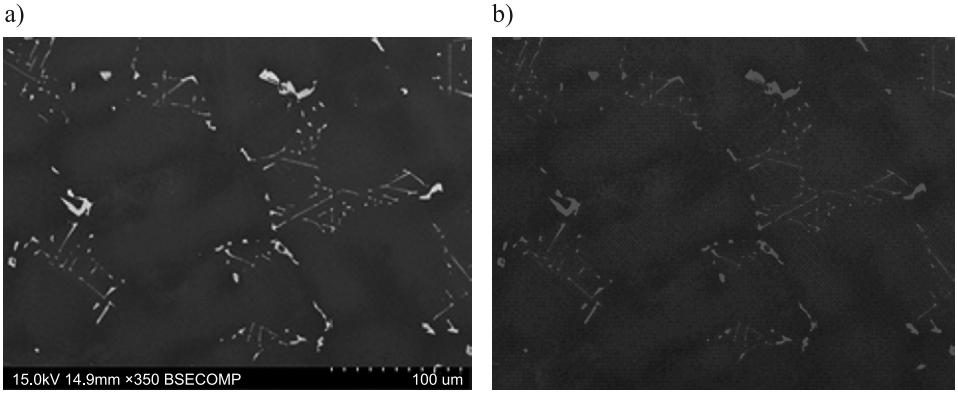

Fig. 4. Carbides precipitates in the Ni-based superalloy at 350×: grey initial image, SEM, BSE (a) and binarization of carbides obtained by means of an image analysis program (b)

The most common imaging mode collects low-energy ($<$ 50 eV) secondary electrons that are ejected from the *k*-shell of specimen atoms. Backscattered electrons (BSE) consist of high-energy electrons originating in the electron beam that are reflected or back-scattered out of the specimen interaction volume. Since heavy elements (high atomic number) backscatter electrons more strongly than light elements (low atomic number), and thus appear brighter in the image, BSEs are used to detect contrast between areas with different chemical compositions. Contrast changes in images taken in scanning electron microscope result from a change in accelerating voltage, spot size (probe current) and tilt angle.

4. Image processing

The term image processing is used to describe operations that are performed on images of microstructures in order to correct them or to make them more accessible for quantitative analysis. Image processing consists of the following steps: image acquisition, digital processing, threshold operations, mathematical morphological operations, manually made corrections (if they are necessary) and measurements. It is a concept based on digital images. Opportunities for image transformations and for measurements depend on the applied software [3].

Image segmentation is an essential task in the fields of image processing and computer vision. It is a process of partitioning of digital images and is used to locate the boundaries into a finite number of meaning full regions which are easier to analyze [4]. The simplest method for image segmentation (enhancement and object detection) is thresholding. The output of the thresholding process is a binary image whose grey level value 0 (black) will indicate a pixel belonging to a print, legend, drawing or target and a grey level value 1 (white) will indicate the background [5].

Preparation of an image representing such a microstructure is a very important factor of a reliable description of a real microstructure. Note that samples of microstructure are usually taken by means of microstructure sampling and converted into the electronic form. The characterization of microstructures usually requires an analysis of a large number of complicated images with each of them containing microstructural elements required as well as some artifacts produced by the imaging technique. This justifies the need for automation and explains the reasons for computer-aided procedures in the characterization of materials.

5. Quantitative image analysis

Modern computer aided methods used for the quantitative description of microstructures take advantage of the progress made in recent years in the field of image processing, mathematical morphology and quantitative stereology [5]. One of the most important issues is a selection of proper magnification for quantitative image analysis. It is essential to take into consideration the magnification at which the images for this analysis were registered. The examples presented in Figs. 4 and 5 can help to understand the effect of applied magnification on the obtained results of quantitative analysis. The example of carbide image registered at 350 times magnification is presented in Fig. 4. In this case, the area fraction

a) b)

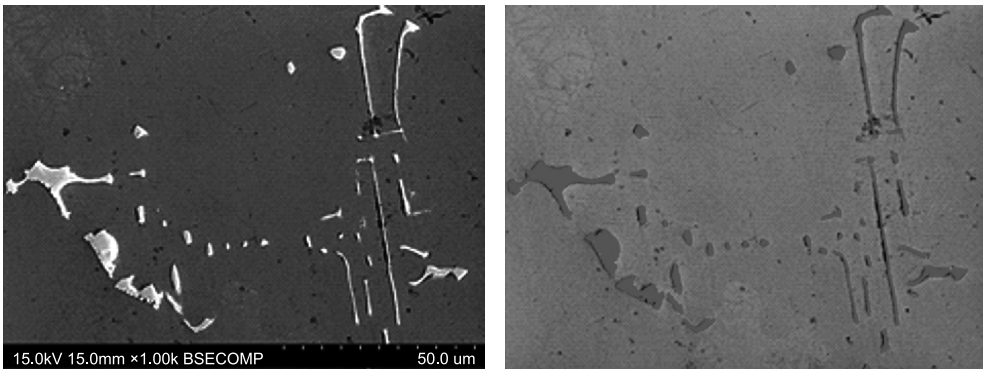

Fig. 5. Carbides precipitates in the Ni-based superalloy at 1000×: grey initial image, SEM, BSE (a) and binarization of carbides obtained by means of an image analysis program (b)

of carbides is equal to 2.28%. On the same material sample, another image with carbides was registered using 1000 times magnification (Fig. 5). At higher magnification you obtain the result of area fraction for carbides amounting to 3.66%. This result is overestimated.

6. Interpretation of results

Each quantitative analysis of a material microstructure should end with proper interpretation of the obtained results. A relative error of the carried out measurements should be estimated. Moreover, a minimal number of measured fields of view should be estimated on the basis of a statistical test (for example the goodness of fit Kolmogorov-Smirnov test of distributions). In the similar way, the repeatability of results of the obtained measurements for selected parameters should be tested.

References

[1] Kurzydłowski K.J., Ralph B., *The Quantitative Description of the Microstructure of Materials*, CRC Press, London 1995.

[2] Łydżba D., Różański A., *Statystyczna charakteryzacja miar geometrycznych mikrostruktur losowych: definicje, właściwości i zastosowania*, Górnictwo i Geoinżynieria, Wyd. AGH, Kraków, 33/2009, 399-410.

[3] Matusiewicz P., Czarski A., Adrian H., *Estimation of materials microstructure parameters using computer program SigmaScan pro*, Metallurgy and Foundry Engineering, **33** (1), 2007, 33-40.

[4] Gonzalez R.C., Woods R.E., *Digital image processing, 2nd Edition*, Prentice Hall, New Jersey 2002.

[5] Mukherjee A., Kanrar S., *Enhancement of Image Resolution by Binarization*, International Journal of Computer Applications, **10** (10), 2010, 15-19.

TECHNICAL TRANSACTIONS | **CZASOPISMO TECHNICZNE**
MECHANICS | MECHANIKA
3-M/2016

ANETA GĄDEK-MOSZCZAK*, JOANNA KORZEKWA**

METHODS OF CORRECTION OF TYPICAL DEFECTS IN THE DIGITAL IMAGES ON THE EXAMPLE OF SEM IMAGES OF ANODIC OXIDE LAYERS

METODY KOREKTY TYPOWYCH WAD OBRAZÓW CYFROWYCH NA PRZYKŁADZIE ORAZÓW SEM ANODOWYCH WARSTW TLENKOWYCH

Abstract

The paper proposes one of the possible methods of image quality improvements. There are materials whose preparation for microstructure observation is difficult and, despite the effort, poor quality images are obtained. Computer image processing techniques allow for image transformation by means of various tools and obtaining much better images, with much more visible details than in the raw image. When it is impossible to prepare the sample better for microscopy observation and microstructural analysis, proper image processing is the only solution to gather information about the tested material.

Keywords: *image processing*, *image analysis*, *shade correction*, *noise*, *microstructure*

Streszczenie

W artykule zaproponowano jedną z możliwych metod poprawy jakości obrazu. Istnieją materiały, których przygotowanie do obserwacji mikrostruktury jest trudne i w efekcie, pomimo najwyższej staranności, otrzymujemy obrazy o słabej jakości. Komputerowe techniki przetwarzania obrazu pozwalają na przekształcenie obrazów za pomocą różnorodnych narzędzi cyfrowej obróbki i uzyskanie obrazów o znacznie lepszej jakości niż obrazy bazowe. Techniki komputerowego przetwarzania i poprawy jakości obrazów stanowią cenne narzędzie w sytuacji, gdy nie jest możliwe powtórne przygotowanie próbek do obserwacji mikroskopowych i analizy mikrostruktury.

Słowa kluczowe: *przetwarzanie obrazu*, *analiza obrazu*, *korekcja cienia*, *szum*, *mikrostruktura*

DOI: 10.4467/2353737XCT.16.116.5727

* Ph.D. Eng. Aneta Gądek-Moszczak, Institute of Applied Informatics, Faculty of Mechanical Engineering, Cracow University of Technology.

** Ph.D. Joanna Korzekwa, Department of Surface Layer Technology, Faculty of Computer and Materials Science, University of Silesia.

1. Introduction

Microstructure analysis of materials microstructure is a standard procedure in developing new materials. It is also a very important stage of the quality control process of material and devices production. Microstructure inspection allows to control if all technology parameters are properly adjusted and the produced material fulfills quality requirements. Depending on the material and the scale of observation, suitable observation equipment must be chosen, like the SEM or TEM optical microscope. After the acquisition of images of microstructure, the quantitative analysis of chosen structural components should be performed if the image quality allows that. Computer image analysis, and the automatic procedure in particular, requires high quality images. Otherwise the obtained detection may fail and the results may be incorrect.

Typical image defects which strongly affect detection results are a high level of noise, unsharp image and the shadow effect. At least one of these defects can be the reason for the conduct of image preprocessing.

The proposed methods for image quality improvement were tested on the SEM images of the anodic oxide layer whose observation was difficult, and working out the proper sample preparation procedure was complicated [2].The image processing procedure presented in this paper allowed for assessing the influence of sample preparation on the quantitative analysis of structure components. For the image processing, it is not the type of object on the image that is the most important issue, but its relation with the background which determines the detection, type of needed analysis, and finally the image defects which must be reduced.

2. Proposed correction method

2.1. Noise reduction

Noise is an unexpected pixel volume fluctuation that does not reflect the true intensity of objects in the frame. Noise is introduced to image at the level of the acquisition process by CCD detectors, electronic data transmission or by a choice to save the image file format. There are lot of types of noise, but the most typical is the uneven, salt and pepper type. This kind of noise can be reduced by linear filters, like the average filter or Gauss filter. Blurring the edges of objects is a disadvantage of linear filtering and can result in enlarging the objects area on the detection images and bias the quantitative analysis. Other proposed solution is to use ranking filters. Ranking filters give good results but they must be chosen according to the noise type. Minimal filter is recommended for the salt type of noise, maximal filter for the pepper type of noise, and median filter for the salt and pepper type of noise. The minimal filter changes the pixel value for the lowest in the neighborhood, while the maximal filter changes the value of analyzed pixel for the highest in the neighborhood. The median filter for a new value of the analyzed pixel chosen is that which is in the middle of the rank list of all pixel values in the neighborhood. The advantage of this filtering is that the objects are blurred inside on the result images but the edges are sharp. The impact of the filter on the image is adjusted by an adequate filter mask size which determines the area of the image,

and in fact the number of pixels considered in the ranking list. Proper filter and its size may be assessed on the basis of profile analysis (Fig. 1a). The profile shows the course of pixel values along the test line, and allows for visualising the intensity of the noise. After

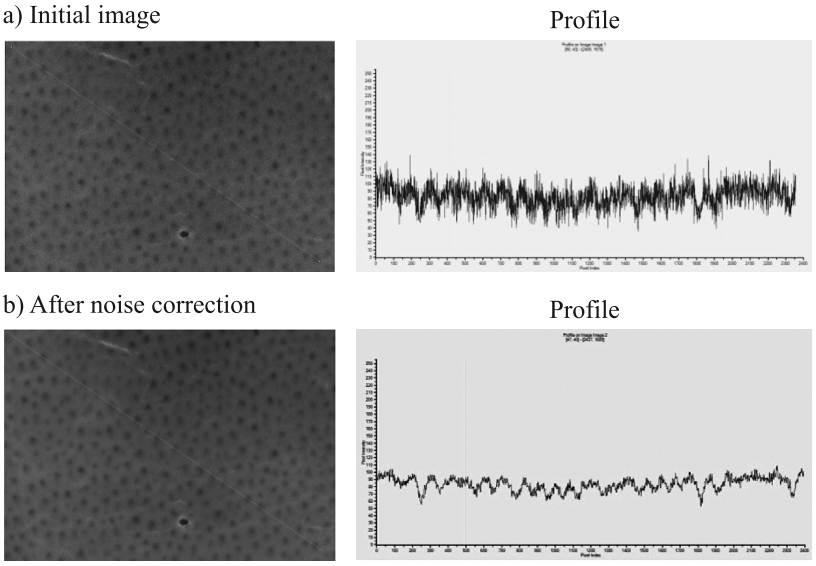

Fig. 1. Noise reduction using median filtering: a) initial image, b) image after noise correction

the noise reduction by means of a median filter, the resulting image is not spectacularly different, but when we compare the profiles of both images it is easier to assess the obtained effect. The profile of the image after noise reduction is significantly smoother, and the local minimally illustrated objects are more visible.

2.2. Image sharpening

Image blurring can be caused by improper equipment adjustment or a specific object surface. Image processing software offers sharpening filters which make images sharper, but it should be taken into consideration that sharpening filters sharpen the image by increasing the local contrast. A side effect of this solution is the enhancement of noise on the image. Sharpening filters are commonly used in computer graphic applications, but for image analysis it is better to use the unsharp masking procedure. The unsharp masking procedure based on a blurred image (Fig. 2b) which is subtracted form the initial image. The obtained image (Fig. 2c) is added to the initial image (Fig. 2a).

a) Initial image b) Blurred image

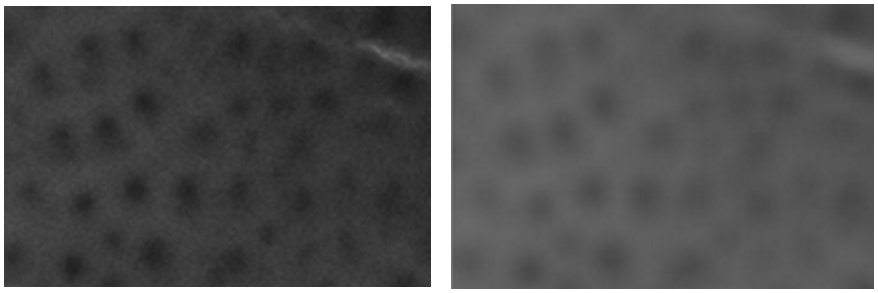

c) Subtract image d) Final image

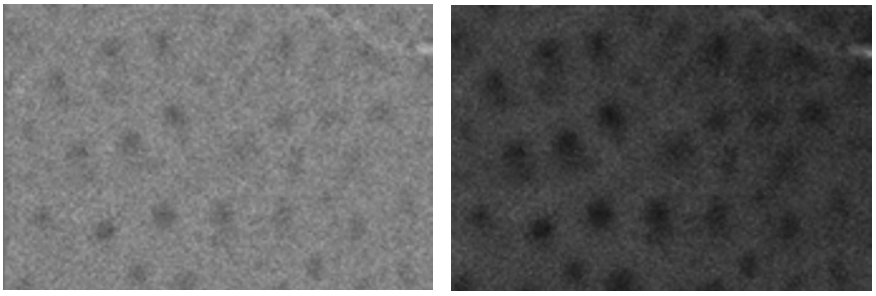

Fig. 2. Unsharp mask

2.3. Shadow correction

The shadow effect on the image is caused by uneven lightening of the object during the acquisition or by uneven surface of the analyzed sample. In both cases it is manifested by uneven background on the image, which may make object detection difficult or impossible, especially when the pixels value of the objects and background is insignificant.

In the literature there can be found numerous methods of shadow correction [1, 3, 4]. The shadow effect can be reduced by bringing out and subtracting the image of the shadow

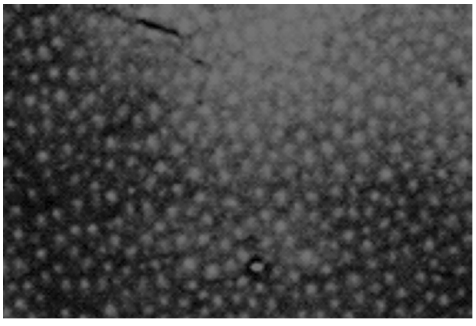

Fig. 3. The result of the detection without the shadow correction

from the initial image. In general, almost all known methods of shadow effect reduction differ in the method of shadow image extraction. The image of a shadow may be generated by means of a mean filter with a large mask, enough to blur out all objects. A frequency filter may be also used, like, for instance, the Fast Fourier Transformation. The shadow might be obtained in the way of morphological transformation, closing with a large size of the matrix. In the considered example, the shadow effect is not visible for the user. However, the problem with correct thresholding and detection showed that the correction must be performed (Fig. 3).

The proposed procedure of shadow correction is so called the proportional method [1] and it starts from generating shadow image by a large closing (Fig. 4b). In the next step, the initial image is divided by the image of a shadow. The resulting image is multiplied by the inverted image of the shadow and added to the initial image. The final image of this set of procedure is presented in Fig. 4c, and the detection result in Fig. 4d.

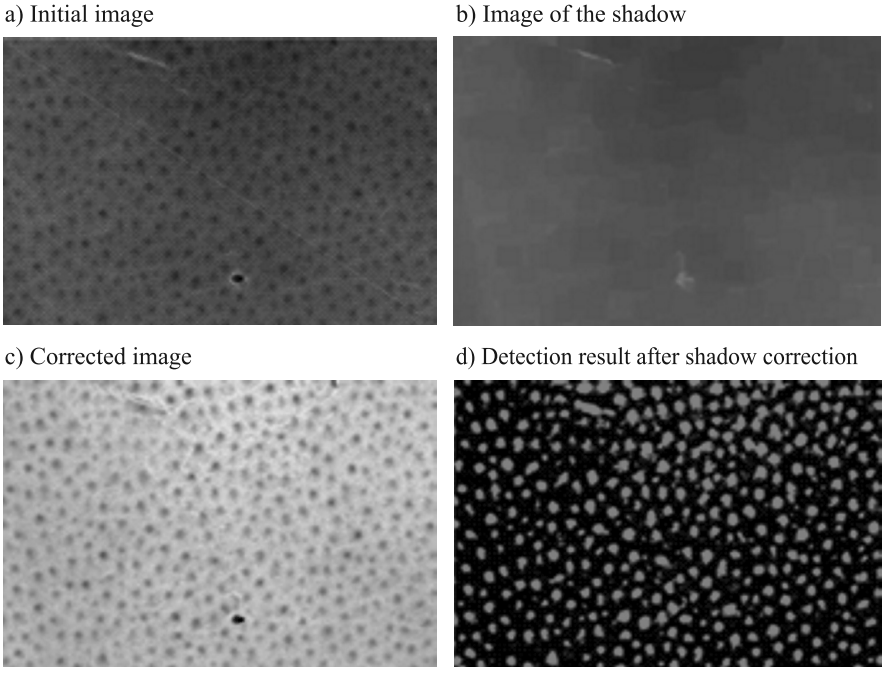

Fig. 4. Shadow correction effect

A set of images presenting an anodic oxide layer was used to test the efficiency of the proposed method of image quality improvement. The result of detection, the pores, have been drawn in yellow. It can be observed that not all pores were detected correctly, some of them were missed and not taken into consideration in quantitative analysis (Fig. 5). However, it must be stressed that without the proposed correction procedure the detection and quantitative analysis were impossible to perform due to the low quality of images.

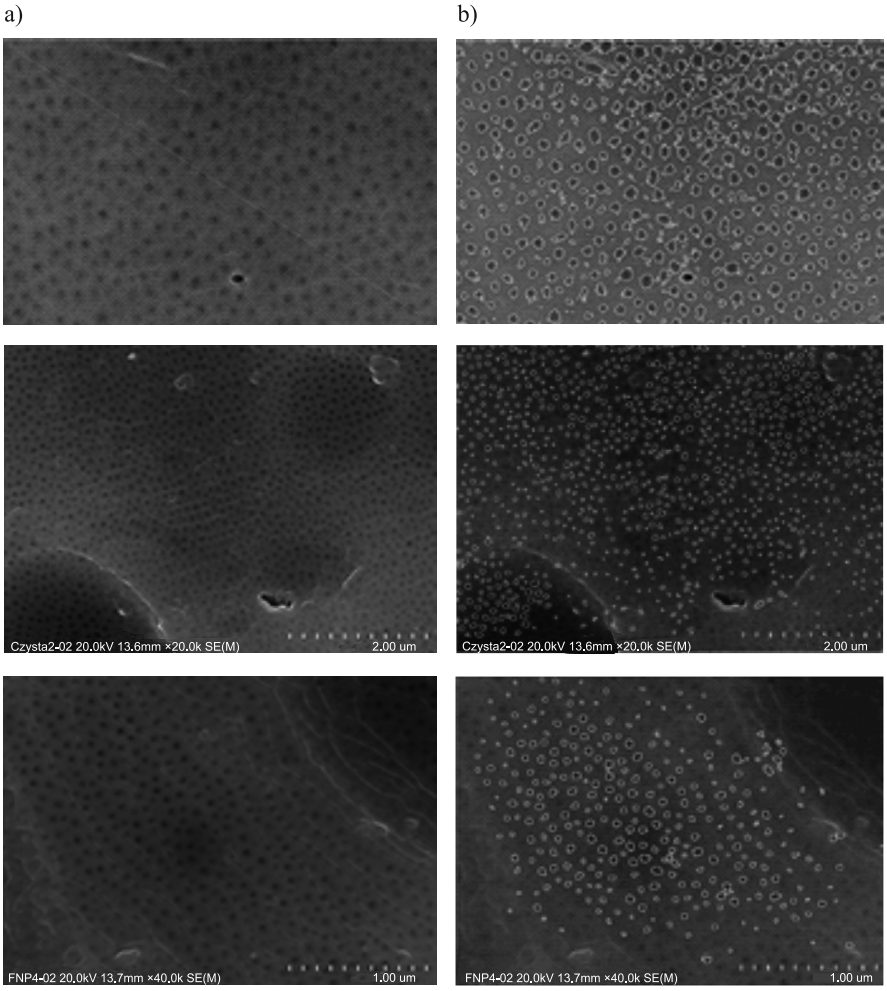

Fig. 5. Result of the detection on the set of tests images: a) initial images, b) detection result of corrected images

3. Conclusion

Advanced imaging techniques allow for obtaining better quality images, but still some problems with proper sample preparation of new materials may cause problems, which may affect the microstructure image quality. Appropriate selection of tools and methods of image processing can result in a significant improvement of image quality and the possibility to perform quantitative analysis of a microstructure.

References

[1] Gądek A., Wojnar L., *Wpływ sposobu 5. korekcji cienia i diboru metody detekcji na wyniki ilościowej oceny porowatości*, Inżynieria Materiałowa, **3**, 2003, 111-116 [in Polish].

[2] Korzekwa J., Gądek-Moszczak A., M Bara, *The influence of sample preparation on SEM measurements of anodic oxide layers*, Practical Metallography, **53** (1), 20016, 3649.

[3] Russ J.C., *The Image processing handbook. Second Edition*, CRC Press, Boca Raton, 1995.

[4] Wojnar L., Kurzydłowski K.J., Szala J., *Praktyka analizy obrazu*, Polskie Towarzystwo Stereologiczne, Kraków 2002 [in Polish].

TECHNICAL TRANSACTIONS | CZASOPISMO TECHNICZNE
MECHANICS | MECHANIKA
3-M/2016

CZESŁAW KUNDERA*, TOMASZ KOZIOR*

INFLUENCE OF PRINTING PARAMETERS ON THE MECHANICAL PROPERTIES OF POLYAMIDE IN SLS TECHNOLOGY

WPŁYW PARAMETRÓW TECHNOLOGICZNYCH NA WŁAŚCIWOŚCI MECHANICZNE POLIAMIDU W TECHNOLOGII SLS

Abstract

This paper presents the research results of the influence of selected process parameters on the tensile strength samples obtained according to the ISO 527 standard. Bio-capable polyamide powder PA 2200 was the material used in the process. The research included such parameters as energy density transmitted to the sintered layer, laser power and speed, printing direction and the number of scanning. A computer program based on artificial neural network was used to analyze the research results. The program allowed us to assess the influence of printing parameters on the tensile strength, based on previously made research without the need to prepare samples according to the experimental plane.

Keywords: Additive Manufacturing, *SLS, Polyamide PA 2200*, *Formiga P100*

Streszczenie

W artykule przedstawiono wyniki badań wpływu wybranych parametrów procesu technologii Selektywnego Spiekania Laserowego na wytrzymałość na rozciąganie próbek wykonanych zgodnie z normą ISO 527 z użyciem poliamidowego proszku PA 2200. Uwzględniono parametry takie jak: gęstość energii, prędkość i moc lasera, kierunek wydruku oraz liczbę naświetleń. Do analizy uzyskanych wyników badań wykorzystano program działający w oparciu o modele sztucznych sieci neuronowych, pozwalający na oszacowanie wpływu opisanych czynników na wytrzymałość uprzednio wykonanych próbek

Słowa kluczowe: Technologie Przyrostowe, *SLS*, *Poliamid PA 2200*, *Formiga P100*

DOI: 10.4467/2353737XCT.16.117.5728

* Prof. D.Sc. Ph.D. Eng. Czesław Kundera, M.Sc. Eng. Tomasz Kozior, Faculty of Mechatronics and Mechanical Engineering, Department of Manufacturing Engineering and Metrology, Kielce University of Technology.

1. Introduction

Unconventional manufacturing technologies, well known as 3D printing have been developing rapidly during the last few years. The first additive technology was invented by Charles Hull in the 80s of the last century. In the last years, a special committee ASTM F42 has prepared a valuable standard where basic terminology related to additive technologies was described. Standard ASTM F2792-10 [2] describes the main phenomena related to additive technologies and standardizes the procedure. Standard ISO 527 [5] and ASTM D638 [3], which are usually used for research in uniaxial tensile tests, are limited in their application because of their layer manufacturing structure. Additive technologies have many advantages e.g. reduction of production time, no need to produce manufacturing tools, small cost in case of singular production and possibility to obtain very complicated shapes, especially inner dimensions. The disadvantages of additive technologies include e.g. anisotropy properties, shrink of material and cost in mass production. There are many papers describing the main area of additive technologies, their mechanical properties and accuracy. In work [9] authors described the influence of proportion of two types of polymer powder which were mixed together, PA12 and HDPE, on mechanical properties in relation to the selected composition. Mechanical properties of selective laser sintering technology were also described in paper [12], where authors determined tensile and bending strength of samples manufactured according to the ISO 527 standard. In work [7], a selective laser sintering technology was used to build two types of element in the form of a shaft and sleeve. The authors determined the influence of selected printing parameters on the accuracy and shape deviations e.g. roundness, cylindricity and straightness. The samples were made in two types of fit which reflect real assembly elements.

Almost all additive technologies have several printing parameters which have a great influence on mechanical properties, accuracy [1] and rheological properties. We can usually set printing direction and layer thickness. Many technologies have additional parameters, especially those which use the laser [11]. In this research, the authors used a computer program based on artificial neural network EASY NN as a calculation tool.

2. Applied Technology

Selective Laser Sintering is one of the oldest additive technologies. It was invented in 1987 at the University of Texas in the United States by Carl Deckard. This technology uses CO_2 laser power to bind sintered powdered material to create a solid structure. In the sintering process, a currently built and previously made layer are joined to obtain a solid model. Building chamber is heated to the temperature little below the melting point. The whole manufacturing process is performed in a chamber filled with neutral gas e.g. nitrogen. In this technology, we can use plastic, ceramic or metal powder to produce objects. The most popular material based on plastic powder is polyamide PA 2200. Cooling process in the SLS technology is quite similar to casting process. In both processes, in case of too fast cooling process in a building model, stresses arise which change model dimensions and can cause damage [8, 10].

3. Research

The aim of the presented research was to determine the influence of 5 printing parameters e.g. printing direction, energy density transmitted to the sintered layer, building layer thickness, laser speed and power on the tensile strength. The samples were designed in the CAD program SolidWorks 2012 and then manufactured by a machine Formiga P100. Polyamide PA 2200 with mechanical properties presented in Table 1 was the material used to build the models. Each type of samples were made in 5 pieces to include statistical calculations. The printing parameters are shown in Table 2. A tensile test machine Inspect Mini 3000N was used to determine mechanical properties. During this research, the samples were subject to tension according to ISO 527 standard. Further, the research results were analyzed by the EASY NN program. In the program it is possible to set a number of hidden neurons and a number of neurons layer. In the calculation phase, the program was used „learning with teacher", which allowed to compare their results with real data obtained from the tensile test. Samples 5, 7 and 13, 15 were excluded from the "learning process" to determine the accuracy of artificial neural network. Placement samples on the virtual platform are shown in Fig. 1.

Table 1

Polyamide PA2200 mechanical properties [4]

Mechanical Properties	Value	Unit	Standard
Young's modulus	1700	[MPa]	EN ISO 527
Shore'a hardness	75	[–]	ISO 868
Density	930	[kg/m^3]	EOS
Melting temperature	176	[°C]	ISO 11357-1/-3

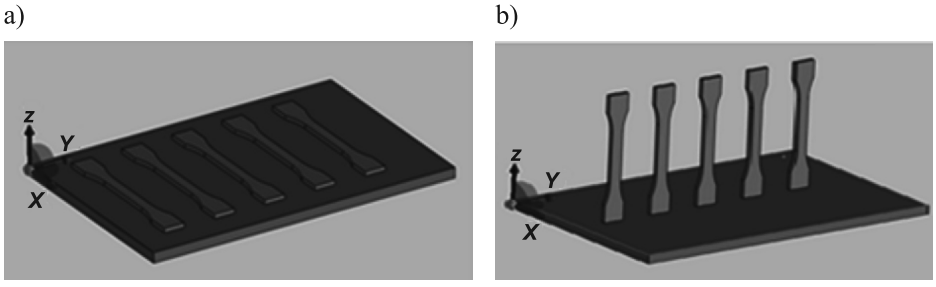

Fig. 1. Placement samples on the virtual platform: a) horizontal samples, b) vertical samples

Energy density transmitted to the sintered layer can be calculated the from relation (1) [12].

$$ED = \frac{P}{vh}x \tag{1}$$

where:

ED – energy density [J/mm^2],

P – laser power [W],
v – laser speed [mm/s],
h – hatching distance [mm],
d – diameter of focussed beam,
x – beam overlay ratio $x = d/h$.

The use of artificial neural network allowed us to set 5 different values of laser power, 4 laser speeds, 5 energy densities, 3 different amounts of exposures and 2 printing directions. The only limitation was the number of input variables, limited to 10.

Table 2

Printing parameters

Samples No.	Laser power [W]	Laser speed [mm/s]	Energy density [J/mm^2]	Number of scanning	Placement on the platform
1	7	3000	0.016	1	Horizontal
2	14	3000	0.031	1	Horizontal
3	25	3000	0.056	1	Horizontal
4	21	2500	0.056	1	Horizontal
5	22	1400	0.1	1	Horizontal
6	22	1000	0.147	1	Horizontal
7	21	2500	0.056	2	Horizontal
8	21	2500	0.056	3	Horizontal
9	7	3000	0.016	1	Vertical
10	14	3000	0.031	1	Vertical
11	25	3000	0.056	1	Vertical
12	21	2500	0.056	1	Vertical
13	22	1400	0.1	1	Vertical
14	22	1000	0.147	1	Vertical
15	21	2500	0.056	2	Vertical
16	21	2500	0.056	3	Vertical

4. Results

The simulation research results obtained by artificial neural networks are shown in Fig. 2. The average absolute error in the EASY NN 1 model was equal to 2.95% for samples 1–8 and 9.8% for samples 9–16. For models EASY NN 2, absolute error was respectively 4.5% and 11.5%. The largest error occured in the samples 5, 7, 13 and 15 was excluded from the learning processes. The average error for samples 5, 7 was 6.9%, and for samples 13, 15–14%.

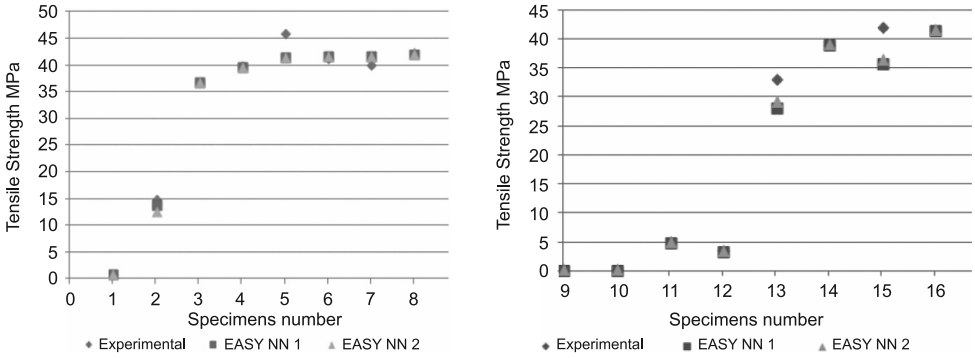

Fig. 2. Tensile strength

Table 3

Research results

Samples No.	Tensile divice [MPa]	EASY NN 1 [MPa]	Absolute error NN 1[%]	EASY NN 2 [MPa]	Absolute error NN 2 [%]
1	1	0.99	1	0.96	4.04
2	15	13.94	7	12.78	15.92
3	37	37	0	37	0
4	40	39.9	0.25	39.9	0.25
5	46	41.61	9.54	41.61	10.55
6	41.5	41.92	1.01	41.92	1.01
7	40.3	41.92	4.01	41.87	3.74
8	42.5	42.18	0.75	42.15	0.82
9	0.2	0.22	10	0.27	31.81
10	0.4	0.26	35	0.32	30.76
11	5	4.99	0.2	4.99	0.2
12	3.5	3.52	0.57	3.52	0.56
13	33	28.2	14.54	29.2	13.47
14	39	38.99	0.02	38.98	0.05
15	42	35.84	14.66	36.35	15.76
16	41.5	41.52	0	41.5	0.09

Table 3 shows the research results of tensile test [9] and simulation results obtained by EASY NN. The marked samples were excluded from the network during the learning process. The lowest tensile strength equals 0.2 and 0.4 MPa, present in samples 9 and 10, where the printing direction was vertical to the building Z-axis and the energy density transmitted to the sintered layer was the lowest. By increasing the number of scanning from 1 (sample 4) to 3 (sample 8), tensile strength increased from 40 MPa to 42.5 MPa in the case

of horizontal print. In the vertical print, for samples 12 and 16 tensile strength increased respectively from 3.5 MPa to 41.5 MPa. By Increasing the energy density from 0.056 J/mm^2 (sample 4) to 0.1 J/mm^2 (sample 5) and 0.147 J/mm^2 (sample 6) tensile strength increased respectively from 40 MPa to 46 MPa and 41.5 MPa for the samples printed horizontally. In case of vertical samples, tensile strength increased respectively from 3.5 MPa (sample 12) to 33 MPa (sample 13) and 39 MPa (sample 14).

5. Conclusion

The analysis of the research results obtained by artificial neural network models indicated that each of the above mentioned printing parameters affects the research results. When energy density is increased above 0.056 J/mm^2 or the number of exposures, tensile strength increases. This is very a positive aspect which allows for minimizing the effects of anisotropy, thereby excluding the influence of the printing direction. Despite the beneficial effects on the mechanical properties, accuracy in these cases decreases. When the number of exposures is increased, the building time significantly increases. The influence of laser power and speed in case of obtaining the same energy density is negligible, as evidenced by the previous research results. The use of artificial neural network models as a calculation tool allows for a quick assessment of the impact of input parameters on the studied phenomena. By increasing the number of neurons in some cases, it can have adverse effect on the results, e.g. Samples 7, 10, 13. For various „printing" directions, the research results obtained by means of the same neural network change. It means that it would be better to design a separate artificial neural network model for each type of printing direction.

References

[1] Adamczak S., Janecki D., Zmarzly P., *Theoretical and Practical investigations of V-block waveness measurement of cylindrical parts*, Metrology and measurement systems, **22** (2), 2015, 181-192.

[2] ASTM F2792-10, Standard terminology for additive manufacturing technologies.

[3] ASTM D638, Standard Test Method for Tensile Properties of Plastics.

[4] EOS COMPANY, Formiga P100 – User Manual, Monachium 2008.

[5] ISO 527-1, Determination of Tensile Properties of Plastics.

[6] Kundera Cz., Bochnia J., *Investigating the stress relaxation of photopolymer O-ring seal models*, Rapid Prototyping, **20** (6), 2014, 533-540.

[7] Kundera Cz., Kozior T., *Ocena luzów technologicznych w modelowym łożysku ślizgowym wykonanym metodą SLS*, Mechanik, **2**, 2015, 345-354 [in Polish].

[8] Wang R.J., Wang L., Zhao L., Liu Z., *Influence of process parameters on part shrinkage in SLS*, Int. J. Adv. Manufacturing Tech., **33**, 2007, 498-504.

[9] Leite J.L., Salmoria G.V., Paggi R.A., Ahreans C.H., Pouzada A.S., *Microstructural characterization and mechanical properties of functional graded PA12/HDPE*, Int. J. Adv. Manufacturing Tech., **59**, 2012, 583-591.

[10] Vaughan R.M., Crawford R.H., *Effectiveness of virtual models in design for additive manufacturing: a laser sintering case study*, Rapid Prototyping Journal, **19** (6), 2013, 11-19.

[11] Leu M.C., Guo N., *Additive manufacturing: technology, applications and research needs*, Frontiers of Mechanical Engineering, **8** (3), 2013, 215-243.
[12] Pilipović A., Valentan B., Brajlih T., Haramina T., Balić J., Kodvanj J., Sercer M., Drstvenšek I., *Influence of laser sintering parameters on mechanical properties of polymer products*, International Conference on Additive Technologies ICAT, 2010.
[13] *EASY NN Neural Planner Software Ltd*, company information, http://www.easynn.com [date of acc. 01.01.2016].

TECHNICAL TRANSACTIONS | **CZASOPISMO TECHNICZNE**
MECHANICS | MECHANIKA
3-M/2016

TOMASZ LIPIŃSKI*

CORROSION ANALYSIS OF THE X2CrNiMoN25-7-4 SUPER DUPLEX STAINLESS STEEL

ANALIZA KOROZJI STALI ODPORNEJ NA KOROZJĘ SUPER DUPLEX X2CrNiMoN25-7-4

A b s t r a c t

Super duplex stainless steels present excellent corrosion resistance of austenite steel and a high mechanical behaviour of ferrite steel. However, performance presented by super duplex stainless steels can be drastically reduced if undesirable phases, such as sigma phase, chi phase, secondary austenite and a lot of rich chromium and carbides precipitate. The purpose of this work was to ascertain how 30-minutes isothermal heat treatments at 530°C and corrosion time effect the relative mass loss and profile roughness parameters of the X2CrNiMoN25-7-4 super duplex stainless steel. The influence of boiling nitric acid on the steel corrosion resistance was investigated using weight loss and roughness parameters.

Keywords: stainless steel, *duplex steel*, *corrosion*, *corrosion rate*, *roughness*

S t r e s z c z e n i e

Stale super duplex posiadają doskonałą odporność na korozję dziedziczną ze stali austenitycznych i wysokie właściwości mechaniczne właściwe dla stali ferrytycznych. Jakkolwiek właściwości stali odpornej na korozję super duplex mogą ulegać gwałtownemu obniżeniu wraz z powstaniem niepożądanych faz, takich jak faza sigma, faza chi, austenit wtórny i wielu innych wydzieleń bogatych w chrom, jak również węglików. Celem tego artykułu było określenie, jak 30 minutowa izotermiczna obróbka cieplna w temperaturze 530°C i czas przetrzymywania materiału w ośrodku korozyjnym wpływa na względny ubytek masy i parametry chropowatości stali odpornej na korozję super duplex X2CrNiMoN25-7-4. Badania wpływu wrzącego kwasu azotowego na odporność korozyjną badano, wykorzystując ubytki masowe i parametry chropowatości.

Słowa kluczowe: stale odporne na korozję, *stale duplex*, *korozja*, *szybkość korozji*, *chropowatość*

DOI: 10.4467/2353737XCT.16.118.5729

* D.Sc. Ph.D. Eng. Tomasz Lipiński, Department of Materials Technology and Engineering, Faculty of Technical Sciences, University of Warmia and Mazury in Olsztyn.

1. Introduction

Duplex stainless steels are among the most popular construction materials. They are used in a wide range of industrial applications, but their properties are continuously studied to improve their qualities. Low maintenance costs, very high material circulation and good environmental reasons are further important arguments for enhancing the selection of these steels. For the most part, the corrosion resistance of a welded joint is slightly lower than the parent material. It is of great importance to have duplex steels readily available to fabricators and end users. Because of this skilled technical support, their well known properties in different temperatures are required to widen the application areas of duplex steels [1–9].

The microstructure and utility properties of steels are determined by phase transformation during its thermal processing [7]. While the phase relationships during the manufacturing process are user-independent, the range of stability or volume fraction of each phase depend of individual maintenance (mainlythermal conditions). The percentage of each phase depends on the composition, technological processes, heat treatments and critical cooling rate obtained by means of the manufacturing method applied [11–12].

Duplex steels are more prone than austenitic steels to the precipitation of phases causing embrittlement and reduced corrosion resistance. The formation of intermetallic phases such as sigma phase occurs in the temperature range of 600–950°C and the reformation of ferrite occurs in the 350–525°C range (475°C embrittlement). However, the performance presented by super duplex stainless steels can be drastically reduced if undesirable phases, such as sigma phase, chi phase, secondary austenite and a lot of rich chromium and carbides precipitate. The sigma phase is rich in chromium and molybdenum and is formed by ferrite decomposition, in the temperature of over 500°C. In normal alloying, heat-treatment or welding processes, the risk of embrittlement is not too high [6]. However, a risk exists for example in a failure that can arise during its operation causing overheating, especially if the cooling is slow. Generally, the higher the superheating temperature the higher the ferrite content. However, steel must be heated to a very high temperature to become completely ferritic. Then heat treatment process for both solution annealing and stress relieving is advisable at certain temperatures with subsequent rapid cooling in water [1, 6]. A lot of authors report that corrosion resistance of stainless steels depends on rich chromium precipitates in microstructure [1, 2, 12].

The purpose of this work was to ascertain how 30-minutes isothermal heat treatments at 530°C and corrosion time affect the relative mass loss and profile roughness parameters of the X2CrNiMoN25-7-4 super duplex stainless steel.

2. Materials and Methods

The experiment was performed with the super duplex stainless X2CrNiMoN25-7-4 steel. The chemical composition of the X2CrNiMoN25-7-4 steel is presented in Table 1.

Table 1

Chemical composition of the X2CrNiMoN25-7-4 steel

Meanchemicalcompositions [wt. %]									
C	Si	Mn	P	S	Cr	Mo	Ni	Cu	N
0.02	0.29	0.5	0.02	0.0005	25.37	3.74	6.82	0.17	0.269

Before experiments, the specimens with the area of 13 cm^2 (4 × 1 × 0.5 cm) were successively polished with 400 grades of emery paper and mechanically cleaned with 95% alcohol.

The samples were held at the temperature of 530°C for 30 minutes and cooled down in the open air, in accordance with the PN EN ISO 3651-1 standard. Determination of stainless steel resistance to intergranular corrosion. Part 1: Austenitic and ferritic-austenitic (duplex) stainless steels. Corrosion test in nitric acid medium by the measurement of loss in mass (the Huey test), corrosive media were represented by the boiling V 65% nitric acid.

The samples of X2CrNiMoN25-7-4 steel (about 10 mg) were analyzed by means of the Dynamic Scanning Calorymetry measurement by NEITSH DSC204 F1 Phoenix and DSC/dt in a nitrogen atmosphere (with the constant flow of 20 ml/min) by means of Neitsch-Proteus 5.1 software. DSC measurements were carried out in the temperature range of 20––610°C and with the heating rate of 10°C/min.

The corrosion rate of the X2CrNiMoN25-7-4 steel measured in mm/year was calculated by means of formula (1), but measurements in g/m^2 were calculated by means of formula (2):

$$r_{\text{corm}} = 8760 \text{ m/Std} \tag{1}$$

$$r_{\text{corg}} = 10\,000 \text{ m/St} \tag{2}$$

where:

m – average mass loss in the boiling solution [g],
S – surface area of the sample [cm^2],
t – time of treatment in the corrosive solution of a boiling nitric acid [hours],
d – sample density [g/cm^3].

The influence of boiling nitric acid on the X2CrNiMoN25-7-4 steel corrosion resistance was investigated using the loss of weight. The mass of samples was measured by Kern ALT 3104AM general laboratory precision balance with the accuracy of measurement 0.0001 g.

Profile roughness parameters were analyzed according to the PN-EN 10049:2014--03 standard (Measurement of roughness average R_a and peak count RPc on metallic flat products) by the Diavite DH5 profilometer.

3. Results

The Dynamic Scanning Calorimetry curves of heating measurement from 400 to 600°C (according to literature – embrittlement temperature of 475°C) the super duplex steel for heating rate 10°C/min is presented as an example in Fig. 1.

The endothermic peak (Fig. 1) involving 8.155 J/g of reaction enthalpy with the Tonset at about 465°C, T_{end} at about 566°C and T_{peak} about 532°C according to literature [3, 4] represents dissolving of chromium-rich α′-phase. The reformation of ferrite which occurs in the range of 350–525°C is determined as the 475°C embrittlement. For this sample Cp is about 0.146 J/(gK).

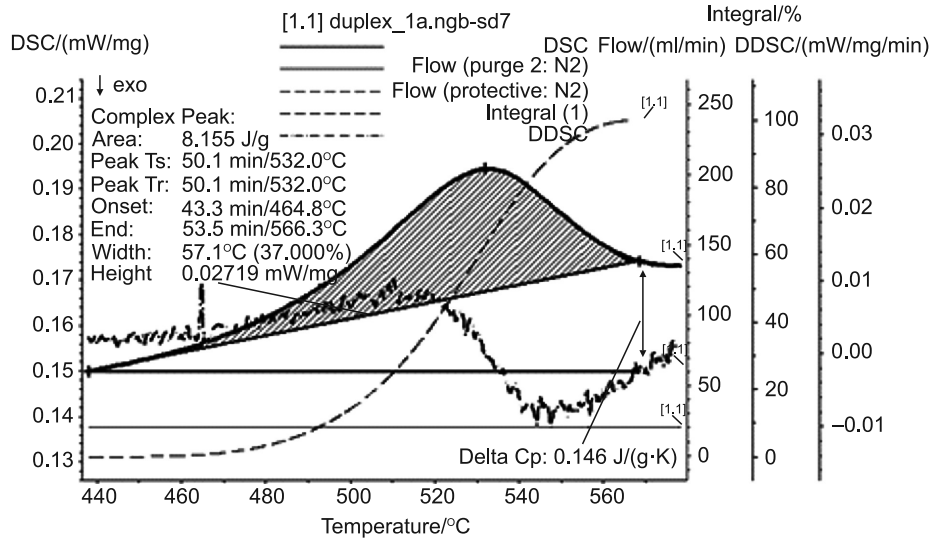

Fig. 1. DSC and DDSC curves of heating measurement the X2CrNiMoN25-7-4 steel. Heating rate 10°C/min

Profile roughness parameters of X2CrNiMoN25-7-4 steel with: R_a – arithmetic average of absolute values [μm], R_p – maximum peak height [μm], R_q – root mean squared [μm], R_t – Maximum Height of the Profile [μm] after corrosion tests in boiling HNO_3 for different boiling time is presented in Fig. 2, regression equation and correlation coefficient r at (3)–(6).

$$R_a = 0.0055t + 2.37 \quad \text{and} \quad r = 0.95 \tag{3}$$

$$R_p = 0.0002t^2 - 0.057t + 23.34 \quad \text{and} \quad r = 0.82 \tag{4}$$

$$R_q = 0.0074t + 2.94 \quad \text{and} \quad r = 0.96 \tag{5}$$

$$R_t = 0.0002t^2 - 0.057t + 23.52 \quad \text{and} \quad r = 0.88 \tag{6}$$

Percentage effects of corrosion time on the relative mass loss (RML) of X2CrNiMoN25-7-4 steel annealed at 530°C for 30 minutes and cooling down in the open air are presented in Fig. 3, regression equation and correlation coefficient r at (7).

$$\text{RML} = 0.21t + 18.3 \quad \text{and} \quad r = 0.98 \tag{7}$$

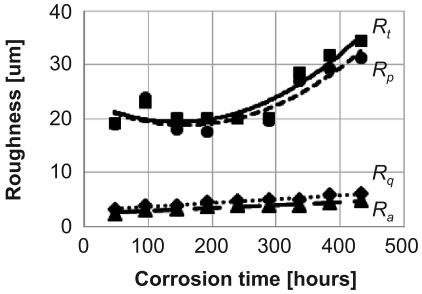

Fig. 2. Profile roughness parameters of X2CrNiMoN25-7-4 steel annealed at 530°C for 30 minutes and cooling down in the open air after corrosion tests in boiling HNO_3 for different boiling time

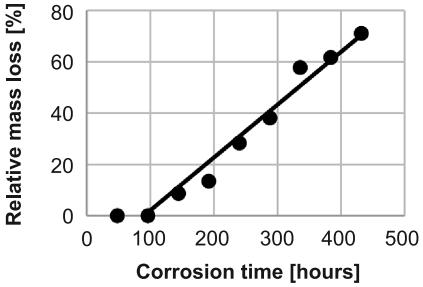

Fig. 3. Percentage effects of corrosion time on the relative mass loss (RML) of X2CrNiMoN25-7-4 steel annealed at 530°C for 30 minutes and cooling down in the open air

Effects of corrosion time on the corrosion rate measured in mm per year of X2CrNiMoN25-7-4 steel annealed at 530°C for 30 minutes and cooling down in the open air are presented in Fig. 4, regression equation and correlation coefficient r at (8).

$$r_{\text{corm}} = 0.062t - 2.69 \quad \text{and} \quad r = 0.96 \tag{8}$$

Effects of corrosion time on the corrosion rate measured in gram per m^2 of X2CrNiMoN25-7-4 steel annealed at 530°C for 30 minutes and cooling down in the open air are presented in Fig. 5, regression equation and correlation coefficient *r* at (9).

$$r_{\text{corg}} = 0.056t - 2.46 \quad \text{and} \quad r = 0.96 \tag{8}$$

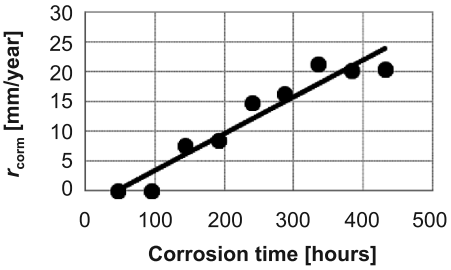

Fig. 4. Effects of corrosion time on the corrosion rate measured in mm per year of X2CrNiMoN25-7-4 steel annealed at 530°C for 30 minutes and cooling down in the open air

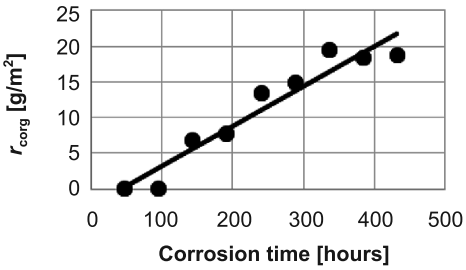

Fig. 5. Effects of corrosion time on the corrosion rate measured in gram per m^2 of X2CrNiMoN25-7-4 steel annealed at 530°C for 30 minutes and cooling down in the open air

4. Conclusions

1. Annealing duplex steels in temperatures from 465°C to 565°C causes dissolving of chromium-rich α′-phase.
2. The results of the tests indicate that the loss of weight of X2CrNiMoN25-7-4 steel annealed at 530°C for 30 minutes and cooling down in the open air is proportional to the time of corrosion.
3. Profile roughness parameters such as R_a and R_q increase with the increase of the time of corrosion process while R_t and R_p in the first stage of corrosion did not change and in the second period increased exponentially.
4. Based on the profiles of roughness parameters every research study can determine the size of duplex steel corrosion.

References

[1] Szabracki P., Lipiński T., *Influence of sigma phase precipitation on the intergranular corrosion resistance of X2CrNiMoN25-7-4 super duplex stainless steel*, Proc. of 23rd International Conference on Metallurgy and Materials METAL 2014 May 21st–23rd 2014, Brno 2014, 476-481.

[2] Dudek A., Wrońska A., Adamczyk L., *Surface remelting of 316 L+434 L sintered steel: microstructure and corrosion resistance*, Solid-State Electronics, **18** (11), 2014, 2973-2981.

[3] Bastos I., Tavares S., Dalarda F., Nogueira R., *Effect of microstructure on corrosion behavior of superduplex stainless steel at critical environment conditions*, Scripta Materialia, **57** (10), 2007, 913-916.

[4] Lipiński T., *Corrosion of X2CrNiMoSi18-5-3 Duplex Stainless Steel*, Proc. of 15th International Scientific Conference Engineering for Rural Development, Jelgava, 25th–27th May 2016, Vol. 15, 946-951.

[5] Tavares S., Pardal J., Lima L.D., Bastos I.N., Nascimento A.M., De Souza J., *Characterization of microstructure, chemical composition, corrosion resistance and toughness of a multipass weld joint of superduplex stainless steel UNS S32750*, Materials Characterization, **58** (7), 2007, 610-616.

[6] Szabracki P., Lipiński T., *Effect of aging on the microstructure and the intergranular corrosion resistance of X2CrNiMoN25-7-4 duplex stainless steel*, Solid State Phenomena, **203–204**, 2013, 59-62.

[7] Petrovic D.S., Pirnat M., Klancnik G., Mrvar P., Medved J., *The effect of cooling rate on the solidification and microstructure evolution in duplex stainless steel, A DSC study*, Journal of Thermal Analysis and Calorimetry, **109**, 2012, 1185-1191.

[8] Szabracki P., Lipiński T., *Effect of aging on the microstructure and the intergranular corrosion resistance of X2CrNiMoN25-7-4 duplex stainless steel*, Solid State Phenomena, **203–204**, 2013, 59-62.

[9] Pietraszek J., Gadek-Moszczak A., *The smooth bootstrap approach to the distribution of a shape in the ferritic stainless steel AISI 434L powders*, Solid State Phenomena, **197**, 2013, 162-167.

[10] Selejdak J., Ulewicz R., Ingaldi M., *The evaluation of the use of a device for producing metal elements applied in civil engineering*, Proc. of 23rd International Conference on Metallurgy and Materials METAL 2014 May 21st–23rd 2014, Brno 2014, 1882-1888.

[11] Scendo M., Radek N., Trela J., *Influence of laser treatment on the corrosive resistance of Wc−−Cu coating produced by electrospark deposition*, International Journals of Electrochemical Science, **8**, 2013, 9264-9277.
[12] Angelini E., De Benedetti B., Rosalbino F., *Microstructural evolution and localized corrosion resistance of an aged superduplex stainless steel*, Corrosion Science, **46** (6), 2004, 1351-1367.

TECHNICAL TRANSACTIONS | CZASOPISMO TECHNICZNE
MECHANICS | MECHANIKA
3-M/2016

RENATA STASIAK-BETLEJEWSKA*

INNOVATIVE WOODEN ENERGY EFFICIENT HOUSES CONSTRUCTIONS

INNOWACYJNE KONSTRUKCJE DREWNIANYCH DOMÓW ENERGOOSZCZĘDNYCH

Abstract

The article presents innovative solutions for wooden energy-efficient constructions which are characterized by low energy power consumption and a high level of performance that ensures a high level of the functional quality and modern design of building interiors. One of the most commonly used modern wooden construction technology is a wooden prefabrication technology whose advantages determine a high level of building energy efficiency. The article presents achievements of selected manufacturers of wooden energy-efficient houses who use prefabrication technology in the context of building construction and interior innovation.

Keywords: the energy efficient buildings, *innovativeness*, *patent*, *wooden prefabricated components*

Streszczenie

W artykule przedstawiono innowacyjne rozwiązania w zakresie drewnianego budownictwa energooszczędnego, które charakteryzuje się niskim zużyciem energii, wysokim poziomem wykonania, zapewniającym wysoki poziom jakości użytkowej i nowoczesne wzornictwo. Jedną z najczęściej wykorzystywanych technologii we współczesnym budownictwie drewnianym jest technologia prefabrykatu drewnianego, którego zalety decydują o wysokim poziomie energooszczędności. W artykule przedstawiono analizę technologii stosowanych przez wybranych producentów drewnianych domów energooszczędnych w kontekście innowacyjności bryły oraz wnętrza budynków.

Słowa kluczowe: budynki energooszczędne, *innowacyjność*, *patent*, *prefabrykaty drewniane*

DOI: 10.4467/2353737XCT.16.119.5730

* Ph.D. Eng. Renata Stasiak-Betlejewska, Institute of Production Engineering, Faculty of Management, The Częstochowa University of Technology.

1. Introduction

The European Directive 2010/31/EU on the energy performance of buildings introduced an obligation on the clean and energy efficient building materials and technologies use. The analysis of the energy buildings standards optimizing methods, carried out by the National Agency for Energy Conservation in Poland (in Polish: KAPE), which took into account economic, environmental and external costs criteria, has confirmed that the increase in energy performance requirements for buildings contributes to the appearance of well--known building materials with improved insulating properties on the market. Materials used for building must provide effective thermal protection using a smaller thickness of the insulation layer [2, pp. 515-520].

An energy efficient building is considered to consume 25–50% less energy than a conventional building. The energy efficiency of a building is not legally defined. Currently in Poland, the demand for heating residential buildings constructed in accordance with building regulations is approximately 65–125 kWh/m^2 of the usable area per year. A building should be energy efficient for heating, ventilation and hot water and to consume no more than 50–70 kWh/m^2 per year [4]. In Western Europe, the technology of energy efficient buildings production with a long-term use of significant house savings in electricity and exploitation of natural environment has a growing popularity. The design process of energy efficient buildings concerns at least construction and materials solutions optimization, taking into account the analysis of building life cycle costs. In accordance with the newest energy efficient constructions, architects have to meet the requirements of customers accustomed to traditional architecture including solutions that provide cost-effective operation and low power consumption [5].

One of the conditions for building energy efficiency is economical operation condition and lower than the average construction costs. These features combine new technological solutions used by contemporary Polish construction companies that experiment with new materials and technologies, so that the buildings can achieve a high level of energy efficiency. However high costs of energy-efficient buildings make consumers/investors look for alternatives, which often provide modern, energy efficient or even passive technologies. Modern technologies of buildings address the following aspects: providing low costs of construction investments, short construction time and cost-effective operation of buildings. Considering these aspects, innovative construction projects involve the use of technologies that ensures: a short construction time, thermal insulation that affect operating costs of the building. Wooden frame construction technology plays significant role in the development of energy efficient constructions. In Germany, there is an increasing demand for energy efficient prefabricated wooden buildings, which results from European energy saving regulations and the popularity of wooden houses [6]. According to the Central Statistical Office, in Poland, in the year 2013, 51 658 new residential buildings in the individual construction were noted, primarily single-family houses built with the application of wooden frame technology (222 buildings), together with 3364 non-individual buildings (1 in the wooden frame technology). According to the Centre for Wooden Construction, there are 750 companies in Poland that deal with the construction of wooden frame constructions and perform each year about 4–5 thousands of buildings in different wooden technologies [1].

2. Contemporary trends in energy efficient wooden constructions – a short review

One of the most interesting construction solutions related to energy efficient constructions is the construction of a building with the wooden dome of Timothy Oulton, which is unique in terms of architecture and a technology. The construction is a result of meticulous planning and design. The space in the dome is made for the interaction between humans in very modern and comfortable conditions. The whole architecture has a minimal impact on the surrounding environment. The dome of the presented house is constructed of prefabricated elements created by Oulton's company and is completely self-supporting, without any columns and pillars. The entire structure has been created by means of wood FSC certified panels and it is built according to the German passive house standard, which is the highest in the world [7]. All the components used in construction of the dome well, keeping extremely tight and well-insulated structure. All the mentioned requirements have been met by architects from the French Studio Djuric Tardio Architects who built a house in a French district with the surface of 262 m^2. Designers experiment with wood and prefabricated structures. They developed a building system that allows for minimizing environmental costs and construction time, but also gives the result of a permanent home and relatively low operating costs. The design of the house consisted of prefabricated elements of the larch Finnish wood. All the components included warming wool and cellulose external facade panels. All technical and interior arrangements were prepared in accordance with energy saving construction trends.

3. Innovative solutions in Polish wooden energy saving constructions – research results

According to CEED Institute report data (Central and Eastern Europe Development Institute), Poland's economy has the potential to become regional leader in terms of innovation. New trends, fashion and customer expectations are forcing manufacturers of building materials, architects and designers to seek innovative solutions. There are two determinants of the construction industry development: energy efficiency and construction ecology. The construction has already been assimilated with solutions-based solar energy [3]. The use of renewable energy sources applied in connection with energy saving sources is concerned to be innovative solution in the construction industry. An analysis of the innovativeness level of Polish enterprises confirmed 95% of domestic applications with patented solutions that include approximately 4500 of patented solutions submitted by construction enterprises in 2010–2015 (e.g. Fakro).

3.1. The characteristics of selected leading construction technologies in Poland

Wooden prefabrication is one of the most popular construction technology in Poland and it enables the realization of a house construction in a few weeks. MultiComfort is one of the Polish enterprises dealing with the production of prefabricated houses that operates in Poland, Germany, Sweden, Switzerland, Latvia, Cyprus and Italy. It is the first company

that has built in Poland a certified passive prefabricated house. Prefabricated houses are manufactured with kiln-dried wood (a wood construction of KVH and BSH type) in German and Austrian sawmills. Properly trimmed elements are arranged in accordance with a detailed design and put together. The stiffness of wooden structure is achieved by building board MFP wood that is nailed to the two sides of the timber frame. The space between posts is filled with mineral wool. On the outer side of the wall external insulation is mounted, which is usually polystyrene, covered in the factory of prefabricated houses with an adhesive and a mesh. The inside wall is attached by a vapour barrier layer and a GKF plate. There are also prefabricated walls, ceilings and roof constructions. Partition walls are covered on both sides with MFP and GKF plates. The accuracy of individual components and advanced prefabrication shortens the construction time. Prefabricated houses are very well insulated. There is a 15 cm thick thermal insulation layer inside the wooden frame and at least 12 cm thick layer on the polystyrene foam facade with the addition of neopor. A U-value below 0.14 W/m^{2}K provides wall insulation. In addition, warm mounting windows (e.g. in the insulation layer), using expansion tapes and flange dealings, eliminates thermal bridges and affects the energy efficiency of a building. An efficient thermal insulation layer is a double layer of mineral wool of minimum 25 cm in thickness. The slab is a plate perimeter with a very low coefficient λ (0.032 W/m·K). Sections of the exterior wall contain: GKF plate, vapour barrier foil (wood construction and insulating mineral wool are protected against moisture), MFP plate (protects a structure against the ingress of moisture, stiffens the structure, strengthens the wall, so that there are no problems with nailing and screwing pins), wooden supporting structure (allows filling the entire space between the joists with insulation material mineral wool), mineral wool (a layer of thermal and acoustic insulation), MFP plate (provides a foundation for the second insulation layer of polystyrene or, optionally, mineral wool and stiffens the structure), glue for external insulation, external insulation (second insulation layer which improves insulating properties), reinforced plaster base grid. Prefabricated wooden houses should be very tight, just as houses constructed in each technology. The tightness of the house is mandatory and must be examined by performing a special leak test – the Blower Door Test. For an energy-efficient house, the leak test should not exceed n_{50} = 1.0. The technology of prefabricated houses applied by MultiComfort obtains test scores on the level of n_{50} = 0.36. It confirms the accuracy of all types of joints in the building: window frames-wall, wall-foundation, wall-like roof structure.

An innovative patented technology for the production of external panel wooden wall elements, absorbing solar energy that can be stored was elaborated on by another Polish construction enterprise Ekoinbud from Gdańsk in Poland. In 2012 it obtained a patent on the performance of wooden structure walls including the assembled system of PE pipes with polyethylene. Pipes receive heat from the walls in the summer, when the sun heats them. Thermal energy is accumulated under the ground, in the land on which the building was mounted. In the winter the stored thermal energy goes back to the walls, providing heating for the house. Ekoinbud production line has the capacity to produce 80 units a year at one shift. Due to the system of a three-shift operation, the production increases to approximately 200 houses a year. The construction of each part of the house – walls, ceilings or roof takes place only in a factory.

3.2. Basic features of the selected energy saving construction

The wooden energy efficient construction is possible thanks to the relatively light weight and modular structure of wooden houses – reconstruction of the attic, construction of an additional floor, removing walls or only modernization that can be carried out simply and practically. The wooden structures offered by Tadeks Fertig Haus enterprise shorten the life of the expansion. Heavy prefabricated wooden elements are created in accordance with the norms and principles of the Polish construction law. However, it is supported by an additional insulation (which is offered by the company Tadeks Fertig Haus as a standard). Energy efficient houses which are based on thoughtful design need 2–3 times less energy than houses built in the traditional way, while providing its users with comfortable living conditions. It is due to the fact that the prefabricated wall of the house is filled in its entirety with an insulator of high thermal parameters. Thermal insulation baffles, determined by the external heat transfer coefficient of partition U [W/m^{2}K], determine how much heat passes through 1 m² within one second at the temperature difference on both sides equal to 1° Celsius. The heat demand of buildings is expressed by the seasonal coefficient of heat demand (EA). In houses that meet the applicable standards of standard EA, it equals approximately 120 kWh/m^{2}a, while the seasonal heat demand for energy-efficient houses ranges between 15–70 kWh/m^2 per year. The analyzed company provides customers with clean and energy efficient wooden houses that combine traditional architectural features with modern technological achievements in the field of construction, which was confirmed by the Technological Certificate DIN-1052 obtained in 1998 and awarded by the MPA LGA Institute in Nuremberg/Germany. While respecting the rigorous rules of technical design and the use of high quality materials, including selected wood KVH and BSH constructions, wooden energy efficient houses provided by the analyzed enterprise are products that meet all European standards. Thermal parameters (heat transfer coefficient $U = 0.15 – 0.07$ W/m^{2}K for the envelope) are synonymous with low energy requirements of our prefabricated houses ($E = 70 – 15$ kWh/m^{2}K).

The standard thickness of external walls in the technology applied by Tadeks Fertig Haus maintains $U = 0.13$ W/m^{2}K, which is only 32.5 cm, where a wall made in the traditional way is acceptable for about 45.0 cm (which greatly increases the cost of house construction and minimizes internal space). The components of the external wall structure – prefabricated structure components include: the insulation wool of ISOVER SUPER-MATA (150 mm λ – 0,033), building board OSB or MFP ECO (12 mm), plasterboard or gypsum fibber (12,5 mm), wooden construction KVH and BSH (60 × 140 mm), vapour barrier stabilized ISOVER STOPAIR 0,60 g/(m^2 (24 h), construction board OSB or MFP ECO (12 mm), graphite styrofoam EPS (100 mm λ – 0,033), grid plaster facade, silicate plaster CERESIT/CAPAROL and plaster facade.

4. Conclusion – the newest technological achievement in the building energy efficiency

The analysis of innovative technologies applied in energy efficient buildings shown several different technical and design solutions. There are other technologies that can affects the final energy efficiency level of the wooden construction.

Tadeks Fertig Haus, as one of the few companies in Poland, applies one of the most modern technology – SIPs (Structural Insulated Panels). The SIP technology consists of three-part panels including two portions arranged outside the OSB or MFP and a polyurethane foam layer forming a core wall. Production materials are carefully selected and the whole thing is based on a prefabricated wooden structure that is made directly in our factory. Ecological character and energy savings are the reasons why the SIP technology is becoming increasingly popular and is gaining wider groups of supporters. The properties and technology of structural panel system provide high resistance to fire or water and the advanced technology and the "dry" method of production and assembly eliminate all kinds of insects, rodents and fungi. The main advantages of SIPs are the following: low production, construction and maintenance costs, short lead time, high level of noise suppression, several times higher rate (about 66%) of energy efficiency than in houses built in the old-fashioned way. Walls in the SIP technology can support a load of 3 tons in 30 cm of construction. The SIP technology is recommended in order to obtain high efficiency, high structural resistance and reduce the costs of heating, cooling and ventilation.

Acknowledgements: *I wish to thank Tadeks Fertig Haus for the information materials on the used technology.*

References

[1] Bekas J., *Ile domów drewnianych buduje 750 firm?*, Gazeta Przemysłu Drzewnego, **4** (207), 2014, 35.

[2] Borkowski S., Stasiak-Betlejewska R., *Analysis of Wooden House Construction Costs in the Chosen Company*, Proc. of the 4th International Conference on Contemporary Problems in Architecture and Construction. Sustainable Building Industry of the Future, September 24–27, 2012, Czestochowa, Poland. Vol. 2., Sekcja Wydawnictw Wydziału Zarządzania Politechniki Częstochowskiej, Częstochowa, Politechnika Częstochowska, 2012, 515-520.

[3] *Report Poland's 10 years in the EU*, CEED Institute, Warsaw 2014.

[4] Kasperkiewicz K., *Wybrane zagadnienia oceny i projektowania energooszczędnych budynków mieszkalnych*, Prace Instytutu Techniki Budowlanej, **2** (134), 2005, 23-37.

[5] Płaziak M., *Technologia tanich domów energooszczędnych jako odpowiedź na kryzys w budownictwie mieszkaniowym*, Przedsiębiorczość–Edukacja, **9**, 2013, 214-226.

[6] Stasiak-Betlejewska R., *Innovative Level in the Wooden House Constructions*, [in:] *Majska konferencija o strategijskom menadzmentu*, Studentski simpozijum o strategijskom menadzmentu. Zbornik izvoda radova, 25–27 May 2012, Bor, Serbia, Univerzitet u Beogradu, Tehnicki fakultet u Boru, Odsek za menadzment, 2012, 32-39.

[7] *Timothy Oulton i jego kopuła z prefabrykatów drewnianych*, http://okraglemiasteczko.net/blog/timothy-oulton-i-jego-kopula-z-prefabrykatow-drewnianych/ [date of acc. 26.06.2016].

TECHNICAL TRANSACTIONS | **CZASOPISMO TECHNICZNE**
MECHANICS | MECHANIKA
3-M/2016

ANNA KIEŁBUS*, GRZEGORZ GAWŁOWSKI*

QUALITY TOOLS OF THE INNOVATIVE PROJECT IN THE PLANNING PHASE ANALYSED ON A CHOSEN EXAMPLE

NARZĘDZIA JAKOŚCI W FAZIE PLANOWANIA INNOWACYJNEGO PROJEKTU NA WYBRANYM PRZYKŁADZIE

Abstract

Project planning is an especially important and difficult part of a project preparation. Errors made at these stages usually cause accumulation of difficulties in the implementation phase, causing for example the need to introduce a number of changes in the schedule or the budget, and may even lead to the failure of the project. This article attempts to outline the characteristics of a selected quality management tool used in the project planning phase. The Product Flow Diagram was presented as one of the elements of product-based planning on the example of a project on developing a prototype system for identifying people.

Keywords: quality of the project, *Product Flow Diagram*, *CTQ Tree*

Streszczenie

Planowanie projektu to szczególnie ważna i trudna część przygotowania przedsięwzięcia. Błędy popełnione w tych działaniach zwykle powodują spiętrzenie trudności w fazie realizacji, wywołując np. konieczność wprowadzania licznych zmian w harmonogramie czy budżecie, a nawet mogą prowadzić do porażki projektu. W artykule podjęto próbę charakterystyki wybranego narzędzia zarządzania jakością projektu stosowanego w fazie planowania. Na przykładzie projektu dotyczącego opracowania prototypu systemu identyfikacji osób zaprezentowano Diagram Następstwa Produktów jako jeden z elementów planowania opartego na produktach.

Słowa kluczowe: zarządzanie jakością projektu, *Diagram Następstwa Produktów*, *CTQ Tree*

DOI: 10.4467/2353737XCT.16.120.5731

* Ph.D. Eng. Anna Kiełbus, M.Sc. Eng. Grzegorz Gawłowski, Production Engineering Institute, Faculty of Mechanical Engineering, Cracow University of Technology.

1. Introduction – Project Management Problems

Planning is one of the most important stages in the process of project management, before the start of implementation phase. It is associated with a thorough analysis of the size, objectives, resources, time, quality and budget of the project. Each of these elements is a potential source of problems, which should be eliminated as soon as possible and without additional funding. In order to prevent the occurrence of unplanned events already in the planning phase, the project team takes measures to identify potential risks. It also proposes a scenario of solutions to problems, so that in the event of their occurrence they can be quickly solved. In the phase of project planning, the essential threats are: the improper assignment of roles and responsibilities in the project team, improper communication and ineffective project planning. This last factor is associated with the invalid defining of design constraints and quality from the point of view of the user and the manufacturer [1].

Problems related to project planning are compounded in the case of innovative projects, i.e. projects with a high or even very high degree of novelty (or originality) [2]. The risk is included in the definition of each project, but in the case of innovative projects the degree is much higher. This is due to the nature and construction of the components of risk in enterprise innovation, such as potential events that may occur, the probability of their occurrence and their consequences.

In order to prevent the risks associated with improper quality planning at the project planning stage, it is necessary not only to have a correct choice of quality planning methods, but also appropriate definition of the process steps of an innovative project with a focus on the quality of product design [3, 4]. The recognition of the right moment for quality planning and quality monitoring of a project by means of the feedback loop effect on minimizing potential problems is raised in the article.

To sum up, the quality planning of a project can generally be treated as taking into account, from the very beginning of the project, the issue of the required quality of the final product of the project. Selected elements of quality management of the project, especially quality planning of the project, will be presented on the example of a project on building a prototype system for identifying people.

2. Characterization of the Innovative Project – the global identity identification prototype system based on frontal sinuses

A front sinus is a pneumatic structure of the frontal bone of the mouth of the hole fronto--nasal of the nasal canal. Each person has an individual shape of sinuses which proves the uniqueness of biometrics. The examination of polimorphic sinus based on the computer analysis of X-ray images helps identify people on the basis of frontal sinuses [5]. The research conducted at the Institute of Applied Informatics at the Cracow University of Technology and the Jagiellonian University shows that the method for identifying people involves the examination of the polimorphic line sinus of a man by means of X-rays and then develops an algorithm of computer image analysis to determine the area sinus [6]. The analysis made a scheme alphanumeric description of frontal sinuses for identification of people.

3. PFD, CTQ Tree and DFMEA dedicated to the global identity identification prototype system

The purpose of quality planning is to provide a solid basis for a common understanding of what the project intends to achieve and above all to guarantee the customer that the product will meet the project's requirements. Proper quality planning can apply methods and techniques aimed at ensuring quality through quality awareness and early defining of problems and possible solutions. In order to illustrate quality planning at the project planning stage we used an example of a prototype system for identifying people based on facial analysis by means of automated image analysis algorithms. Items related to project quality planning can be traced in a classic project management, but also in the PRINCE2 methodology.

At the stage of product-based planning, PRINCE2 recommends the establishment of a Product Structure Diagram (DSP) [7]. It provides information that tangible and intangible elements are necessary to produce the product design. After building the Structure Diagram Product, the next step is to proceed to a detailed description of each element of the diagram. Enter the ID, name, purpose, composition, origin, appearance, people assigned to the manufacture of the product and the criteria, methods of control and tolerance for quality. Already at this stage there is an initial review of the characteristics of the elements that the final product should have. In the case of a prototype system for identifying people, distinguished DSP for products belong to the group: the system (software, hardware, products integrating) and the core group of product integration (managers). Drew up: the Product Description was chosen on the basis of multi-criteria, a comparison of the criteria validity and creation of linguistic matrix of pairwise comparison, showing the criteria and the extent to which they are more important than others. The importance of each criterion α_i according to the rule of Saaty was established [8]:

$$\alpha_i = \frac{\sqrt[n]{\prod_{j=1}^{n} a_{ij}}}{\sum_{k=1}^{n} \sqrt[n]{\prod_{j=1}^{n} a_{kj}}} \tag{1}$$

and then each criterion was assigned a utility function. Aggregation was done according to the method of Sewastian [9], according to three different methods: Maximum pessimism criterion (DD_1), multiplicative criterion (DD_2) and Additive criterion (DD_3):

$$DD_1 = \min(\mu_1(x_1)^{\alpha_1}, \mu_2(x_2)^{\alpha_2}, \ldots) \tag{2}$$

$$DD_2 = \prod_{i=1}^{n} \mu_i(x_i)^{\alpha_i} = \mu_1(x_1)^{\alpha_1} \cdot \mu_2(x_2)^{\alpha_2} \cdot \ldots \tag{3}$$

$$DD_3 = \prod_{i=1}^{n} \alpha_i \mu_i(x_i) = \alpha_1 \mu_1(x_1) + \alpha_2 \mu_2(x_2) + \ldots \tag{4}$$

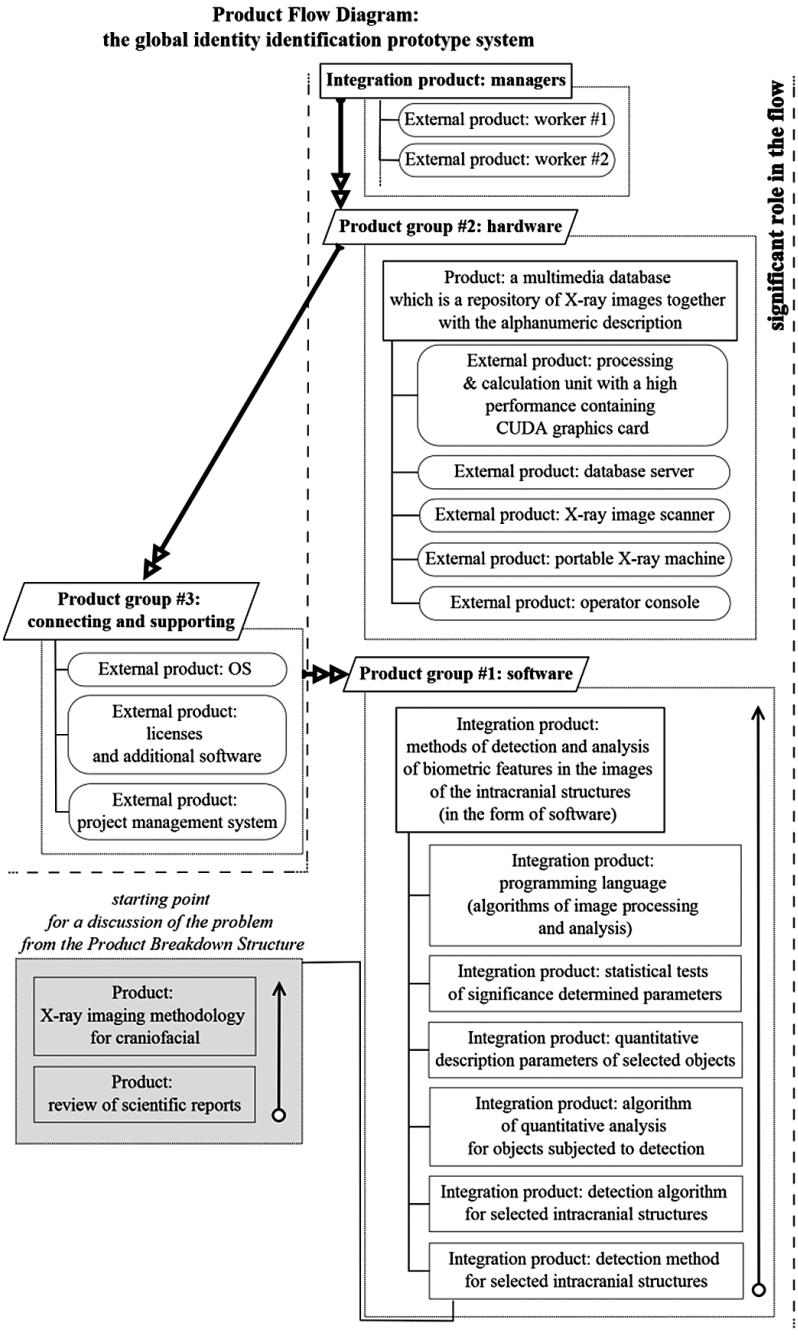

Fig. 1. Product Flow Diagram for the global identity identification prototype system (source: own calculations based on data from [7, 10])

where:

x_i – quality parameters,
$\mu_i(x_i)$ – total utility (functions),
α_i – relative importance of criteria (coef ficients),
i – 0 ... n, n = 7.

The final stage of product-based planning is the construction of Diagram Aftermath Products [7]. It shows the sequence of production and interdependencies of the products listed in the Product Structure Diagram. In the discussed system, a full DNP identification of people was presented in the diagram in Fig. 1.

Knowing the needs and requirements of the customer concerning the product project, potential hazards that may occur in their environment must be identified. We must prevent the effects of possible defects that may occur in the designing stage. Expectations are fulfilled by the DFMEA method (Design Failure Mode and Effects Analysis) – analysis of the types

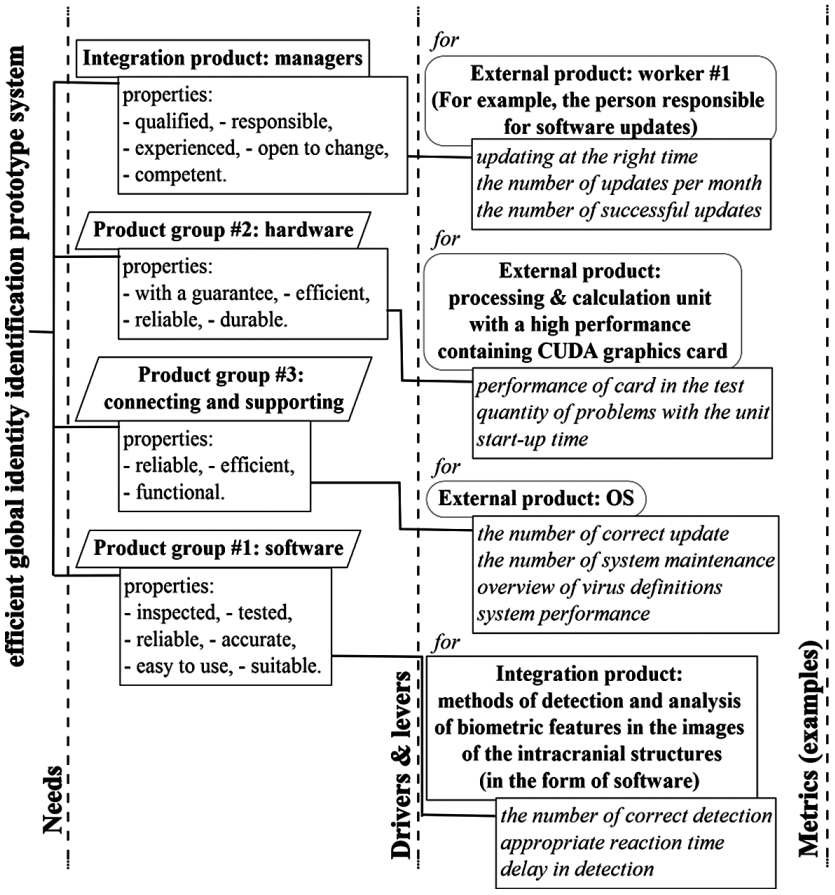

Fig. 2. Simplified CTQ tree dedicated to the efficiency of the system
(source: own calculations based on data from [7, 10])

and effects of possible errors [11]. The presented need for an efficient system to identify in a CTQ tree (Fig. 2) automatically becomes the function of the system, which must be examined in the DFMEA.

4. Conclusions

Planning is a type of immune mechanism against all kinds of wrong decisions. It requires solving some important problems at a time when there is possibility of a choice between different options of these solutions [12]. Abraham Lincoln aptly captured this when he said: "If I have six hours to chop a tree, I will use the first four for sharpening the axe". This means that good preparation for work makes it easier and more resistant to failure. In connection with project planning itself, we should answer at least two questions: what should we do? (Requirements) and how should we do it? (Design and specification). The course of planning depends on the competence of individuals, as they have a significant impact on the requirements, design and project budget, which translates into the success or failure of the project.

The article presents product planning based on the example of an innovative system for identifying people as a way/methodology which leads to project quality management, maximizing the quality of products and the success of the project. That alone, trying to develop a methodology for identification of people, to implement and create a prototype device and introduce this innovative product to the market is a tool of entrepreneurship by means of which the change makes the opportunity to take a company to a new action of economic or provision of new services. Yet biometric systems is still a growing industry not only in the Polish market, but in the whole world [13]. Since the first identification solutions were made, revenue from their sale continues to grow. Thus, the challenges of biometrics in the field of identification of people is one of the opportunities for entrepreneurs and innovators.

References

[1] Ahern T., Leavy B., Byrne P.J., *Knowledge formation and learning in the management of projects: A problem solving perspective*, International Journal of Project Management, **32** (8), 2014, 1423-1431.

[2] Trocki M., Grucza B., *Zarządzanie projektem europejskim*, Warszawa 2007 [in Polish].

[3] Marsh G., *Bombardier throws down the gauntlet with CSeries airliner*, Reinforced Plastics, **55** (6), 2011, 22-26.

[4] Cooper R.G., *How Companies are Reinventing Their Idea-To-Launch Methodologies*, Research Technology Management, **52** (2), 2009, 47-57.

[5] Karpisz D., *Komputerowa analiza obrazu RTG zatok czołowych jako podstawa identyfikacji osób*, PhD thesis, Kraków 2009 [in Polish].

[6] Karpisz D., Kowalski P., Tabor Z., Wojnar L., *An automatic recognition of the frontal sinus in X-ray images of skull*, IEEE Transactions on Biomedical Engineering, **56** (2), 2009, 361-368.

[7] Kiełbus A., Gawłowski G., *Planowanie oparte na produktach na przykładzie prototypu systemu identyfikacji tożsamości*, Proc. of XVIII Conf. „Innowacje w Zarządzaniu i Inżynierii Produkcji" 1st–3rd March 2015, Zakopane, vol.1, 568-578 [in Polish].
[8] Bryndza J., Dudycz H., *Zastosowanie macierzy graficznej w metodzie analizy hierarchicznej problemu*, Prace Naukowe Akademii Ekonomicznej, nr 1051, Wrocław 2004 [in Polish].
[9] Dymowa L., Kaczmarek K., Sewastianow P., *Problemy metodologiczne optymalizacji portfela i nowoczesne podejście do ich rozwiązywania*, Zeszyty Naukowe Uniwersytetu Szczecińskiego „Finanse. Rynki finansowe. Ubezpieczenia", **6** (1), 2007, 199208 [in Polish].
[10] Jones E., *Quality Management for Organizations Using Lean Six Sigma Techniques*, CRC Press, New York 2014.
[11] Fabiś-Domagała J., *Application of FMEA matrix for prediction of potential failures in hydraulic cylinder*, Technical Transactions, 1-M/2013, 97-104.
[12] Berkun S., *Sztuka zarządzania projektami*, Wyd. Helion, Gliwice, 2006 [in Polish].
[13] Kiełbus A., Furyk K., *Nowe technologie i zastosowania w biometrii − analiza rynku*, Proc. of XVII Conf. „Innowacje w Zarządzaniu i Inżynierii Produkcji" 23rd–25th February 2014, Zakopane, vol. 2, 147-158 [in Polish].

TECHNICAL TRANSACTIONS | CZASOPISMO TECHNICZNE
MECHANICS | MECHANIKA
3-M/2016

NORBERT RADEK*, AGNIESZKA SZCZOTOK**

HETEROGENOUS SURFACES FORMED BY HIGH ENERGY TECHNIQUES

POWIERZCHNIE NIEJEDNORODNE KSZTAŁTOWANE TECHNOLOGIAMI WYSOKOENERGETYCZNYMI

A b s t r a c t

The paper concerns testing Cu−Mo coatings deposited over carbon steel C45, which were then eroded with a laser beam. The analysis involved the measurement of macrogeometry and microhardness of selected areas after laser treatment. The coatings were deposited by means of an ELFA-541 device and they were laser treated with a Nd:YAG laser, the parameters being variable.

Keywords: electro-spark deposition, *laser treatment*, *coating*

S t r e s z c z e n i e

W artykule przedstawiono wyniki badań powłok Cu−Mo nałożonych na stal węglową C45, które zostały poddane procesowi erodowania wiązką laserową. Wykonano pomiary makrogeometrii i mikrotwardości na wybranych obszarach po obróbce laserowej. Powłoki nanoszono za pomocą urządzenia ELFA-541, które zostały poddawane obróbce laserem Nd:YAG przy różnych parametrach.

Słowa kluczowe: obróbka elektroiskrowa, *obróbka laserowa*, *powłoka*

DOI: 10.4467/2353737XCT.16.121.5732

* D.Sc. Ph.D. Eng. Norbert Radek, Assoc. Prof., Centre for Laser Technologies of Metals, Faculty of Mechatronics and Machine Design, Kielce University of Technology.

** Ph.D. Eng. Agnieszka Szczotok, Institute of Materials Science, Faculty of Materials Science and Metallurgy, Silesian University of Technology.

1. Introduction

During tribological investigations it was found that employed heterogeneous surfaces models into boundary interaction of solid surfaces make significant improvement [1–4]. Surfaces described as heterogeneous consist of areas which differ one from another in geometrical, physicomechanical or physicochemical properties. The heterogeneity of surfaces is frequently due to application of more than one technology, and can be constituted by:

- shaped surface features such as grooves, pits or channels resulting from milling, eroding, etching, laser-beam forming, etc.;
- areas with different physicochemical and physicomechanical properties, e.g. areas with diversified hardness and mechanical strength accomplished by local surfacing or selective surface hardening (e.g. electron-beam machining, laser-beam forming or thermochemical treatment);
- areas with diversified surface microgeometry, e.g. areas eroded at the points of focus (laser treatment or electro-spark deposition), or areas with formed surface microgeometry, for instance, in terms of desired microroughness directivity or load capacity (laser and ESD technologies).

Heterogeneous surfaces can be measured by different methods [5], the laser treatment of electro-spark deposited coatings being one of them [6]. Electro-Spark Deposition (ESD) is one of the methods that require concentrated energy flux. The method which developed into a number of varieties allows us not only to produce coatings but also modify their surface microgeometry [7, 8]. Steels with different properties are an alternative to the use of ESD technologies [9].

The electro-spark deposition coating is characterized by a non etching structure. It remains white after etching. The surface layer is constituted in the environment of local high temperature and high pressure. It has been suggested that ESD coating quality can be improved by applying laser technologies. A laser beam used for surface smoothing, surface geometry formation and surface sealing is able to reduce surface roughness and change the profile form of the irregularities. For smoothing purposes, it is recommended that power density should be small and laser beam diameters big so that the melting process affects the coating at a small depth. The aim of laser concentration is to reduce coating porosity and dispose of scratches, cracks and delaminating, and, in consequence, to improve coating density. The predicted advantages of laser treatment of ESD coatings include: better smoothness, smaller porosity, better adhesion to substrate material, better resistance to wear and seizure, more compressive stresses resulting in better resistance to fatigue, better resistance to corrosion, shaping of surface.

2. Experimental

Two investigation stages were carried out. First of all, Cu-Mo coatings were electro-spark deposited on C45 steel coupons and after that they were modified by a Nd:YAG laser beam. The copper inside coatings is a fundamental material to the creation of low-friction surface layers. It is itself also a compensator of internal stresses. This material is characterized by

good thermal conductivity, which can be very helpful in highly loaded contacts – heat can be taken away into material core from the friction zone. The other selected element was molybdenum as it significantly strengthens the surface content. Mo is also helpful in the creation of hard phase compounds, e.g.: MoC. In the practical meaning, this compound will improve durability of tools of kinematics pairs. The electro-spark deposition of Cu and Mo wires with a diameter of 1 mm was performed by means of an ELFA-541, a modernized device made by a Bulgarian manufacturer. The subsequent laser treatment was performed with the aid of a BLS 720 laser system employing a Nd:YAG type laser operating in the pulse mode.

The parameters of the electro-spark deposition established during the experiment include: current intensity I = 16 A (for Cu I = 8 A); table shift rate V = 0.5 mm/s; rotational speed of the head with electrode n = 4200 rev/min; number of coating passes L = 2 (for Cu L = 1); capacity of the condenser system C = 0.47 μF; pulse duration T_i = 8 μs; interpulse period T_p = 32 μs; frequency f = 25 kHz.

The main aim of the investigations was:
- observing the surface state by means of a stereoscopic microscope,
- analyzing the surface macrogeometry,
- measuring the microhardness with the Vickers method.

3. Results and discussion

The heterogeneous Cu–Mo coatings structure after electro-spark deposition on steel coupons and erosion by laser beam were investigated. The observation was done by an OLYMPUS SZ-STU2 stereoscopic microscope.

The erosion was performed with the point pulsed-laser technique by means of a Nd:YAG type laser under the following conditions:
- laser spot diameter, d = 0.7 mm,
- laser power, P = 10; 20; 30; 40; 50; 100 and 150 W,
- beam shift rate, v = 1200 mm/min,
- nozzle-sample distance, h = 1 mm,
- pulse duration, t_i = 0.8; 1.2; 1.48; 1.8; 5.5 and 8 ms,
- frequency, f = 8 Hz.

The investigations of the effects of the laser erosion involved measuring the diameters and depths of the cavities obtained at different laser powers. The results of the measurement performed with a PG-2/200 form surfer are presented in the form of graphs in Fig. 1 and 2. It was noticed that higher laser beam power gives a greater diameter and depth of the cavities. The cavity depth produced at 150 W is an exception. The value is smaller than the one obtained at 100 W (Fig. 1). This might have been due to a considerable pulse duration (t_i = 8 ms), the laser power being 150 W. However, if P = 100 W, the pulse duration t_i was 5.5 ms. In the case of lasers operating in the pulse mode, the power is averaged in time; thus, if pulse durations are long, the laser beam is less effective.

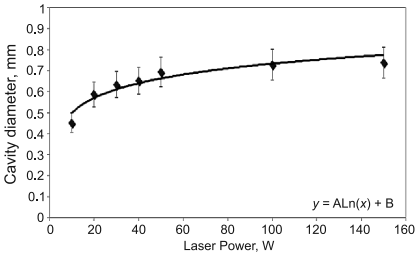

Fig. 1. Cavity diameter as a function of laser power

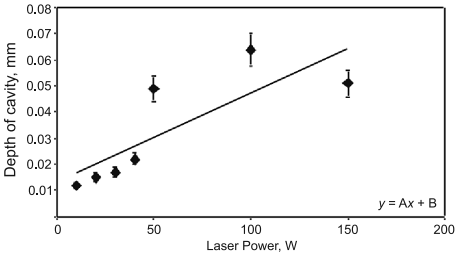

Fig. 2. Cavity depth as a function of laser power

A 3D macrogeometry of the developed heterogeneous surface eroded by the laser craters for the used specimens with A-A cross section built in 2-D crater is shown in Fig. 3a and 3b.

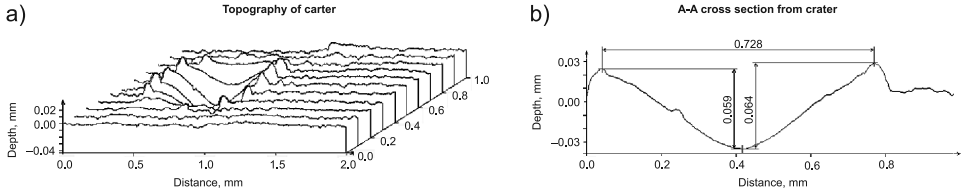

Fig. 3. Macrogeometry and cross section of a crater eroded by laser: a) 3D crater topography, b) A-A cross section on crater

As can be concluded from these graphs, crater edges are sharp and are protruding 0.03 mm above the average height, just treated by ESD surface, which is within the range of tolerances for the designed clearance fit. The average size of the crater shown on Fig. 1 produced by laser power of 100 W is about 0.7 mm in diameter and the total depth of about 0.06 mm. The crater is going below the so-called "ground zero level" by down to 0.030 mm. For instance, the crater displayed in Fig. 2, produced by laser power of 20 W, is about 0.05 mm in diameter and has a depth of 0.015 mm. The produced crater profile (picks and valleys) and also order of craters location, depending on the required or desired surface performance, could be controlled and adjusted to the acceptable level.

At the next stage, the Vickers microhardness test was conducted using a load of 0.98 N. The measurement was carried out on Cu-Mo coatings laser-eroded at 20 W. The distribution of microhardness is shown in Fig. 4.

It was established that there was an increase in microhardness at the points of laser machining, the increase being strictly related to the changes in the coating structure, and therefore, to the method of laser treatment. The surface hardening at the points of laser interaction and in the heat-affected zone (HAZ) follows the phase changes occurring in the material first heated and then immediately cooled. The average microhardness of the C45 steel substrate was 300 HV, while that of the ESD coatings amounted to about 430 HV. The laser treatment of the ESD coatings caused an increase in microhardness to approximately 850–880 HV. In the heat-affected zone, the microhardness fluctuated around 580–630 HV.

The laser beam surface forming resulted in changes in the microhardness of electro-spark deposited Cu-Mo coatings.

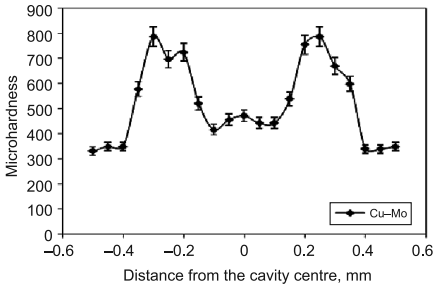

Fig. 4. Distribution of microhardness on the surface of a laser-treated Cu–Mo coating

It was established that there was an increase in microhardness at the points of laser machining, the increase being strictly related to the changes in the coating structure, and therefore, to the method of laser treatment. The surface hardening at the points of laser interaction and in the heat-affected zone (HAZ) follows the phase changes occurring in the material first heated and then immediately cooled. The average microhardness of the C45 steel substrate was 300 HV, while that of the ESD coatings amounted to about 430 HV. The laser treatment of the ESD coatings caused an increase in microhardness to approximately 850–880 HV. In the heat-affected zone, the microhardness fluctuated around 580–630 HV. The laser beam surface forming resulted in changes in the microhardness of electro-spark deposited Cu–Mo coatings.

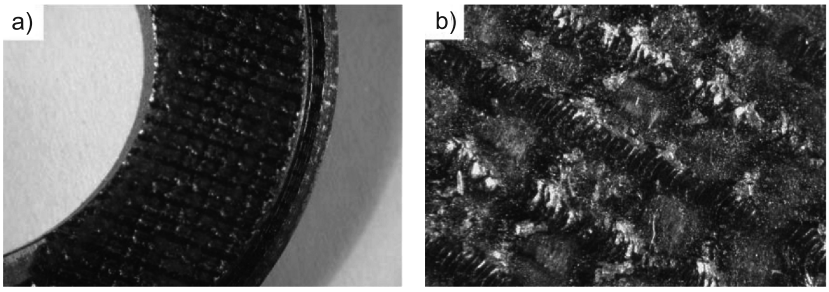

Fig. 5. Stereoscopic photographs of the laser-treated Cu-Mo surfaces: a) ×6 magnification, b) ×40 magnification

The next stage of the experiment involved analyzing the changes in the macrogeometry of Cu–Mo coatings. The laser treatment causing the formation of new surface geometry was performed with a Nd:YAG laser operating in the pulse mode, with the following process parameters: laser spot diameter, d = 1.5 mm, laser power, P = 30 W; beam shift rate, v = 250 mm/min, nozzle-sample distance, h = 1 mm, pulse duration, t_i = 0.8 ms, frequency, f = 8 Hz. Examples of the images obtained with a stereoscopic microscope for laser-treated Cu–Mo coatings are given in Fig. 5.

4. Summary

It is possible to diversify the surface of electro-spark deposited coatings, i.e. to obtain heterogeneous surfaces. The laser-affected areas are characterized by the occurrence of regular cavities, hardened areas and varied roughness.

Surface heterogeneity (i.e. the cavities) is desirable in sliding friction pairs. They may be used as reservoirs of lubricants as well as sources of hydrodynamic forces increasing the capacity of a sliding pair.

A concentrated laser beam can effectively modify the state of the surface layer, i.e. the functional properties of electro-spark coatings can be achieved.

References

[1] Antoszewski B., Evin E., Audy J., *Study of the effect of electro-spark coatings on friction in pin--on-disc testing*, J. Tribology-Transactions of the ASME, **3**, 2008, 253- 262.

[2] Antoszewski B., *Influence of laser surface texturing on scuffing resistance of sliding pairs*, Advanced Materials Research, **874**, 2014, 51-55.

[3] Gyk G., Etison I., *Testing piston rings with partial laser surface texturing for friction reduction*, Wear, **216**, 2006, 792-796.

[4] Wan Y., Xiong D.S., *The effect of laser surface texturing on frictional performance of face seal*, J. of Mater. Proc. Technol., **197**, 2008, 96-100.

[5] Radziszewski L., *The influence of the surface load exerted by a piezoelectric contact sensor on testing results: Part I, The displacement field in the solid*, Arch. of Acoustics, **28**, 2003, 71-91.

[6] Pietraszek J., Radek N., Bartkowiak K., *Advanced statistical refinement of surface layer's discretization in the case of electro-spark deposited carbide-ceramic coatings modified by a laser beam*, Solid State Phenom., **197**, 2013, 198-202.

[7] Radek N., Sladek A., Broncek J., Bilska I., Szczotok A., *Electrospark alloying of carbon steel with WC–Co–Al_2O_3: deposition technique and coating properties*, Advanced Materials Research, **874**, 2014, 101-106.

[8] Chang-bin T., Dao-xin L., Zhan W., Yang G., *Electro-spark alloying using graphite electrode on titanium alloy surface for biomedical applications*, Appl. Surf. Sci., **257**, 2011, 6364-6371.

[9] Jankech P., Fabian P., Broncek J., Shalapko J., *Influence of tempering on mechanical properties of induction bents below 540°C*, Acta Mechanica et Automatica, **10** (2), 2016, 81-86.

TECHNICAL TRANSACTIONS | **CZASOPISMO TECHNICZNE**
MECHANICS | MECHANIKA
3-M/2016

KRZYSZTOF KNOP*, KRZYSZTOF MIELCZAREK*

SIGNIFICANCE OF VISUAL CONTROL TYPES IN AUTOMOTIVE INDUSTRY

ZNACZENIE RODZAJÓW KONTROLI WIZUALNEJ W BRANŻY MOTORYZACYJNEJ

A b s t r a c t

The results of the assessment of visual control (VC) types in 10 enterprises from the Silesian province which operate in the automotive industry were presented in this article. These enterprises specialize in production for the automotive industry and constitute companies from Tier 1 and Tier 2 groups in the supply chain. The meaning of visual control was presented in TPS, research methodology and research results. Importance series were used as the basic tool of data analysis. A comparison of importance series was made for the purpose of stating characteristic relations in the scope of importance of the analyses types of VC.

Keywords: visual control, *BOST method*, *importance series*, *automotive industry*

S t r e s z c z e n i e

W artykule przedstawiono wyniki z zakresu oceny rodzajów kontroli wizualnej (zarządzania wizualnego) w 10 przedsiębiorstwach z branży motoryzacyjnej z województwa śląskiego. Były to przedsiębiorstwa stanowiące w łańcuchu dostaw firmy z grupy Tier 1 i Tier 2. Przedstawiono znaczenie kontroli wizualnej w TPS, metodykę badawczą oraz wyniki badań. Jako podstawowe narzędzie analizy danych wykorzystano szeregi ważności. Dokonano porównania szeregów ważności w celu stwierdzenia charakterystycznych zależności w zakresie ważności badanych rodzajów kontroli wizualnej.

Słowa kluczowe: kontrola wizualna, *metoda BOST*, *szeregi ważności*, *branża motoryzacyjna*

DOI: 10.4467/2353737XCT.16.122.5733

* M.Sc. Eng. Krzysztof Knop, M.Sc. Eng. Krzysztof Mielczarek, Institute of Production Engineering, Faculty of Management, Czestochowa University of Technology.

1. Introduction. Visual control in the Toyota Production System

Visual control in the Toyota Production System is known as visual management, visual communication or *mieruka* (見える化). Visual control is the process of translating live information into visible information so that both problems and kaizen opportunities are identified immediately [7]. Visual control is any communication device used in the work environment that tells us at a glance how work should be done and whether it is deviating from the standard [9].

Visual control is often understood in Toyota with 5S practice [8]. 5S is a tool for workplace organization so that everything has a place and everything is identified. The main intent of 5S is the same as the visual control system – to make problems visible immediately. The most important fact in visual control is that it leads to undertaking a specific action, which in Toyota indicates problem-solving process [11].

Visual control has a special place in the Toyota Motor Company. It is one of the production techniques connected with company's perfection that is integrated with the process of increasing added values [9]. Visual control is a heart of the Toyota Production System [6], it is a very important element which completes and intensifies other elements of this system. Visual control is a fundamental element in Toyota's production system, a particularly important tool in the "pillar" named Jidoka [9]. Toyota plants use in Jidoka visual control tools such as a problem display board system called andon. Other examples of visual control in TPS include kanban, daily production boards, signs classifying sections, coloured lines on the floor indicating how a product is to be stacked, metal clipboards, containing information that is needed at your fingertips [10]. Two kinds of visual control which are deeply rooted in the Toyota culture, are: visual indicators that contain graphs, charts, andon and kanban systems and the A-3 report standard. One of the greatest innovations of Toyota in the field of visual control is obeya [9]. TPS visual controls system have four main goals: informative, instructional, identification and planning.

The 7th rule of the Toyota management claims is "use visual control so that no problems remain hidden" which means:

- use simple visual signals to help employees continuously check whether the process is a standard that differs from the standard;
- avoid using computer screens if you distract the worker in the workplace;
- design simple visual inspection systems in the workplace to support movement and "pulling";
- whenever possible, limit the report to a single page - even if it concerns the most important financial decisions [9].

The implementation of the visual control system brought Toyota specific and notable benefits in the form of increased productivity, reduced number of defects and errors, help in meeting dates, facilitation of communication, improvements in safety, reduction of costs, and providing employees with greater control over their own environment [9, 11].

2. Research methodology

The BOST survey was the basic tool used to evaluate the significance of visual control types. The full name of this method is BOST – Toyota's management principles in questions [1, 2]. It is a tool of transformation of Toyota's management principles into questions. It serves to assess the practical use of management approach subscribed at Toyota among manufacturing and service companies in Poland. The BOST research aimed at proving thatin companies operating in Poland, regardless of the ownership form, the crew subconsciously uses the elements of management principles, which they may have never heard before. These principles are Toyota's management principles (14). Toyota's management principles in the BOST method are described by characteristic factors. The sets of factors are called areas. Toyota's management principles are divided into four parts, while the BOST survey has two versions: a version for employees and superiors [3].

The issue of visual control types evaluation in the BOST questionnaire form appears in the E7 area. The content of E7 area is the answer to the seventh principle of Toyota management. The question in E7 area is the following: *What is the most important element in the visual control?* In the box, types 1, 2, 3, 4, 5, 6 are presented (6 as the most important factor) [4, 5].

CS		Cleanness/Order
EP		Flow
TI		Information board
UP		Participation in production places
ME		Monitoring
GW		Graphic presentation of results

To assess the significance of visual control types in the BOST survey, a six ordinal scale described numerically is used [6].

The BOST survey was carried out in 10 companies from the automotive industry in order to obtain the opinion about the significance of visual control types. The researched companies from the automotive industry specialize in delivering products to the automotive industry, dealing with delivering products for the first or second assembly (Tier 1 and Tier 2 suppliers). These companies conduct their activity in the area of the Silesian province. This research area was chosen due to the crucial meaning of this business for the economic development of this part of Poland, which is confirmed by statistical data. Producing companies, among others, motor vehicles, located in the Silesia province generated in 2014 the highest value of production sold in million zloty, more than mining and extractive industry [12]. A sample of enterprises was selected in the quasi-random way. An essential condition of the selection of enterprises from the automotive industry was a confirmed use of visual control (in the course of preliminary analyses). Next, 10 enterprises were drawn from among the rated enterprises from the examined businesses and a sample of production workers was examined by means of the BOST survey. The sample of workers from the population was selected also in the quasi-random way. For BOST examinations, a proven contact with

the system of visual control was an essential criterion for the selection of production workers (on the basis of preliminary analyses). Altogether, 356 production workers were examined from 10 researched enterprises and their opinions about the importance of visual control types were collected.

An essential tool of results analysis in the scope of the meaning of visual control types was the scale of Thrustone comparative assessments [13] (result of applying the method of Thrustone comparative assessments). It was used for the purpose of creating importance series for the types of visual control (Fig. 1).

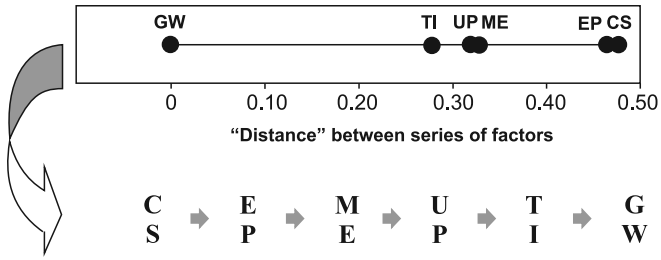

Fig. 1. Scale of Thrustone comparative assessments and importance series created on its base

The examined numbers of importance series were subjected to a detailed analysis on account of the place of appearing of visual control types in these individual series.

3. Research results

As a result of the assessment of visual control types made by production workers in 10 examined enterprises from the automotive industry, importance series were created. It results from the preliminary analysis of the importance series of visual control types that numbers of the examined types of visual control are individual and specific for the examined enterprises from the automotive industry – the lack repeats (at least one) of arrangement of the importance of visual control types in the half set (in the scope of places 1–3 and 4–6) and total (examining all places in the importance series) in the range of 10 enterprises.

A summing up analysis was made in the scope of the location of individual factors of the seventh principle of Toyota (visual control types) in the importance series for 10 enterprises from the automotive industry. The most important type of visual control in 3 enterprises was cleanness/order (CS) and flow (EP). Participation in production places (UP) was among the most important types of visual control in 5 enterprises. Information board (TI) and graphic presentation of results (GW) were the less important types of visual control (in 5 enterprises). Graphic presentation of results (GW) was the least important type of visual control in 5 enterprises. Generally, cleanness/order (CS) and participation in production places (UP) were the more important types of visual control (in 7 enterprises). In all the examined enterprises from the automotive industry, graphic presentation of results (GW) was the less important type of visual control.

The summarized importance series of visual control types for the automotive industry (in 10 enterprises) are presented by the following model:

$$\begin{matrix} \mathbf{C} \\ \mathbf{S} \end{matrix} \Rightarrow \begin{matrix} \mathbf{E} \\ \mathbf{P} \end{matrix} \Rightarrow \begin{matrix} \mathbf{M} \\ \mathbf{E} \end{matrix} \Rightarrow \begin{matrix} \mathbf{U} \\ \mathbf{P} \end{matrix} \Rightarrow \begin{matrix} \mathbf{T} \\ \mathbf{I} \end{matrix} \Rightarrow \begin{matrix} \mathbf{G} \\ \mathbf{W} \end{matrix} \quad (1)$$

Cleanness/order (CS), flow (EP) and monitoring (ME) there are the most important types of visual control in the automotive industry. Graphic presentation of results is the least important type of visual control (GW), in the second order there are information boards (TI) and participation in production places (UP).

4. Conclusions

How big is the meaning of visual control tools in the scope of keeping cleanness and order in the automotive industry? Such a big meaning of that type of visual control tools could not be related to without 5S Practises. Visual control is connected with 5S Practises and inversely, these two systems support each other (synergy effects). The need for implementing visual management results from the desire for effective application of 5S practices in the production. After workers get accustomed to actions connected with the maintenance of cleanness and order in "gemba", they become a part of their everyday duties. Workers apparently noticed some benefits in having a well-organised and tidy place of employment and pride in the fact that their workstations and surroundings are clean and tidy. Such changes are easily noticeable by everyone in the surroundings, not only by workers from the 5S practices area. Keeping a place of employment constantly in neatness and order requires a lot of effort from workers. Involving workers in keeping cleanness in their workstations and surroundings that is supported by the use of visual control tools, contributes to the increasing meaning of 5S practises and the visual control system. It should also be emphasized that 5S practices are one of the most often implemented tools of the Lean manufacturing conception among enterprises from production branches. The process of the introduction of changes in a company which consists in implementing less or more advanced conception of both improving the quality and the production often starts with implementing 5S practices. The measurability benefit of 5S practices, general universality of this program in the examined production companies, major effort connected with the maintenance of cleanness and order (trainings, audits, complicity in implementation and maintenance), easiness of noticing such changes by all workers, were undoubtedly the aspects that contributed to the highest assessments of the importance of 5S practices and visual control tools connected with them in the automotive industry.

Flow (EP) and monitoring (ME) are tools that were recognised as essential in the visual control system in the examined enterprises from the automotive industry. Different types of visual tools were used in the examined enterprises for the purpose of passing products from one position to another in a systematic, unchanging and incessant way: kanban cards, colourful lines, Hejiunka boards, so-called one piece cells of the flow, i.e. lines in the shape of the "U" letter at a large stake of assembly works. An important element of equipping the factory floors was also luminous showing parameters of the course of the process, the size

of the production plan, current number of produced goods, pointing at places of problems appearance what monitoring and steering the course of a production process. The system of monitoring in chosen enterprises included also applying cameras in the critical areas of the process that created the value added.

Superiors actively joined the process of problem solving in the production places by identifying problems, using the sense of sight and available for this purpose tools of visual control – participation in production places (UP).

Information board (TI) and graphic presentation of results (GW) are comparatively the least important types of visual control. Their role in revealing problems in the workshop and their meaning in the system of visual control was relatively smaller according to the workers.

References

[1] Borkowski S., *Toyotaryzm. Wyniki badań BOST*, Wydawnictwo Menedżerskie PTM, Warszawa 2012 [in Polish].

[2] Borkowski S., *Toyotaryzm. Zasady zarządzania Toyoty w pytaniach*, Wydawnictwo Menedżerskie PTM, Warszawa 2012 [in Polish].

[3] Borkowski S., Ingaldi M. (red.), *Toyotaryzm. Zagadnienia kontroli w metodzie BOST*, Oficyna Wydawnicza Stowarzyszenia Menedżerów Jakości i Produkcji, Częstochowa 2012 [in Polish].

[4] Borkowski S., Knop K., *Measurement and Analysis of Visual Control Importance in a Company of Automotive Branch*, Proc. of CO-MAT-TECH 2012 "Global Crises − Opportunities and Threats, 20th International Scientific Conference", October 10th–12th, 2012, Trnava, Slovak Republic, Vydavatel'stvo Alumnipress, Trnava, 64-75.

[5] Borkowski S., Knop K., *Visual Control as a Key Factor in a Production Process of a Company from Automotive Branch*, Production Engineering Archives, **1**, 2013, 2528.

[6] Borkowski S., Knop K., Rutkowski T., *Meaning of Visual Control Types in Production Improvement. Chapter 9*, [in:] Borkowski S., Konstanciak M. (eds.), *Production Improvement*, Tripsoft, Trnava, 2011, 117-128.

[7] Hirano H., *5 Pillars of the Visual Workplace: The Sourcebook for 5S Implementation*, Productivity Press, Portland, OR, 1995.

[8] Knop K., Borkowski S., *Evaluation of Visual Control in 5S and 5M*, Proc. of "Ekonomika a manazment podnikov 2011. Medzinarodna vedecka konferencia. 4 a 5 oktobra, 2011", Zvolen 2011, 118-126.

[9] Liker J.K., *Droga Toyoty. 14 zasad zarządzania wiodącej firmy produkcyjnej świata*, MT Biznes, Warszawa 2005 [in Polish].

[10] Mann D., *Creating a Lean Culture Tools to Sustain Lean Conversion*, Productivity Press, New York 2005.

[11] Moulding E., *5S: A Visual Control System for the Workplace*, AuthorHouse, Central Milton Keynes 2010.

[12] *Rocznik Statystyczny Województwa Śląskiego*, GUS, Warszawa 2015 [in Polish].

[13] Sagan A., *Analiza preferencji konsumentów z wykorzystaniem programu Statistica – analiza Conjoint i skalowanie wielowymiarowe*, StatSoft, Kraków 2009 [in Polish].

TECHNICAL TRANSACTIONS | **CZASOPISMO TECHNICZNE**
MECHANICS | MECHANIKA
3-M/2016

DARIUSZ KARPISZ*

DESIGN OF MANUFACTURING DATABASES

PROJEKTOWANIE PRZEMYSŁOWYCH BAZ DANYCH

A b s t r a c t

The article presents specific cases appearing in the design of manufacturing databases. In particular, a decomposition of entity model to the physical data model is presented. Understanding of significant differences between them makes it possible to build such structures of industrial databases that include special cases which occur in them. Different strategies for the transition from hierarchical entities model to targeted database tables are described. Additionally, an overview of problems associated with unary entities is outlined in this document.

Keywords: manufacturing databases, *ERD*, *PDM*, *super-entities*, *sub-entities*

S t r e s z c z e n i e

W artykule przedstawiono specyficzne przypadki spotykane w projektowaniu przemysłowych baz danych. W szczególności zajęto się dekompozycją modelu encji ERD do fizycznego modelu struktur danych PDM. Zrozumienie istotnych różnic między nimi daje możliwość zbudowania takich struktur przemysłowych baz danych, aby uwzględniały szczególne przypadki w nich występujące. Przedstawione różne strategie przejścia od modelu z hierarchią encji do docelowych tabel bazy danych

Słowa kluczowe: przemysłowe bazy danych, *ERD*, *PDM*, *hierarchia encji*, *encje podrzędne*

DOI: 10.4467/2353737XCT.16.123.5734

* Ph.D. Eng. Dariusz Karpisz, Institute of Applied Informatics, Faculty of Mechanical Engineering, Cracow University of Technology.

1. Introduction

Modeling relational databases is based on a well-defined theory [1, 2]. Despite the existence and availability of a number of graphical tools for database design, creation of the correct model is difficult and time consuming.

In every industry area, there is a variety of custom cases which require specific design mechanisms. Such cases can be found also in databases for manufacturing systems. The Entity Relationship Diagram (ERD) is a basic tool for database design [3], but its logic elements – entities representing a fragment of reality do not necessarily correspond to the target database tables. This way it is possible to result in flexible logical description of the topic database separate from the implementation (usually in the SQL language). Transformation of the ERD diagram into correct data storage structures is realized by means of the Physical Data Model (PDM). Importantly, the number of entities and tables after the transition may vary significantly.

2. Methods

No particular difficulties from the perspective of relational theory are encountered when using classical methods of database design, including normalization, up to the 3rd Normal Form. However, there are special cases in which the details of the types of entities relationships have a significant impact on the implementation and operation of the system.

2.1. Data Flow representation

In the case of designing entities based on data flow responsible for the order of operations, it is possible to use classic model with unary (recursive) entities relationships when both the Participants in the relationship are the same entity. Such an approach is shown in Fig. 1 and 2.

In the case shown in Fig. 1, subsequent process steps follow each other, each operation is always preceded by only one other operation. The figure shows a simplified entity *Workpiece Operation* (state of the workpiece in manufacturing process as an example in [4]) with

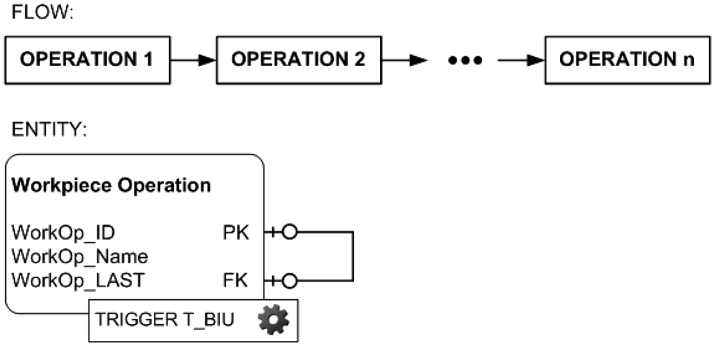

Fig. 1. Example of simple process flow represented by unary relationship entity

WorkOp_ID Primary Key and Foreign Key *WorkOp_LAST*, but the Foreign Key is the same entity (unary relation). Martin Notation is used in the ER model (Crow's Foot notation) to show the participation of entities in the relationship. As default in unary relations must be used in correlations *0:1*, *1:1* or *1:many* (*1:* as perpendicular line, *many:* as Crow's Foot) with both side optionality (indicated by the open circle). The optionality is required in order to be able to insert and modify data in targeted database table.

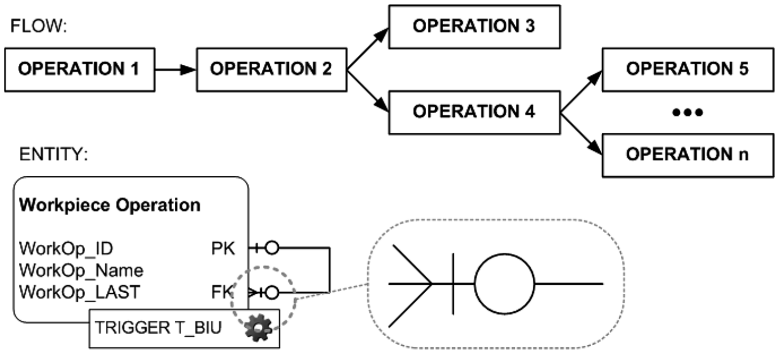

Fig. 2. Example of process flow with branchiny represented by unary relationship entity

In the case shown in Fig. 2, the following operations can be due to branching of the process. Operations can be executed parallely, allowing the case of any number of parallel operations. The ER model from Fig. 2 differs only in the entity relationship *1:many* from the ER Model in Fig. 1. To implement this functionality, database procedures activated by events called triggers [5] are to be used. In the given problem it is recommended to use a trigger type *Before Insert* or *Update* (example in [6]) to check whether there is a previous or next operation defined in the process.

2.2. Supertype and Subtype Entities

A unique design case is a description of reality in the main entity (Supertype Entity) and its subtypes (Subtypes Entities). An example of such an approach is presented in Fig. 3. The *Machine* entity case (e.g. *n*-axis CNC) is described by a set of factors represented by the *Machine Factors* entity.

In the example, the factors were divided into 4 classes:

– *Nominal Factors* − nominal monovalent,
– *Range Factors* − range from/to,
– *Fuzzy Factors* − described as fuzzy values (e.g. set: low, middle, high),
– *Timed Changing Factors* − time-varying values.

The *Machine* entity remains in a constant relationship *1:n* with the *Machine Factors* entity. The additional *Sample* entity designed to store data from the measurement of specific time-dependent factors is in relationship only with the subtype *Timed Changing Factors* entity. This is one of the standard cases in databases used in the Total Productive Maintenance Systems (TPM as example in [7]).

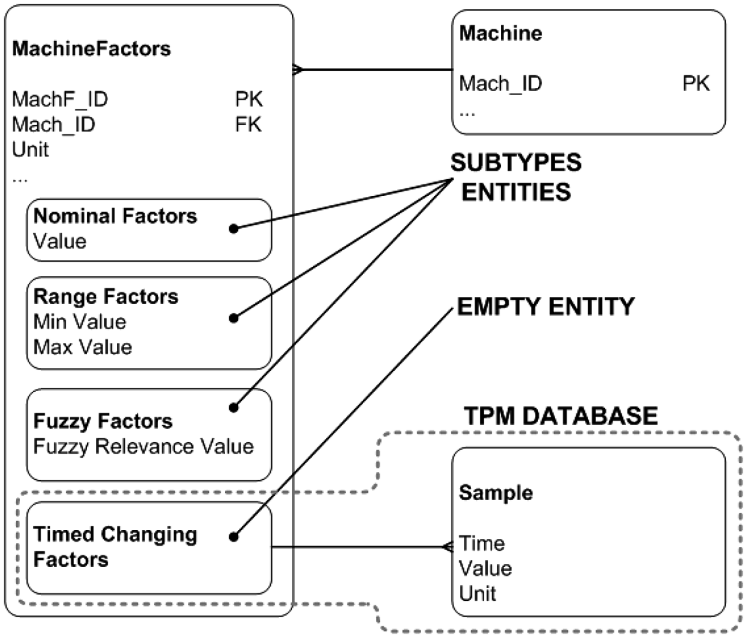

Fig. 3. Example of Supertype and Subtype entities in the Manufacturing Database

The presented example also shows the use case known as the Empty Entity (*Timed Changing Factors*) without any private attributes. Such an entity signals the need to use a different context of the subtype entity, in this case, with time dependencies.

3. Discussion

Presented in Fig. 1 and 2 unary relationships of the entities are often present in design practice. In fact, the shown cases are not difficult to implement, but usually full implementation to the PDM model with dedicated triggers is skipped due to the insufficient knowledge of developers generating data model of the ICT system from application classes created in the Object-Oriented Programming (OOP) style. The use of such practices as generating data model from the Object-Oriented Application with the Object-Relational Mapping is a wrong approach because it does not guarantee data consistency and compliance with the design of correct data layer.

In the case of Subtypes Entities, there are three solutions for transitioning from the ER Model to the PDM model:

1. For all Subtypes Entities, separate database tables are created which contain foreign key from the parent entity.
   Advantages:
   – Database structure is transparent,
   – Ease to define data integrity restrictions of the FK by the SQL code,

– Ability to add tables corresponding to subtypes entities without interference with existing data.

Disadvantages:

– Search data will require many join operations between tables which can significantly affect system performance.

2. For each Subtype Entity a separate table with a set of attributes from the parent entity is created.

   Advantages:

   – Fast searching when data is collected only from a particular table corresponding subtype,
   – No Foreign Keys are necessary to build a table for the subtype.

   Disadvantages:

   – High redundancy in the case of the parent entity with a large list of attributes and the lack of distinction between subtypes entities,
   – Ambiguity in relations with other tables of database that have previously been in relationships with subtypes entities.

3. Creation of a single table with a set of attributes of the parent entity and subtypes entities.

   Advantages:

   – Fast data searching – everything in one place,
   – Lack of Foreign Keys necessary for table creation for subtype entity.

   Disadvantages:

   – The table raw may require a large amount of storage space,
   – Potential issue with a high number of NULL values impacting performance.

There is no guidance as to the preference of methods to be chosen to decompose the Entity Relationship Diagram to the relational database data model (the Physical Data Model). It all depends on the design assumptions adopted in the analysis of the functionality of target system and the amount of information that is needed to be saved, modified and searched in the system.

References

[1] Codd E.F., *A Relational Model of Data for Large Shared Data Bank*, Communications of the ACM, **13** (6), 1970, 377-387.

[2] Elmasri R., Navathe S.B., *Fundamentals of Database Systems (3th Edition)*, Addison Wesley, 2000.

[3] Date C.J., *An Introduction to Database Systems, 8 edition*, Pearson, 2003.

[4] Gawlik J., Kiełbus A., Karpisz D., *Application of an Integrated Database System for Processing Difficult Materials*, Solid State Phenomena, **223**, 2015, 35-45.

[5] Widom J., Ceri S., *Active database systems: triggers and rules for advanced database processing*, Morgan Kaufmann, 1996.

[6] Karpisz D., *Implementation of assertion for relational databases with ORACLE examples*, Technical Transactions, 1-M/2011, 179-186.

[7] Gawlik J., Kiełbus A., *Application of artificial intelligence in supervising the technological equipments and quality of products*, [in:] Sikora T., Giemza M. (eds.), *The Practice of Quality Management of the 21st Century*, Wyd. Naukowe PTTŻ, Kraków 2012, 508-534.

TECHNICAL TRANSACTIONS | CZASOPISMO TECHNICZNE
MECHANICS | MECHANIKA
3-M/2016

JOLANTA MARIA RADZISZEWSKA-WOLIŃSKA*

FIRE PROPERTIES OF ANTICORROSION COATINGS FOR ROLLING STOCK

WŁAŚCIWOŚCI OGNIOWE ANTYKOROZYJNYCH ZABEZPIECZEŃ LAKIEROWYCH TABORU SZYNOWEGO

A b s t r a c t

The article presents current requirements and the results of fire tests for surface protection systems proposed for rolling stock securing. The influence of coating thickness and the type of filler used on the determined parameters is shown.

Keywords: fire spread, *paint coatings*, *filler*, *rolling stock fire safety*

S t r e s z c z e n i e

W artykule przedstawiono aktualne wymagania i wyniki badań ogniowych dla systemów ochrony powierzchni proponowanych do zabezpieczenia taboru szynowego. Omówiono wpływ grubości powłoki oraz rodzaju zastosowanej szpachli na określane parametry.

Słowa kluczowe: rozprzestrzenianie ognia, *powłoki lakierowe*, *szpachla*, *bezpieczeństwo pożarowe taboru szynowego*

DOI: 10.4467/2353737XCT.16.124.5735

* Ph.D. Eng. Radziszewska-Wolińska, Materials and Structure Laboratory, Railway Research Institute, Warsaw.

1. Introduction

Paint coatings for rolling stock have to meet a number of requirements regarding their mechanical, physico-chemical, protective and decorative properties. However, until recently, the most important features considered were: protection of structural material from the effects of corrosive agents under operating conditions and giving a product a desired aesthetic appearance. Striving to achieve a product that meets the expectations of manufacturers and operators of rail vehicles (or making the product permanent − retaining its properties at the required level as long as possible) as well as easy application and exploitation of the product, affected the development of paint industry. For these reasons, new materials were introduced (acrylic, alkyd-phthalate, epoxy, polyurethane, polyester), as well as their various combinations and modifications. However, the development of research in the field of rolling stock fire safety (also with taking into account the analysis of events as they occur) lead to the conclusion that paint coatings also have an impact on the development of possible fire in the rail vehicle. A fire in the Rydultowy, where a spread of fire on paint coatings of a wagon and locomotive took place [1, 2], is an example confirming the necessity of implementing safety requirements also for paint coatings.

2. Fire requirements

Initially, introduced fire requirements were related to non-metallic materials intended only for construction and interior equipping of vehicles. Exterior paint coatings were not taken into account. However, the real examples of fire spread upon paint coatings as well as the fact that coatings weight in currently built vehicles in the range of 150 to 300 kg/unit (which gives a substantial share in the total mass of non-metallic materials used in rail vehicles, typically of 1 700−8 700 kg/unit) led to the conclusion that this product cannot be ignored in assessing fire safety. Therefore, at the turn of the century, in some countries, including Poland, the need to meet the criteria of fire requirements of paints has already been introduced. Below, current Polish and European requirements in force in this field are described.

2.1. Test methods and requirements according to Polish standards

In Poland, only three parameters were initially standardized. Then, with the development of voluntary certification for coatings in compliance with the PN-K: 02511:2000 [3], other parameters for fire properties were included into to test range. Currently, until the end of the transitional period related to the implementation of European requirements, i.e. EN 45545: 2013 [4] and TSI LOC & PAS [5], the following leading standards are obligatory:

– for passenger rolling stock PN-K-02511: 2000 [3]
– for electric traction vehicles PN-K-02506: 1998 [6]
– for combustion traction vehicles PN-K-02507: 1997 [7].

These standards include the need to meet requirements for the following parameters.

Flame spread along the surface. Tests in accordance with PN-K-02512:2000 [8] consist in subjecting a sample to thermal radiation of the intensity of 35 kW/m^2 in the presence of a gas pilot burner whose role is to attempt to set fire to the emitted products of thermal decomposition. During the test the following parameters are recorded: the time in which the flame front passes through each zone of sample surface as well as the initial and the maximum flue temperature in the chimney. The *Flame Spread Index (I)* is calculated by means of the formula given in the standard. Safety requirements according to PN-K-02511:2000 [3] are as follows: for a coating on the ceiling: $I \leq 20$ [–] and for other elements: $I \leq 75$ [–].

Smoke properties. In a test performed according to PN-K-02501:2000 [9], a sample is placed in a closed chamber with a volume of approx. 0.56 m^3 and treated with a flame of a gas burner. Then changes of the light passing through the chamber intensity over time is determined. The result of the test are: *exposure S* [lx s] during the first four minutes of the test and the *light intensity* after 4 minutes of testing E_4 [lx]. Safety requirements according to PN-K-02501:2000 [3], PN-K-02511: 2000 [3] and the UIC 564-2 [10] App. 15 are as follows: $S \geq 9000$ lx s, $E_4 \geq 20$ lx.

Concentration of gases toxicity. A test in accordance with PN-K-02505:1993 [11] consists in subjecting a crushed material sample in a closed chamber with a volume of 0.56 m^3 to pyrolysis. The sample is placed at a quartz dish set on an electric heater with the power of 500 W. After 5 minutes *concentration of carbon monoxide and carbon dioxide* is measured for the extracted gas samples with use of Drager tubes. The safety requirements according to PN-K-02505: 1993 [11], PN-K-02511:2000 [3] are as follows: 20 CO + + $CO_2 \leq 6000$ ppm.

Combustible properties. The method according to p.4.1 PN-K-02508:1999 [12] (in accordance with the UIC Code 564-2 [10] App. 4) consists in an alcohol flame impingement on a sample arranged in a frame inclined at the angle of 45 ° to the horizontal position. During the test the *time of the sample burning* (*t*) after putting off the burner is measured as well as the course of burning is observed. After the test the *surface of the sample burned part* (*s*) is measured. The safety requirements according to PN-K-02508:1999 [12], PN-K-02511:2000 [3] and the UIC 564-2 [10] App. 4 are as follows: no falling burning particles, $t \leq 10$ s, $s \leq 150$ cm^2.

Oxygen index. A test according to PN-EN ISO 4589-2: 2006/Ap1: 2006 [13] is performed in accordance with the UIC Code 564-2 [10] App. 7. It consists in determining the lowest concentration of oxygen in a mixture of oxygen with nitrogen, at which minimal burning of material remains. The safety requirements according to PN-K-02511: 2000 [3] and the UIC 564-2 [10] App. 7 are as follows: *Oxygen index* OI $\geq 28\%$.

2.2. Test methods and requirements according to EN 45545-2: 2013

The European standard EN 45545-2: 2013 [4] introduced the need for mandatory testing of coatings, making the type of required tests as well as criterial values of individual parameters dependent on the location of paint coatings. Table 1 presents categories of requirements assigned to individual groups of materials. The next Table 2 shows types of required tests and criteria values of individual parameters.

Table 1

Categories of requirements for vehicle components covered with paintings according to EN 45545-2 [4]

Product No.	Name of painted elements	Requirement
IN1A	Interior vertical surfaces	R1
IN1B	Interior horizontal downward-facing surfaces	
IN1C	Interior horizontal upward-facing surfaces including body shell	R10
EX1A	Walls of external body shell	R7
EX1B	External surfaces of cab housing	R17
EX2	Roof of external body shell	R8
EX3	Under frame of external body shell	R7

Table 2

Test methods and criterial values for parameters for each category of R requirements, taking into account HL threat levels according to EN 45545-2 [4]

Test method, parameter	Requirement	Values required for particular hazard level HL		
		HL1	HL2	HL3
ISO 5658-2, CFE [kWm^{-2}]	R1, R7	$\geq$ 20 a	$\geq$ 20 a	$\geq$ 20 a
	R17	13 a	13 a	13 a
EN ISO 9239-1, CHF [kWm^{-2}]	R8, R10	$\geq$ 4,5	$\geq$ 6	$\geq$ 8
ISO 5660-1, MARHE [kWm^{-2}]	R1$^{*)}$, R7$^{*)}$, R17$^{*)}$	a –	$\leq$ 90	$\leq$ 60
	R8$^{**)}$	–	$\leq$ 50	$\leq$ 50
EN ISO 5659-2, $D_s(4)$ [–]	R1$^{*)}$	$\leq$ 600	$\leq$ 300	$\leq$ 150
EN ISO 5659-2, $D_s$max [–]	R7$^{*)}$, R8$^{**)}$, R17$^{*)}$	–	$\leq$ 600	$\leq$ 300
	R10$^{**)}$	$\leq$ 600	$\leq$ 300	$\leq$ 150
EN ISO 5659-2, VOF_4 [min]	R1$^{*)}$	$\leq$ 1 200	$\leq$ 600	$\leq$ 300
EN ISO 5659-2, CIT_G [–]	R1$^{*)}$, R17$^{*)}$	$\leq$ 1,2	$\leq$ 0,9	$\leq$ 0,75
	R7$^{*)}$, R8$^{**)}$, 10$^{**)}$	–	$\leq$ 1,8	$\leq$ 1,5

$^{*)}$ test for the radiation intensity of 50 kWm^{-2},

$^{**)}$ test for the radiation intensity of 25 kWm^{-2}, a – if flaming droplets are reported or the material does not ignite in ISO 5658-2 [14], required additional test acc. to EN ISO 11925-2 [15].

Below, the relevant test methods are described.

Test according to ISO 5660-1 [16]. The test is performed with use of the cone calorimeter, wherein the principle used is an oxygen consumption calorimetry [17]. During the test a number of parameters is measured, but for classification according to EN 45545-2 [4], parameter MARHE [kW/m^2] *Maximum Average Rate of Heat Emission* (*MARHE*) is determined during 20 minutes of the test.

Test according to ISO 5658-2 [14]. The method consists in subjecting a vertical sample to an external heat flux of a standardized density distribution. During the measurements, the time of flame transition in the central part of the sample is recorded. After the test, the length of the burned part of the sample is determined in order to be calculated with the numerical code of the *Critical Flux at Extinguishment CFE* [kW/m^2].

Test according to EN ISO 9239-1 [18]. The method consists in subjecting a vertical sample to an external heat flux of a standardized density distribution. During the measurement, the time of flame transition through succeeding zones is recorded. After the test, the length of the burned part of the sample is determined in order to be calculated with the numerical code of the *Critical Heat Flux CHF* [kW/m^2].

Test according to EN ISO 5659-2 [19]. The method consists in subjecting a horizontally located sample of a thermal irradiation of 25 or 50 kW/m^2 in an closed chamber, with or without the use of a pilot burner. The reduction of light beam intensity passing through the smoke emitted is measured. The results are given as *optical density* D_s and as VOF_4 – the *cumulative value of specific optical densities* in the first 4 min of the test**.**

Test according to EN ISO 5659-2 [19] and EN 45545-2 [4] Annex C. The test consists in determination, by means of a spectrophotometer, of the emission of toxic gases during combustion of a sample in a smoke chamber, according to EN ISO 5659-2 [18]. On the a basis of concentrations of CO_2, CO, HBr, HCl, HCN, HF, NO_x, SO_2 gases, the *Conventional Index of Toxicity CIT* parameter [–] is calculated.

3. The test results

3.1. The test results according to PN

The results of the tests of surface protection systems designed for body shell of rail vehicles show that the tested products meet Polish requirements. For most parameters, the values obtained were within relatively narrow ranges (very close to each other), regardless of the coating thickness and composition. They were as follows:

– Oxygen index at a very good high level of – OI: 46–48%,
– Concentration of toxicity of the emitted gases at a very good low level of – 20 CO + + CO_2: 813–1080 ppm,
– Smoke Properties at a very good high level of *S*: 22830–23600 lxs, E_4: 89–99 lx,
– Combustible properties at a very good low level of *t*: 0 s, *s*: 18–33 cm^2.

Only in the case of the *Flame Spread Index* over the surface, the influence of coating thickness and type of the fillers on value *I* was observed. As shown in the diagram (Fig. 1), the coating with epoxy filler revealed lower values of this parameter, however increasing

with the thickness of coating on 8,5 to 35,0 [–]. For shells with polyester filler parameter *I* changed from 23,5 to 65,8 [–]. However, it should be noted that the thickness of the tested systems does not exceed 500 µm, which means that the applied layer of putty was very thin. For paint systems that do not contain filler, index *I* was below the value of 10,0 [–].

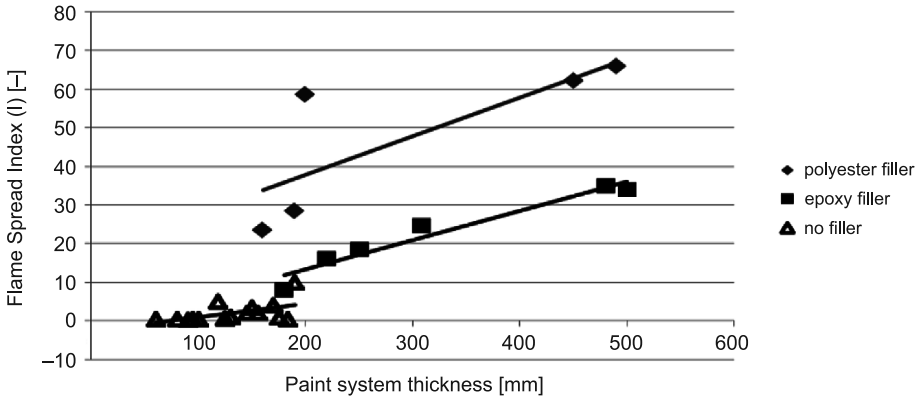

Fig. 1. Test results of *Flame Spread Index (I)* [–] of surface protection systems for rolling stock (archive IK, 2000–2014)

3.2. The test results according to EN

The results of the already completed tests of coatings designed for steel substrate show that the following parameters comply with the requirements of EN 45545-2:2013 [4] for the requirements of R1, R7 and R17 for HL1 and HL2 (however, the influence of the thickness of coatings and their composition is visible):

– $D_s(4)$ – for sets with epoxy filler < 100 [–], for sets with polyester putty 100–280 [–],
– $D_s\max$ – for sets with epoxy filler < 100 [–], for sets with polyester putty 100–300 [–],
– VOF_4 – for sets with epoxy filler: 139–286 min, for sets with polyester putty: 242–585 min,
– CIT_g – (0.01 to 0.06 [–]).

However, as results from the following plots (Fig. 2 and 3), requirements for the *MARHE* and CFE are difficult to meet for paint systems containing a polyester putty. In terms of the *Maximum Average Rate of Heat Emission* (*MARHE*) coating with the epoxy filler revealed lower values, increasing with the thickness of coating from 25.3 to 54.8 kW/m^2. But for coatings with polyester filler this parameter changed from 58.2 to 149.5 kW/m^2.

In the case of the *Critical Flux at Extinguishment* (*CFE*), much better results were obtained similarly for systems with epoxy filler (19.0–32.8 kW/m^2) than with polyester (7.3–21.5 kW/m^2). Also, for both variants, a deterioration of properties with increasing coating thickness occurred. It should also be noted that these thicknesses reached oven to 2 500 µm, which reflects the real conditions on the wagons. In contrast, all systems that did not include fillers met the requirements.

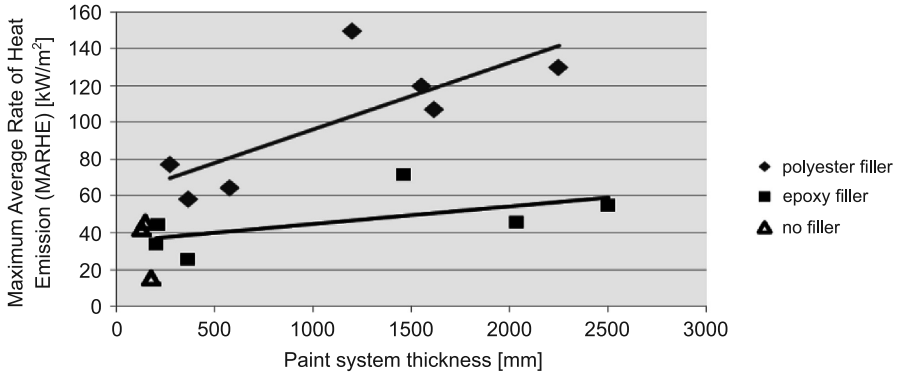

Fig. 2. Test results of *Maximum Average Rate of Heat Emission* (*MARHE*) [kW/m^2] of surface protection systems for rolling stock (archive IK, 2014–2015)

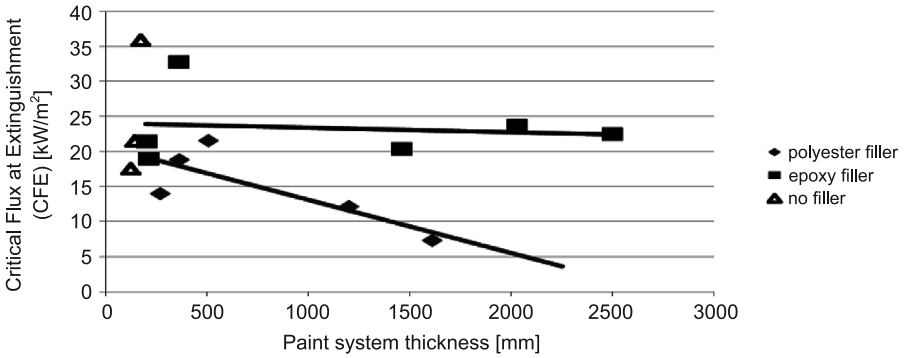

Fig. 3. Test results of *Critical Flux at Extinguishment* (*CFE*) [kW/m^2] of surface protection systems for rolling stock (archive IK, 2014–2015)

4. Summary and Conclusions

The results of the already completed studies at the Railway Institute show that coatings systems used for anticorrosion protecting of rail vehicles meet the requirements of PN-K-02511:2000 [3], but the determined values are worse when the coating thickness increases.

In contrast, the tests carried out in accordance with EN 45545-2: 2013 [4] show that:

– Systems with epoxy fillers are characterized by more favourable, in terms of fire safety, coatings fire properties than those with polyester fillers, which in most of the cases did not meet the requirements;
– With increasing thickness of the coatings, their fire performance becomes worse. In this connexion, during renovation of vehicle old paint should be fully removed;
– Because of favorable physical and mechanical properties (elasticity, adhesion, resistance to punching and bending) of the polyester putty in relation to the epoxy putty, paint industry is facing another challenge for modification of these products.

References

[1] Radziszewska-Wolińska J., *Passenger train fire in a tunnel*, Proc. of the 2nd Int. Conf. "Long Road and Rail Tunnels", 09–11.05.2002, Hong Kong, Tunnel Management International Ltd., Kempston, UK, vol. 5, No. 4, 2002, 109-118.

[2] Radziszewska-Wolińska J., *Zagrożenia pożarowe w tunelach kolejowych*, Problemy Kolejnictwa, **137** (18), 2003, 73-84 [in Polish].

[3] PN-K-02511:2000 Tabor kolejowy. Bezpieczeństwo przeciwpożarowe materiałów. Wymagania [in Polish].

[4] EN 45545:2013 Railway applications – Fire protection on railway vehicles.

[5] Rozporządzenie Komisji (UE) nr 1302/2014 z dnia 18 listopada 2014 r. odnoszącej się do podsystemu „*Tabor – lokomotywy i tabor pasażerski*" systemu kolei w Unii Europejskiej dalej zwane TSI Loc&Pas 1302/2014 [in Polish].

[6] PN-K-02506:1998 Elektryczne pojazdy trakcyjne. Zabezpieczenie przeciwpożarowe. Wytyczne konstrukcyjne [in Polish].

[7] PN-K-02507:1997 Spalinowe pojazdy trakcyjne. Zabezpieczenie przeciwpożarowe [in Polish].

[8] PN-K-02512:2000 Tabor kolejowy – Bezpieczeństwo przeciwpożarowe materiałów – Metoda badania wskaźnika rozprzestrzeniania się płomienia [in Polish].

[9] PN-K-02501:2000 Tabor kolejowy – Właściwości dymowe materiałów – Wymagania i metody badań [in Polish].

[10] UIC Code 564-2 Regles relatives a la protection et a la lutte contre l'incendie dans les vehicules ferroviaires du service international, transportant des voyageurs, ou vehicules assimiles, 3 edition of 1.1.1991 and 2 Amendments,

[11] PN-K-02505:1993 Tabor kolejowy – Stężenie tlenku i dwutlenku węgla wydzielanych podczas rozkładu termicznego lub spalania materiałów [in Polish].

[12] PN-K-02508:1999 Tabor kolejowy – Właściwości palne materiałów – Wymagania i metody badań [in Polish].

[13] PN-EN ISO 4589-2:2006 Tworzywa sztuczne – Oznaczanie zapalności metodą wskaźnika tlenowego – Badanie w temperaturze pokojowej [in Polish].

[14] ISO 5658-2 Reaction to fire tests – Spread of flame. Part 2 Lateral spread on building products in vertical configuration.

[15] EN ISO 11925-2 Reaction to fire tests − Ignitability of products subjected to direct impingement of flame − Part 2: Single-flame source test.

[16] ISO 5660-1 Fire test – Reaction to fire Part1 Rate of heat release.

[17] Peacock R.D., Bukowski R.W., Markos S.H., *Evaluation of Passenger Train Car Materials in the Cone Calorimeter*, Fire and Materials, **23**, 1999, 53-62.

[18] EN ISO 9239-1 Reaction to fire tests for floorings Part 1 Determination of the burning behaviour using a radiant heat source.

[19] EN ISO 5659-2 Plastic – Smoke generation. Part 2: Determination of optical density by a single chamber test.

TECHNICAL TRANSACTIONS | **CZASOPISMO TECHNICZNE**
MECHANICS | MECHANIKA
3-M/2016

DOROTA KLIMECKA-TATAR*

FLOW OF TECHNICAL INFORMATION IN THE PRODUCTION PROCESS OF PROSTHETIC RESTORATIONS

PRZEPŁYW INFORMACJI TECHNICZNYCH W PROCESIE WYTWARZANIA UZUPEŁNIEŃ PROTETYCZNYCH

Abstract

In the implementation of specialized services a large attention is paid to the flow of information between cells which determine the proper execution of the task. In engineering services related to dentistry there appears to be a significant discrepancy connected with knowledge awareness. The article presents three areas of knowledge (in the range and possession of the required knowledge) and information flow between the patient, dentist and dental technician. A technical solution to increase the possibilities of obtaining information at the design stage of the restoration has also been proposed, by introducing a system of material selection and engineering techniques in dentistry.

Keywords: information flow, *dental restoration*, *dental engineering*, *material selection*

Streszczenie

W realizacji usług specjalistycznych dużą uwagę kładzie się na przepływ informacji pomiędzy poszczególnymi komórkami decydującymi o właściwej realizacja zadania. W usługach dotyczących inżynierii dentystycznej pojawia się znaczna rozbieżność w zakresie posiadanej wiedzy. W artykule zaprezentowano trzy obszary przechowywania wiedzy i przepływu informacji pomiędzy pacjentem, dentystą a technikiem dentystycznym. Zaproponowano również techniczne rozwiązanie zwiększenia możliwości pozyskania informacji na etapie projektowania uzupełnienia protetycznego przez wprowadzenie systemu doboru materiału i technik w inżynierii dentystycznej.

Słowa kluczowe: przepływ informacji, *uzupełnienie protetyczne*, *technika dentystyczna*, *dobór materiałów*

DOI: 10.4467/2353737XCT.16.125.5736

* Ph.D. Eng. Dorota Klimecka-Tatar, Institute of Production Engineering, Faculty of Management, Czestochowa University of Technology.

1. Introduction

According to data from the literature [1–6], in the process of individual production it is required to have specialist knowledge, which guarantees precise requirements determination and ensures the appropriate level of quality. Production unitary is marked by a specific set of requirements for implementation. This is connected with an individual approach to individual order. The fact that the individual production is controlled through direct dialogue between the contractor and the client is an additional factor. Execution of prosthetic restorations by dental technician is this kind of production on special order.

The material selection is an increasingly more complex task, not only because of the very wide choice of material and availability of the offer, but mainly due to the consequences of an improperly used material. Digital material selection tools have a great potential not only in technical terms but also in evolution and development of the design process [7–9]. These tools give the possibility to know the basis of the project and create conditions for innovative performance of prosthetic restoration. There are many available databases of material, but it is important to create a database for familiar materials. Similar materials, whose characteristics differ from each other, however, are used in a specified field of science. In this case, creating a base of dental materials allows for the selection of materials from all engineering materials groups that are used at various stages of restoration manufacturing.

Creating a functional base of the dental materials selection is one of the demands of the rapidly growing market for these materials. Constantly striving to improve the quality of patients' (users') life through an increased number of aesthetic restorations makes patients want to be fully informed and, what is more, to be able to make their own decisions on the creation of their image (in this case their restoration) [8–10]. The functioning of the above database can have a significant impact on the flow of information between the three cells, which are the dentist, dental technician and patient. Implantation of a database in a dental office can also help to increase the confidence of patients to "their" dentists [9, 10]. The patients will be 100% informed what the price for the dental-prosthetic service includes and they will be able to decide on the possible reduction of costs by finding substitutes. The DeMISS base may become an essential tool for creating a clear and explicit material-processing-aesthetic orders. In order to create a useful and reliable database of commercial dental materials it is necessary to carry out research in the market of dental materials. It is obvious that if the database is to be created with proper acceptance of dentists and dental technicians, it will be necessary to carry out extensive research among these professional groups. To compile information on dental materials which are mostly offered to patients and most often used by dental technicians, an extensive survey should be created – all dental materials that are released for sale are under the strict control of the International Standards Organization (ISO) and the American Society for Testing and Materials (ASTM), which places high demands on the stage of material parameters determination [9, 10].

Creating the algorithm of searching and selection of proper dental materials involves carrying out multi-step trials research in dental practices and dental laboratories in order to improve the flow of information streams. Stage of the base synthesis process (e.g. dental materials integral selection system – DeMISS) would be carried out the external studies,

on a group of customers, i.e. patients who will be able to decide freely about the kind of materials their dentures will be made of.

2. Objective of the research

The aim of the research is to introduce the idea and primary project of the Dental Materials Integral Selection System (DeMISS), which will become a functional tool during the design stage of total and partial dental restorations. The idea of the system includes advanced control functions of the material choice from the point of view of construction materials requirements and expectations of both aesthetic and economic subjects. One of the elements of the system will also be the possibility of individual virtual designing of dental restorations by the dentist, dental technician and patient, based on the unit prices of necessary materials and based on labor coefficient required to create a supplement.

3. Characteristics of information stream flow

The main problem in the implementation of orders (restoration project) from the range of dental engineering, is the fact that there is a one-way flow of information. In this system, there are three cells: the customer (patient), dentist and dental technician (Fig. 1). In this system, the patient is in direct contact with the doctor who performs the treatment and decides on the type of required restoration [11–14]. The dentist forwards recommendation to the dental technician. In this system, the contact between the patient and the dental technician is completely omitted. This means that, in theory, the patient does not have a major impact on the type of order and has no possibility to submit requirements. The dentist is an intermediary in communication during the process of determining the details of project. It should be noted that, in most cases, the patient has no possibility of selecting operational parameters of restoration (the choice of materials and manufacturing techniques, taking into account the characteristics and prices of the final product) – therefore we refer to a one-way flow of information in the patient – dentist – dental technician system.

Fig. 1. The flow of information in the patient-dentist-dental technician system

It can be assumed that each of the participants of the system has its own requirements, expectations and knowledge. Fig. 2 presents the basic information (knowledge), requirements and expectations of the system elements (competencies of the dentist and dental technician have been determined on the basis of the framework of teaching faculties).

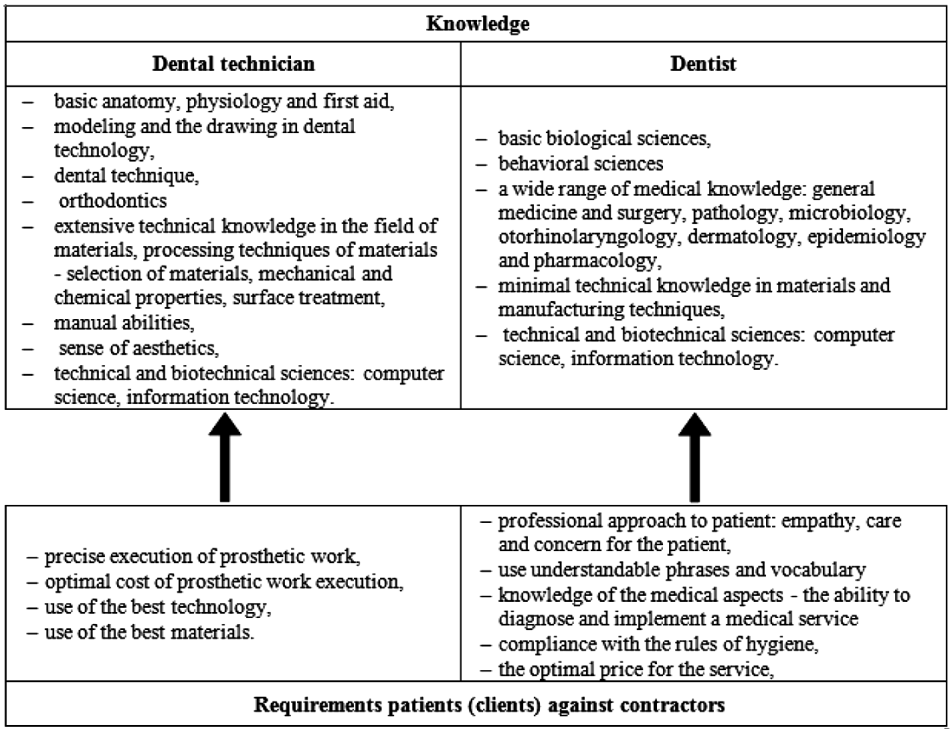

Fig. 2. Knowledge and requirements for contractors of prosthetic individual orders

In prosthetic orders, quite an interesting relationship occurs in the flow of information. The first key factor is the client (patient) that comes to a dental office to use medical services – diagnosis, treatment and denture fitting. The customer sets very high expectations of the service. The patient has direct requirements for the doctor to focus on the professional approach to the patient and to have wide knowledge of medicine as well as indirect demands on the dental technician during the implementation of the restoration project realization. The patient expects that its restoration will fulfill all the aesthetic requirements, will be made from the finest materials and by means of the best technology, while maintaining the best prices. Completion of an order with such a flow of information is difficult, because the dentist should have extensive knowledge of medicine, and only minimal knowledge of the materials and techniques used in dentistry. Thus, the dentist is not fully able to provide the information that for the patient may be the core of order. Technical information would help to make the right project. It should be noted that the dental technician does not have permission (the lack of legal provisions) to contact the patient, and the only unit of connecting the information flow in the patient – dental technician relation is the dentist. The patient does not have any information on the technical aspects of the production of the prosthesis and does not have any possibility to interfere in the project work [12]. It is worth emphasizing that the prices of dental restorations are determined not only by the type and size of the restoration, but also by materials selection (apparently similar

materials differ in performance characteristics, and consequently the price), technology and the use of technical devices. The use of modern techniques (computer-aided) and high standardization of work affects the final price. Therefore, the Dental Integral Material selection System (DeMISS) is very helpful for dental offices as a form of communication between the client and the contractor of prosthetic work [13]. The Dental Integral Material Selection System (DeMISS) is an innovative concept of communication in the plane of the patient--dental technician. The Fig. 3 presents the general scheme of action and the information flow during orders by the DeMISS system.

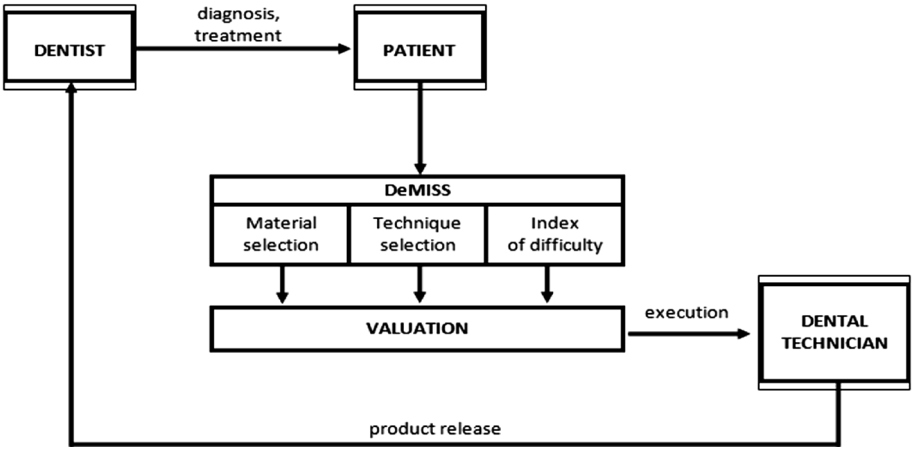

Fig. 3. General scheme of action and the information flow during orders by the DeMISS system

The use of the restorations self-designing system (DeMISS) does not force on the patient the knowledge of the basic principles of materials, techniques and their selection. The system is based on the clearly referred set of operating parameters. The system information shows the dependence between prices and durability of the products, and the cost of labor - factor of complexity (this factor should be calculated individually), based on the dental technician's skills presented in the database. Start of the DeMISS system in practice requires an empirical estimation of difficulty coefficients and the creation of a database of commercially available materials as well as techniques available to selected laboratories of dental technique. The proposed solution is a substitute for the flow of information between the patient and dental technician. It must be remembered that, according to the current law, the dental technician is not authorized to have a direct contact with the patient, who makes quick adjustment to special order requirements.

4. Conclusion

The introduction of the system to dental offices allows the patient to select materials and techniques used during the manufacturing process of a dental supplement. It is a technical solution which increases the possibility of contact between the patient and dental technician.

The proposed systems (The Dental Integral Material Selection System – DeMISS) gives the patient the possibility to fully and directly express their expectations for the restoration without having to mediate (in this case the dentist is the intermediary). Such a system can positively affect the quality of services and overcome errors resulting from the improper flow of technical information during the ordering process.

References

[1] Ciaputa T., Ciaputa A., *Podstawy wykonania prac protetycznych*, Wydawnictwo Elamed, Katowice 2009 [in Polish].

[2] Donovan T.E., *The selection of contemporary restorative materials*, Calif. Dent. Assoc. J., **34**, 2006, 129-134.

[3] Radomska K., Klimecka-Tatar D., Jagielska-Wiaderek K., *Dental Alloy Corrosion Characteristics Remanium G (Ni–Cr–Mo) Melting/Casting by Different Techniques*, Ochrona przed Korozją, **57** (7), 2014, 262-268.

[4] Klimecka-Tatar D., Radomska K., *The Quality Determinants in the Acrylate Denture Manufacturing*, Proc. of Conf. „Inżynieria Stomatologiczna – Biomateriały. Teoria, praktyka, doświadczenie", Ustroń 2013, 65-75.

[5] Radomska K., Klimecka-Tatar D., Pawlowska G., *The All-Ceramic Structures of Zirconium Oxide – the Harmony of Beauty and Functionality*, Inżynieria Stomatologiczna – Biomateriały, **11** (1), 2014, 7-9.

[6] Radomska K., Pawlowska G., Klimecka-Tatar D., *Wpływ parametrów technologicznych na właściwości materiałów inżynierskich stosowanych w medycynie odtwórczej*, Proc. of Conf. „Inżynieria stomatologiczna – Biomateriały. Nowoczesne materiały i technologie, stosowane w diagnostyce i terapii stomatologicznej", Ustroń 2015, 75-81 [in Polish].

[7] Buchanan J.A., *Experience with virtual reality-based technology in teaching restorative dental procedures*, J. Dent. Educ., **68**, 2004, 1258-1265.

[8] Ashby M.F., Brechet Y., Cebon D., Salvo L., *Selection strategies for materials and processes*, Mater. Des., **25**, 2004, 51-67.

[9] Ramalhete P.S., Senos A.M.R., Aguiar C., *Digital tools for material selection in product design*, Mater. Des., **31**, 2010, 2275-228.

[10] Ali J., Md Y.I., Faizal M., Salit M.S., *Material selection based on ordinal data*, Mater. Des., **31**, 2010, 3180-3187.

[11] Hu J., Luo E., Song E., Xu X., Tan H., Zhao Y., Wang Y., Li Z., *Patients' attitudes toward online dental information and web-based virtual reality program for clinical dentistry: a pilot investigation in China*, Int. J. Med. Informatics, **78** (3), 2009, 208215.

[12] Kilfeather G.P., Lynch C.D., Sloan A.J. et al., *Dentist – dental technician communication*, Dental Abstracts, **55** (5), 2010, 239-240.

[13] Della Bona A., Wozniak W.T., Watts D.C., *International dental standards – Order out of chaos?*, Dent. Mater., **27** (7), 2011, 619-621.

[14] Doméjean-Orliaguet S, Léger S., Auclair C., Gerbaut L., Tubert-Jeannin S., *Caries management decision: Influence of dentist and patient factors in the provision of dental service*, J. Dent., **37** (11), 2009, 827-834.

TECHNICAL TRANSACTIONS | **CZASOPISMO TECHNICZNE**
MECHANICS | MECHANIKA
3-M/2016

PRZEMYSŁAW OSOCHA*

THE EFFECTIVENESS OF E-LEARNING IN ENGINEERING EDUCATION

EFEKTYWNOŚĆ E-LEARNINGU W EDUKACJI INŻYNIERSKIEJ

Abstract

Changes in technology, availability of video casts and the general increase of information and knowledge value result in the advent of educational technology. As the first step toward validation of the effectiveness of e-learning in engineering education, a research on a group of students was carried out. The open-source and free software educational platform Moodle was used to conduct a selected course in the form of blended e-learning. The course was prepared and presented to the students during one semester time period. The effects of learning were verified through knowledge tests and their results were collected for analysis. Students in the test group achieved results equal or even better than other groups, validating the effectiveness of e-learning in engineering education. During the experiment also other positive aspects of e-learning were noted: students appreciated freedom of time and place where they learn and for the teacher high effort connected with course preparation could be rewarded by multiple use of the developed course at a later time.

Keywords: *e-learning*, *collaborative systems*, *technology enhanced learning*, *smart university*

Streszczenie

Zmiany technologiczne, dostępność wideotransmisji i ogólny wzrost wartości informacji i wiedzy doprowadziły do rozkwitu technologii edukacyjnych. Pierwszym krokiem w kierunku walidacji efektywności e-learningu w nauczaniu inżynierskim było przeprowadzenie badań na grupie studentów. Darmowa i otwarta platforma edukacyjna Moodle została użyta do przeprowadzenia wybranego kursu w formie mieszanego e-learningu. Kurs został przygotowany i przedstawiony studentom w czasie jednego semestru nauki. Efekty kształcenia były weryfikowane za pomocą testów wiedzy, a ich wyniki zbierano do dalszej analizy. Studenci w grupach testowych osiągnęli wyniki nie gorsze niż w innych grupach, potwierdzając tym samym efektywność e-learningu w nauczaniu inżynierskim. Podczas eksperymentu dostrzeżone zostały także inne pozytywne aspekty e-learningu: studenci doceniali swobodę czasu i miejsca gdzie mogą się uczyć, a wykładowcy dostrzegli, że duży nakład pracy poświęcony na przygotowanie kursu może zostać zrekompensowany przez późniejsze jego wielokrotne użycie.

Słowa kluczowe: *e-learning*, *systemy współpracy*, *nauka wspomagana technologią*, *inteligentna uczelnia*

DOI: 10.4467/2353737XCT.16.126.5737

* Ph.D. Przemysław Osocha, Institute of Applied Informatics, Faculty of Mechanical Engineering, Cracow University of Technology.

1. Introduction

In the last decades we have witnessed enormous development and growth in the electronic technology market. Electronic devices are getting smaller, more powerful and are pervasively blending into human environment. The ubiquitous connectivity of all kinds of devices through wired or wireless networks which utilizes numerous communication standards is even more important for this process of irrepressible spreading than the small form factor and raising computational power. Examples of such devices in personal service include smart TV sets, laptops, tablets, smartphones, smartwatches, together with all the wired and wireless infrastructure providing connectivity. Those changes impact most of the human life areas: how we work, how we rest and entertain and also how we learn.

The raise of mobility of electronic devices and significant increase of data transfer bandwidth are the main game changers for educational technology advent. E-learning is not limited anymore to plain text as educational data maybe presented in the form of high quality videos as well as sound and interactive advanced demonstrations.

On the other hand, there is a raising appetite in our population to consume more and more information. Manual labor loses its importance in favor of knowledge. People of all ages are looking for opportunities to leverage their education to a higher level. And this is where technical informational revolution and human needs meet together in the form of educational technology [1].

There is a number of e-learning definitions and approaches; even learning by means of an electronic device like calculator can be called e-learning. However, let us stick to the well accepted definition where e-learning is online distance learning [2, 3]. And it is worth mentioning that there are some variants of e-learning, e.g. hybrid or blended learning, where traditional stationary learning is reduced but not eliminated, and is replaced with some e-learning. Looking back in history, one of the first examples of e-learning, as we understand it today, is a system introduced by the University of Illinois in 1960, where informational resources were provided by computer terminals together with recorded lectures available by remotely linked television or audio devices. In the mid-1980s, many college libraries already offered courses in the electronic form. But the real dawn of online distant learning was a solution provided by the Open University in Britain and the University of British Columbia which used the Internet to deliver web-based trainings and online discussions for students. In 2003, the number of students using e-learning reached 1.9 million mark, and started to increase by 25% every year. Nowadays most of educational institutions offer some form of e-learning for their students. The Council of Europe endorsed in 2008 a statement that e-learning has potential to drive equality and education improvements in the whole European Union. Nowadays higher education in Poland is looking for possibilities to lower costs of the teaching process. The introduction of e-learning could be not only an economic solution, but in fact a way to spread the wings by attracting even more students and leaving to personnel of the university more time for research work. The goal of this paper is to present and analyse the introduction of e-learning in one course of engineering studies.

2. Materials and Methods

Moodle is a leading, free and open-source e-learning platform used for blended learning and distance education in schools, universities and for corporate and private websites with online courses and trainings [4]. The system is written in the PHP language and distributed under the General Public License (GNU). Moodle uses pedagogical approach to learning and incorporates a number of features like calendars, gradebooks and plugins system which extend it even more. Customizable themes, often based on the responsive web design, allow courses to be used also on mobile devices. The Cracow University of Technology uses Moodle as its official e-learning platform for students [5]. It is called ELF for e-learning framework. All students who start studies at the university are required to create an account in that e-learning system. The current version of Moodle in use at that platform is 2.5.2.

The Moodle software provides teachers with numerous options of how to implement the learning process. From that wide range of possibilities, a subset of core functionalities was selected. One of the most popular way of providing the content in the last years is video transmission. It is easily observable how the Youtube service has gained popularity worldwide, and how many similar services have emerged in the last decade. This phenomenon of ubiquitous online video casting through the Internet was only possible thanks to the technology progress, especially in electronic miniaturization and wide band data transmission.

3. Results

The selected course was to some extent implemented in the form of e-learning. The course subject "Algorithms and Data Structures" is one of the basic courses for applied informatics students. It was taught in the form of lectures and computer laboratories. The lectures and in some part laboratories were implemented in the form of e-learning system. As a base for the electronic version of the course, an official e-learning platform of the Cracow University of Technology was used. The platform elf2.pk.edu.pl is based on the open source software called Moodle. The first lecture was provided in a blended form, both live in the classroom and also in the electronic version for a later review by students. At the first meeting, except for the first part of the course, students were informed about the aim, range and requirements of the course, the e-learning platform was presented and, what is important, they had the opportunity to meet their teacher in person.

There is a number of ways to register to the e-learning course, ranging from teacher registering every student individually to a fully open course where every student may attend at his will. In the case of the discussed course, students obtained registration key per students group and registered themselves. In this way, there was less work for the teacher, and later it was easy to sort students by student group for final classification. It is worth mentioning that all students at the university already have verified accounts in the official learning platform, so there is little probability of an unwanted person getting access to course materials. Furthermore, before opening access to the materials, the teacher verifies registered students and closes registration for the course. The material of the course is presented to

students in parts available in defined time periods, similar to the life course where meetings are every one or two weeks. This method builds in students systematic approach to learning. Students can memorize better and understand every part of the lesson, because they are not overwhelmed by the availability of all the course material at once, since sections of the course are published in parts in defined time frames. On the other hand, students are not overloaded with too much data at the end of the course, since every part of the course ends with a test that has to be timely solved, making it impossible to learn in an unsystematic way.

Every section of learning material is composed of a lecture in the form of a video screencast and a corresponding PDF file containing presentations slides, together with a selection test verifying understanding of the provided courseware.

The most attractive part of the course is a video of the lecture. It is only possible to provide content in that form due to massive advances in electronic and connectivity technologies made in the last years. Videos presented in the course are screencasts of MS Power Point presentation, together with the recorded voice of a lecturer. Drawings and notes made live in the presentation with the stylus of a PC computer are an important part of the teaching process. It is possible due to the use of tablet computes with a stylus and digitizer screen. This way the lecturer may highlight important parts of the slide, draw additional pictures or write additional explanatory texts on the screen.

It is important that a video may be played not only on the computer, but on any device equipped with a web browser, at any time and in almost any place.

Students may freely review and download slides from presentations in the PDF format. It allows them to review the lecture material, make notes or print out for a later use. During video playback students concentrate on the presented material, knowing that slides are available for a later review.

Every section of teaching materials ends with a selections test verifying if the presented lecture was actually reviewed and well understood by students. The test is a set of 5 questions randomly selected from about 20 questions prepared for a particular section. Every question may have multiple correct answers, so it is possible that there is only one correct answer, two or three correct answers, or even all the answers may be correct. This way students must carefully review all the answers and cannot stop after the first one which seems to be correct. It is worth mentioning that the order of presented answers is also random, so it is impossible to memorize only the question number and the correct answer position, and the student has to learn the entire problem and its solution. Together with the presentation of section lecture material, there opens a time window of 2 weeks when it is necessary to solve the test. After that time the test closes and it is not possible to gather points for that one, if not solved in the predicted time.

The course was presented to the two groups of students at the second semester of bachelor studies of applied informatics. There were 37 students in total taking part in the course. The course is presented in numbers in Table 1. The whole course was divided into 8 sections which were presented every two weeks to the students. Every section contained several movies of variable time length. The selection test in each section was composed of 5 questions with 4 answers. The questions were randomly selected from a larger set of questions. Table 1 presents also the mean result of grades received by students in every course section.

Preparation of an e-learning course takes significantly more time than running the same course live in the classroom. Definitely, the most time consuming work is recording of video screencasts. First of all, one has to prepare for a particular lecture presentation, which takes more or less the same amount of time as for the live presentation. Then the recording takes more time than a live presentation due to technical issues, repetitions of some recordings, edition of the already recorded material and other reasons. Teachers know that, opposite to live presentations, the recorded videos will be watched many times by many users, so they try to do their best, which is why repetitions of recordings happen and that takes more time. In case of the presented course, the recording of 1 hour of video material took on average 3:12 hours. After the video is recorded, it is necessary to master it to the final form, for which in the case of this course MP4 format was used. It consumes additional time. Also, creation of test questions is additional work that has to be done. Finally, also entering the test questions into the e-learning system is quite time consuming.

Table 1

The course data by sections

Section number	Number of movies	Time [h:m:s]	Number of test questions	Mean evaluation result [%]
1	7	1:11:07	24	95.9
2	5	0:52:09	20	90.9
3	7	1:00:54	14	92.0
4	7	1:29:45	20	92.5
5	8	1:22:44	20	94.4
6	6	1:07:07	14	93.6
7	8	1:13:08	22	93.2
8	7	1:06:33	21	93.4

4. Discussion

The presented results show that preparation of e-learning course is far more time consuming than just running it live in the classroom. In the presented case, only recording of video screencasts takes 3 times more time than a classical course, not to mention other labor necessary for the finalization of on-line training. On the other hand, an e-learning course may be used many times later on. The effort of work is remunerative if the course is used in the future for a few subsequent years, or is taught parallelly to many students groups, which would require separate live presentations made by teacher for each group. In addition, to plain time and work calculation, there are some additional advantages of running an e-learning course. Students prefer e-learning because it gives them the freedom to manage their time and a choice of localization in which they learn. They may learn in the most appropriate time for them and not waste unnecessarily time commuting to the university classroom if it is not necessary. The possibility to repeat the recorded video as

many times as it is necessary for students to understand the presented problem is yet another advantage. In live lectures some aspects may be violated, since the lecture goes on and it is not possible to stop and discuss every single nuance of the subject. There is also a number of advantages for the teacher who prepared an e-learning course. It actually frees his time when live classes should took place. He may use that particular time for other assignments. Moreover, that freedom repeats in the future every time when e-learning is used. Material prepared one time can be used many times in the future. What is more, since students learn in their favorite time and may repeat material as many times as they wish, they learn better, which gives satisfaction to the teacher. The possibility to monitor progress of students by following their grades in every section tests is a practical advantage for the teacher. Finally, e-learning system automates final grades calculation, releasing the teacher from some work. To conclude the discussion on the presented e-learning course, it ought to be said that this solution is well accepted by students due to individual approach to their learning process. The results of teaching are no lower than with classical classroom learning. Considering all the advantages and results, it is recommended to widen the e-learning offer for students. In the current economy and technology conditions it could be a winning factor for some high schools on the market.

References

[1] Stacey E., Gerbic, P., *Success factors for blended learning*, Proc. of Ascilite 2008, Melbourne 2008, 964-968.
[2] Littlejohn A., Pegler Ch., *Preparing for blended e-learning*, Routledge, London–New York 2007.
[3] Wankel Ch., Blessinger P., *Increasing student engagement and retention in e-learning environments: Web 2.0 and blended learning technologies*, Vol. 6, Emerald Group Publishing, 2013.
[4] *Moodle – Open-source learning platform*, http://moodle.org [date of acc. 30.01.2016].
[5] *ELF, e-learning framework of the Cracow University of Technology*, http://elf2.pk.edu.pl, [date of acc.: 30.01.2016].

TECHNICAL TRANSACTIONS | **CZASOPISMO TECHNICZNE**
MECHANICS | MECHANIKA
3-M/2016

MONIKA GWOŹDZIK*

WEAR OF WORKING PART OF SURGICAL DRILLS

ZUŻYCIE CZĘŚCI ROBOCZEJ WIERTEŁ CHIRURGICZNYCH

A b s t r a c t

The paper presents the results ofstudies onthe topography of surgical borers flank after their operation. The studies were carried out on borers made of X39Cr13 martensitic steel, which was subject to heat and surface (plasma nitriding) treatment. Test drilling was performed in beef bones, which were fixed in a vice to ensure appropriate stability, a borer 6 mm in diameter and 160 mm long was used. The studies on the topography of flank comprised studies on roughness, which were carried out by means of a profilographometer designed for 2D and 3D studies on the surface by means of a contact method. The studies were carried out for borers of flank formed by successive drilling cycles.

Keywords: surgical drills, *martensitic steel*, *surface treatment*

S t r e s z c z e n i e

W artykule przedstawiono wyniki badań topografii powierzchni przyłożenia wierteł chirurgicznych po eksploatacji. Badania przeprowadzono na wiertłach ze stali martenzytycznej X39Cr13, które poddano obróbce cieplnej oraz powierzchniowej (azotowanie jarzeniowe). Testowe wiercenia wykonywano w kościach wołowych, które mocowano w imadle, w celu zachowania odpowiedniej stabilności, użyto wierteł o średnicy 6 mm i długości 160 mm. W ramach badań topografii powierzchni przyłożenia przeprowadzono badania chropowatości, które realizowano z zastosowaniem profilografometru przeznaczonego do badań 2D i 3D powierzchni metodą stykową. Badania przeprowadzono dla wierteł o powierzchni przyłożenia ukształtowanej poprzez kolejne cykle wiercenia.

Słowa kluczowe: wiertła chirurgiczne, *stal martenzytyczna*, *obróbka powierzchniowa*

DOI: 10.4467/2353737XCT.16.127.5738

* Ph.D. Monika Gwoździk, Institute of Materials Engineering, Faculty of Production Engineering and Materials Technology, Czestochowa University of Technology.

1. Introduction

Intensive development of technology causes continuously increasing requirements for surface engineering [1–9] and biomaterials engineering [1, 6–8, 10–15], both in the field of operational life and biocompatibility. Material wear occurs mainly on the surface, therefore the development of surface treatments creates broad possibilities to manufacture products of required properties based on the existing materials. Numerous attempts are made to shape the usable properties of biomaterials by means of surface engineering techniques [1, 6–8], which enable forming the microstructure, phase and chemical composition or the internal stresses state in the layers. Surgical instruments comprise a very wide, functionally and geometrically diversified group of products [13, 14]. The usable features of such instruments depend on the proper selection of materials used for individual components. The expected characteristics distinguishing surgical instruments in terms of design and operation include: high reliability, safety of use for the operator and the patient, ease of operation, specified set of mechanical properties as well as geometry useful to perform a specific procedure, design enabling full sterilisation of the instrument or device [13, 14]. The borers used in bone surgery should be stable, i.e. should not move on the bone bark during drilling. Such borers feature primarily appropriate geometry of the drill point and appropriate rotational speed during drilling.

The paper presents the results of studies on the topography of surgical borers flank after their operation. Both heat treated and plasma nitrided borers were used.

2. Material and experimental methods

The object of studies consisted of surgical borers made of martensitic steel which belongs to a group of X39Cr13 stainless steels. Test drillings were carried out using borers: (a) quenched + low-temperature tempered, 300°C (Q + LT), (b) quenched + low-temperature tempered + nitrided (Q + LT + N), (c) quenched + high-temperature tempered, 620°C + + nitrided (Q + HT + N).

Test drillings were carried out using borers: (a) quenched + low-temperature tempered, 300°C (Q + LT), (b) quenched + low-temperature tempered + nitrided (Q + LT +N), (c) quenched + high-temperature tempered, 620°C + nitrided (Q + HT + N).

Test drillings were carried out using borers: (a) quenched + low-temperature tempered, 300°C (Q + LT), (b) quenched + low-temperature tempered + nitrided (Q + LT + N), (c) quenched + high-temperature tempered, 620°C + nitrided (Q + HT + N).

Test drillings were carried out using borers: (a) quenched + low-temperature tempered, 300°C (Q + LT), (b) quenched + low-temperature tempered + nitrided (Q + LT + N), (c) quenched + high-temperature tempered, 620°C + nitrided (Q + HT + N).

The heat treatment consisted of compressed nitrogen quenching from the austenitising temperature of 1050°C. The time of holding at this temperature was 20 minutes. After quenching the borer was subject to two-hour tempering at 300°C with compressed nitrogen cooling. Instead, prior to nitriding the steel was tempered at 300°C and 620°C. A precise description of the nitriding process execution was presented in paper [7].

Operational tests were carried out on borers, 6 mm in diameter and 160 mm long, used in the bone tissue surgery (Fig. 1).

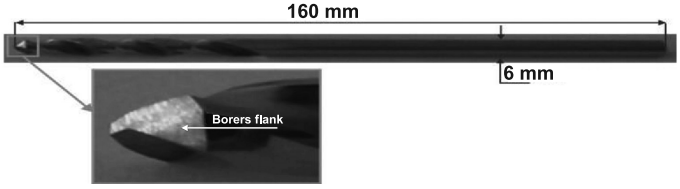

Fig. 1. Surgical borer

A special stand was arranged for borers' operational tests, consisting of:

– a drill mounted on a stable stand. Borer's pressure was ensured by the load of 3.5 kg mounted on a 30 cm long arm. This resulted in the feed force of around 200 N, i.e. an average manual feed force – of a drill's operator;
– a meter (time-measurer), which automatically stopped measurements after the preset drilling time (60 s);
– an external stabilised power source, to which the drill and the meter were connected.

Test drilling was performed in beef bones, which were fixed in a vice to ensure appropriate stability. The drilling was performed in four cycles. During each cycle the drilling time which lasted 60 seconds, and the depth of individual holes were registered. After 60 seconds of drilling the sterilisation procedure was applied and the next drillings were carried out.

The sterilisation by steam was carried out in an ASVE type autoclave at $T = 134°C$ and pressure $p = 0.21$ MPa during 30 min.

Stereometric examinations of the borers flank were carried out by means of a FormTaly Series 2 profilographometer made by Taylor Hobson, applying the contact method. All operations and computations on the measurement files were performed by means of the TalyMap Universal software. The obtained file represented the original surface subject to further analysis and a stereometric description. The stereometricdescription of each measured specimen consisted of: visualisation (2D) using a photographic simulation; Abbott's curve (load capacity curve) together with a graphical interpretation of its basic parameters; isometric image (3D) of surface fragments.

The topography of studied borers was determined on the flank. For the specimens examined, 0.85 mm × 0.85 mm surface was the measurement area. The sampling interval in X and Y axis was 1 μm, the measuring speed was 0.5 mm/s.

3. Results of examinations

The obtained results of studies have shown that after 60 seconds of drilling (the first drilling cycle) the total depth of drilled holes amounted to 35.46 mm for Q + LT borers, 25.34 mm for Q + LT + N, and 28.74 mm for Q + HT + N borers. Instead, significant differences in the depth of drilled holes are visible after the fourth drilling cycle. After this

drilling time the depth amounted to 32.63 mm for Q + LT borers, 9.66 mm for Q + LT + N and 17.76 mm for Q + HT + N borers.

Stereometric measurements carried out on borers' flanks have shown substantial differences in the studied parameters (Fig. 2–4).

Quenching + low-temperature tempering (Q + LT)

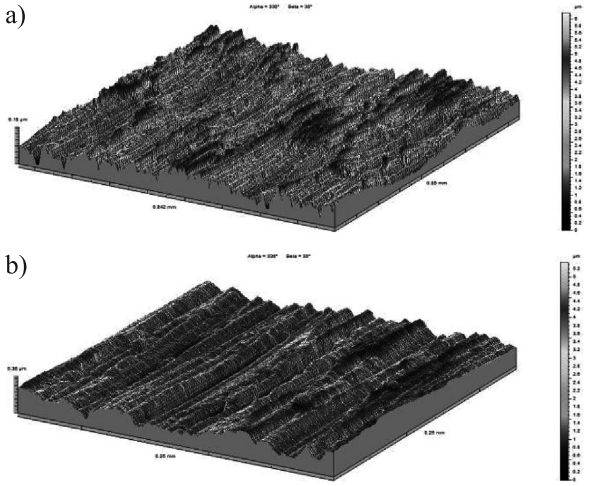

Fig. 2. The topography of borers flank after the fourth drilling cycle: isometric image (3D) of the studied surface (a) and enlargement of its selected fragments (b)

Quenching + low-temperature tempering + nitriding (Q+LT+N)

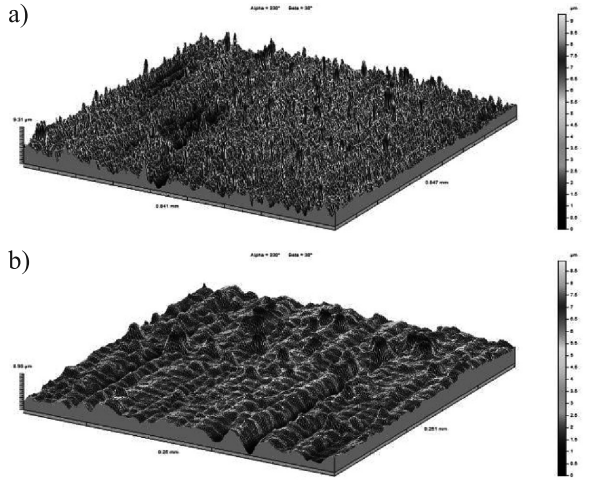

Fig. 3. The topography of borers flank after the fourth drilling cycle: isometric image (3D) of the studied surface (a) and enlargement of its selected fragments (b)

After the fourth drilling cycle the greatest wear of the studied surface was observed for Q + LT + N borers. The obtained 3D images show substantial differences in the topography of this layer. Local chippings of the nitrided layer are visible. These defects caused considerable blunting of borer's working part, which is proven by a smaller depth of the drilled holes. The application of plasma nitriding treatment to surgical borers is unfavorable, because on the one hand the borer edges blunt quickly, while on the other hand the chipped layer may get to the body and thereby cause adverse outcomes.

Quenching + high-temperature tempering +nitriding (Q + HT + N)

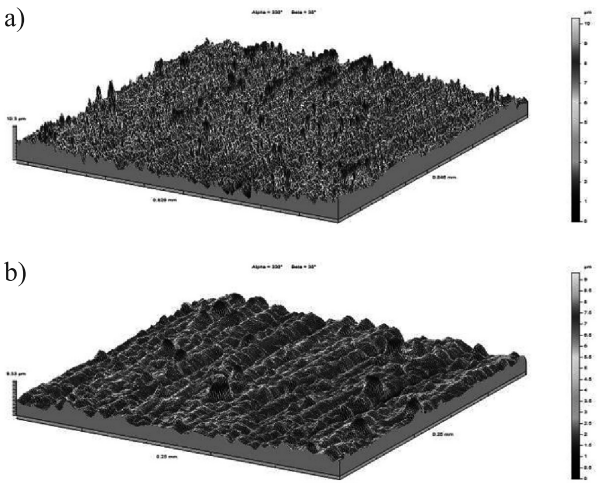

Fig. 4. The topography of borers flank after the fourth drilling cycle: isometric image (3D) of the studied surface (a) and enlargement of its selected fragments (b)

4. Summary of results

Heat and surface treated (plasma nitrided) borers used in bone surgery were analysed. The studies on the topography of borers flank after operation were carried out by means of a profilographometer, which allowed for a precise determination of the degree of borers wear. The studies have shown that the borers subject only to heat treatment were worn to a substantially lower degree than the borers with a nitrided layer. The obtained results have shown greater local chipping of the nitrided layer with previous low-temperature tempering (T = 300°C) as compared to high-temperature tempering (620°C). The application of plasma nitriding as a surface treatment for surgical borers is unfavourable due to the possibility of leaving nitrided layer chips in the body. Instead, such surface treatment may increase the operational life of instruments used in soft tissue surgery.

References

[1] Gwoździk M., Nitkiewicz Z., *Wear resistance of steel designed for surgical instruments after heat and surface treatments*, Archives of Metallurgy and Materials, **54** (1), 2009, 241-246.

[2] Szafarska M., Iwaszko J., *Laser remelting treatment of plasma-sprayed Cr_2O_3 oxide coatings*, Archives of Metallurgy and Materials, **57** (1), 2012, 215-221.

[3] Iwaszko J., *Surface remelting treatment of plasma-sprayed Al_2O_3+13wt.% TiO_2 coatings*, Surface & Coatings Technology, **201**, 2006, 3443-3451.

[4] Kulesza S., Bramowicz M., *A comparative study of correlation methods for determination offractal parameters in surface characterization*, Applied Surface Science, **293**, 2014, 196-201.

[5] Labisz K., *Microstructure and mechanical properties of high power diode laser (HPDL) treated cast aluminium alloys*, Materials Science and Engineering Technology, **45**, 2014, 314-324.

[6] Gwoździk M., *Evaluation of the surface condition of steel used for surgical instruments by means of atomic forces microscope (AFM)*, Engineering of Biomaterials, **89–91**, 2009, 74-76.

[7] Gwoździk M., *Optimization of heat and surface treatment of X39Cr13 steel designated for surgical instruments*, [in:] *Materials Engineering 2009, Material and exploitation problems in modern Materials Engineering*, Stradomski Z. (ed.), Wydawnictwo Wydziału Inżynierii Procesowej, Materiałowej i Fizyki Stosowanej Politechniki Częstochowskiej, Częstochowa 2009, 73-93.

[8] Gwoździk M., Nitkiewicz Z., *Topography of X39Cr13 steel surface after heat and surface treatment*, Optica Applicata, **39** (4), 2009, 853-857.

[9] Jagielska-Wiaderek K., *Depth-profiles of corrosion properties of carbonitrided AISI 405 steel*, Archives of Metallurgy and Materials, **57** (2), 2012, 637-642.

[10] Klimecka-Tatar D., Radomska K., Pawłowska G., *Corrosion Characteristics in Alkaline, and Ringer Solution of Fe68-xCoxZr10Mo5W2B15 Metalic Glasses*, Journal of the Balkan Tribological Association, **21** (1), 2015, 204-210.

[11] Augustin G., Zigman T., Davila S., Udilljak T., Staroveski T., Brezak D., S. Babic S., *Cortical bone drilling and thermal osteonecrosis*, Clinical Biomechanics, **27**, 2012, 313-325.

[12] Albertini M., Herrero-Climent M., Lázaro P., Rios J.V., Gil F.J., *Comparative study on AISI 440 and AISI 420B stainless steel for dental drill performance*, Materials Letters, **79**, 2012, 163-165.

[13] Marciniak J., *Biomateriały w chirurgii kostnej*, Wyd. Politechniki Śląskiej, Gliwice 1992 [in Polish].

[14] Paszenda Z., Tyrlik-Held J., *Instrumentarium Chirurgiczne*, Wyd. Politechniki Śląskiej, Gliwice 2003 [in Polish].

[15] Liu Y., Huang J., Niinomi M., Li H., *Inhibited grain growth in hydroxyapatite–graphene nanocomposites during high temperature treatment and their enhanced mechanical properties*, Ceramics International, **42**, 2016, 11248-11255.

TECHNICAL TRANSACTIONS | **CZASOPISMO TECHNICZNE**
MECHANICS | MECHANIKA
3-M/2016

AGATA WROŃSKA*, AGATA DUDEK**

FORMATION OF MICROSTRUCTURE AND PROPERTIES OF SINTERED STEEL THROUGH REMELTING OF SURFACE LAYER

KSZTAŁTOWANIE MIKROSTRUKTURY I WŁAŚCIWOŚCI STALI SPIEKANYCH POPRZEZ PRZETOPIENIOWĄ OBRÓBKĘ WARSTWY WIERZCHNIEJ

Abstract

This study presents the findings concerning the effect of remelting on microstructure and selected properties of sintered duplex steel. It was demonstrated that the methods of processing lead to homogenization and elimination of porosity in the surface layer of sinters, which substantially affects their properties (surface roughness, microhardness and resistance to friction wear). It was found that the degree of tribological wear in the steel used in the study depends primarily on the microstructure and phase composition and less on porosity.

Keywords: duplex sintered steel, *surface layer remelting*

Streszczenie

W artykule przedstawiono wyniki badań mających na celu określenie wpływu obróbki przetopieniowej na mikrostrukturę oraz wybrane właściwości warstwy wierzchniej spiekanych stali duplex. Wykazano, że zastosowana obróbka prowadzi do ujednorodnienia mikrostruktury oraz wyeliminowania porowatości w warstwie wierzchniej spieków, co istotnie wpływa m.in. na ich mikrotwardość oraz odporność na zużycie ścierne. Dowiedziono, że stopień zużycia tribologicznego badanych spieków zależy głównie od mikrostruktury oraz składu fazowego warstwy wierzchniej, natomiast w mniejszym stopniu od porowatości.

Słowa kluczowe: spiekane stale duplex, *przetapianie warstwy wierzchniej*

DOI: 10.4467/2353737XCT.16.128.5739

* Ph.D. Eng. Agata Wrońska, Polskie Zakłady Lotnicze Sp z o.o., ul. Wojska Polskiego 3, 39-300 Mielec.

** D.Sc. Ph.D. Eng. Agata Dudek, Assoc. Prof., Institute of Materials Engineering, Faculty of Production Engineering and Materials Technology, Czestochowa University of Technology.

1. Introduction

In the period of high demand on technologies and both cheap and ecological products, the increased interest in powder metallurgy and sintered goods in e.g. automotive industry seems to be justified. Although costs of the operation of production line for manufacturing sinters are high, the unit product price in serial production might be several times lower than in the case of a product manufactured with conventional methods [1–3]. In the case of stainless steel, mechanical properties can be considered as secondary, especially because porosity seems to be desirable in order to obtain a product with reduced mass. Porosity also substantially affects tribological properties of sintered steel [4]. This study proposes remelting processing by means of the GTAW welding methodology. The effects obtained were compared to the results of pulsed laser remelting. The idea and description of the method have been contained in e.g. [3]. The previous method of formation of surface layers has been used extremely rarely to develop surface layers on sintered duplex steel. Therefore, the authors aimed to describe microstructural changes in the surface layer of stainless steel, with particular focus on the evaluation of functional properties of sinters after remelting.

2. Materials and Methods

We used corrosion-resistant stainless steel obtained from water-atomized powders of 316L austenitic steel (16.7% Cr, 12.3% Ni, 0.9% Si, 0.1% Mn, 2.20% Mo, 0.025% C) and ferritic 434L steel (16.2% Cr, 0.98% Mo, 0.8% Si, 0.1% Mn, 0.015% C). The powders were mixed with the following proportions: 80% 316L + 20% 434L, 50% 316L + 50% 434L and 20% 316L + 80% 434L. The names of the sinters were adopted with regard to the proportions of powders: 80A-20F, 50A-50F, 20A-80F. The procedure of sinters preparation was described in detail in the study [3].

The microstructure of sinters revealed through etching in aqua regia was represented by a multi-phase structure, different than in the case of conventional duplex steel. The metallographic cross-sections showed light areas of austenite, grey areas of acicular component and dark cross-sections of pores. The percentage of the acicular component was approximately proportional to the percentage of ferritic steel 434 L. Porosity of the steel was examined by means of a quantitative method by means of Image Pro Plus software. Ten microscopic images of non-etched metallographic cross-sections were analyzed. Porosity of individual sinters was around 8%, 11% and 5%, respectively.

The sinters were subjected to arc surface remelting with the following parameters: current intensity from 30 A to 40 A, voltage ~10 V, feed rate 340 mm/min. Selection of the parameters was described in the study [3]. Pulsed laser remelting was carried out by means of impulse laser NdYAG according to the parameters chosen experimentally. Impulses with the power of 3.5 kW, 5 kW and 7.5 kW were generated by changing the degree of laser spot overlapping (from 50% to 90%). The laser spot diameter was 1.5 mm. This publication analyzed the examinations conducted for 50A-50F sinters after remelting with pulses with the power of 5 kW with overlapping of ~85%.

The effects of the remelting were initially evaluated based on macroscopic observations. Microstructural examinations were carried out on etched metallurgical cross-sections by means of Axiovert 25 metallurgical microscope.

Microhardness measurements used the Vicker's method with the load of 490 mN.

Examinations of friction wear resistance were carried out by means of T-05 block-on-ring wear tester in dry sliding contact. Test parameters were selected experimentally: $F_N \approx 49.05$ N, rotational speed of the roll: 3.55 rps. Test duration was 120 minutes (8 cycles for 15 minutes). Total friction distance was ~2809 m.

3. Results and Discussion

Microscopic observations were employed after remelting to examine specimen surface. In the case of sinters after GTAW method, further examinations involved remelting of samples with arc with intensity of 35 A and linear speed of 240 mm/min, for which no defects were found (i.e. craters, excessive penetration or lack of penetration). For pulsed laser remelting, the best surface quality was found for the specimen remelted with pulses with the power of 5 kW with overlapping of 85%. However, the surface of the specimen was characterized by substantially higher degree of surface development compared to arc remelting. The overlapping of individual laser spots on the sinter surface caused formation of flash, exhibiting a characteristic relief. This effect does not occur for arc remelting due to a continuous mode of tool operation, ensuring even the distribution of liquid metal across the remelted volume.

Microscopic observations revealed uniform microstructure in the surface layers of sinters after arc remelting (Fig. 1). The treatment was accompanied by the fast heat transfer and high gradient of temperature, which resulted in formation of the primary structure with columnar crystals oriented according to the direction of heat transfer (in sinters 80A-20F and 50A-50F). Microscopic examinations showed also epitaxial character of nucleation and growth of primary structure cells, initiated in the transition zone formed as a result of base material remelting. A cellular-dendritic structure was formed in the microstructure of surface

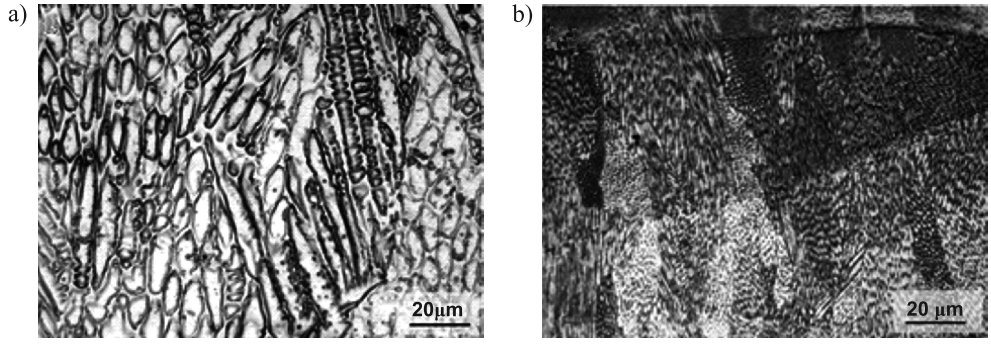

Fig. 1. Microstructure of surface layer for 50A-50F sintered steel after remelting: a) GTAW method, b) laser method

layer of 20A-80F sinter after arc remelting. Complete description of the microstructure of surface layer of the sinters after remelting was contained in the study [3].

In the case of 50A-50F sintered steel after laser remelting, a cellular-dendritic structure was formed on the surface layer. Cooling rate for laser treatment was by several orders of magnitude higher compared to the arc method, which consequently led to the formation of a much finer structure (Fig. 1b). Similar as in GTAW method, nucleation and growth of cells had also an epitaxial character. A clear transient zone was not observed. It was found that both methods ensured the development of a homogeneous surface layer without voids. Figures 1a, b show example images of microstructure of sinter surface layers (50A-50F) after remelting.

Measurements of microhardness (Fig. 2) supported the results obtained from the microscopic observations. Substantial variation in hardness, resulting from presence of various phases and structural components and pores was observed in the area of core material. Furthermore, an insignificant increase in hardness with respect to mean hardness of sinters in the initial state was observed for remelted layers, regardless of the method used. Insignificant deviations from mean values of microhardness (Fig. 2) suggest a substantial homogenization of the microstructure.

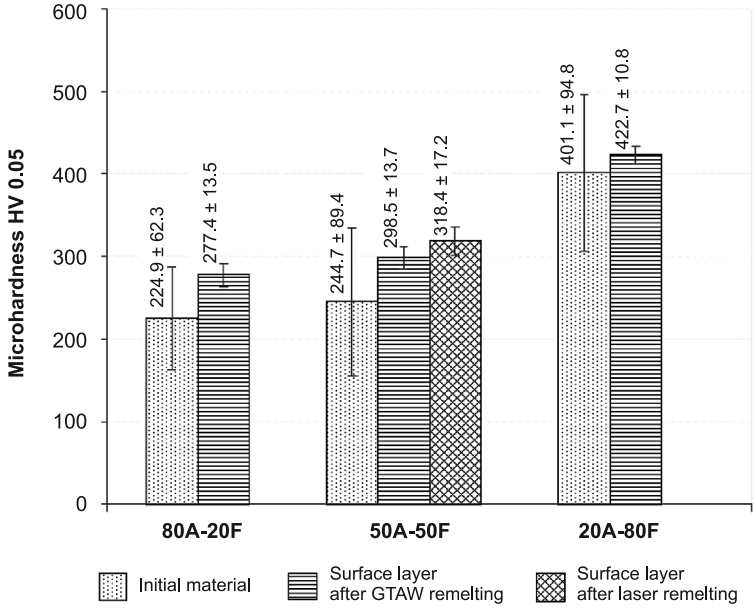

Fig. 2. Microhardness of sintered steel in the initial state and after remelting

Resistance to friction wear of sintered steels represents the effect of several factors, e.g. microstructure, hardness, porosity and surface quality. The studies have demonstrated that improved resistance to friction wear in the group of austenitic-ferritic sinters is observed for steels with non-homogeneous microstructure and higher hardness [2]. Fig. 3 presents the results of measurement of specimen mass reduction after tribological test.

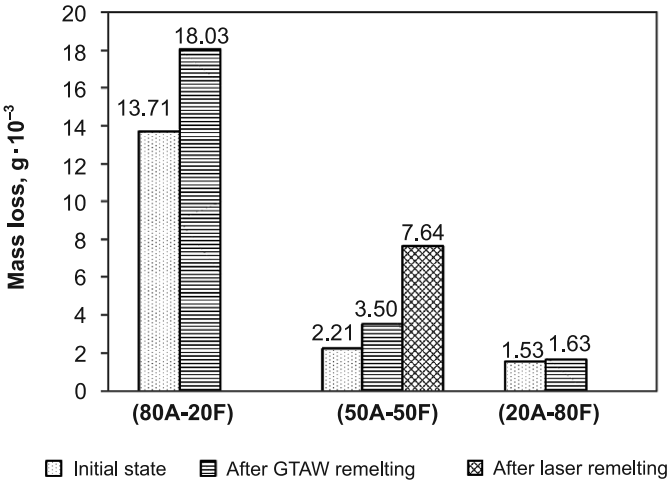

Fig. 3. Decrease in mass of sintered steel after examination of resistance to friction wear

Among the sinters remelted using GTAW method, the best resistance to friction wear was observed for (20A-80F) sinters, for which the reduction in mass after tribological test was 1.63 mg, whereas for sinters in the initial state, this value was 1.53 mg (Fig. 3). Higher reduction in mass was also observed for remelting of (80A-20F) and (50A-50F) sinters. Furthermore, the analysis of diagram in Fig. 3 shows a relationship: the resistance to friction wear was higher for higher percentage of ferritic steel powder in the sinter i.e. for higher hardness. In conclusion of the above observations, the most important factor that determined friction wear of sintered steel was microstructure and hardness of sinter, whereas porosity played the secondary role. The multi-phase acicular component present in the microstructure of sinters, with a relatively high hardness, is likely to have acted as an "inhibitor" of material wear. The substantial loss of mass of the specimen after laser treatment results not only from the homogenization of microstructure but also from the presence of unevenness (relief) on the contact surface of the specimen.

4. Conclusion

The remelting of sintered austenitic-ferritic steels leads to substantial changes in the microstructure of surface layer and, consequently, changes the properties of sinters. The findings presented in the paper, which represent a continuation of the investigations contained in [3], led authors to the following conclusions:

– Remelting is an adequate method for homogenization of microstructure, especially for the elimination of porosity in the surface layer area of sinters. Furthermore, GTAW method allows for the reduction in sinter roughness, whereas using the laser method results in the appearance of relief, which negatively affects tribological properties of sinters. It is recommended to perform additional finishing (e.g. rolling or burnishing) after pulsed laser remelting;

– The treatment used in the study leads to an insignificant increase in hardness in the surface layer of sintered steel;
– In order to improve resistance to friction wear of sintered steel, it is desirable to carry out remelting with the addition of an alloying element or compound.

References

[1] *Economic Considerations for Powder Metallurgy Structural Parts*, http://www.ipmd.net/Introduction_to_powder_metallurgy/Economic_Considerations.
[2] Martin F., Garcia C., Blanco Y., Aparicio M.L., *Tribocorrosion behavior of powder metallurgy duplex stainless steels sintered in nitrogen*, Tribology International, **57**, 2013, 76-85.
[3] Dudek A., Wronska A., Adamczyk L., *Surface remelting of 316L+434L sintered steel: microstructure and corrosion resistance*, Journal of Solid State Electrochemistry, **18**, 2014, 2973-2981.
[4] Ceschini L., Palombarini G., Sambogna G., Firrao D., Scavino G., Ubertalli G., *Friction and wear behaviour of sintered steels submitted to sliding and abrasion tests*, Tribology International, **39** (8), 2006, 748-755.

TECHNICAL TRANSACTIONS | **CZASOPISMO TECHNICZNE**
MECHANICS | MECHANIKA
3-M/2016

MARTA JAGUSIAK-KOCIK*

USE OF OVERALL EQUIPMENT EFFECTIVENESS INDICATOR FOR ANALYSIS OF WORK TIME OF TEST BENCH

WYKORZYSTANIE WSPÓŁCZYNNIKA OGÓLNEJ EFEKTYWNOŚCI URZĄDZENIA DO ANALIZY CZASU PRACY STACJI WZORCOWNICZEJ

A b s t r a c t

This article presents information about the Overall Equipment Effectiveness indicator – a key measure used in the Total Productive Maintenance. The research object has been characterized – test bench, which enables a simultaneous, multiposition calibration, adjustment and verification of single- phase or three- phase electricity meters. In the research part, the analysis of effectiveness of the test bench by means of TPM and Overall Equipment Effectiveness indicators was presented.

Keywords: Overall Equipment Effectiveness indicator, *test bench*, *calibration*, *adjustment*, *verification*

S t r e s z c z e n i e

W artykule zaprezentowano informacje dotyczące Całkowitej Efektywności Urządzenia – kluczowego miernika stosowanego w Kompleksowym Utrzymaniu Maszyn TPM. Scharakteryzowano obiekt badawczy – stację wzorcowniczą, która umożliwia jednoczesną, wielostanowiskową kalibrację, adiustację i legalizację jednofazowych i trójfazowych liczników energii elektrycznej. W części badawczej zaprezentowano analizę efektywności stacji wzorcowniczej z zastosowaniem współczynników TPM i współczynnika Całkowitej Efektywności Urządzenia.

Słowa kluczowe: współczynnik Całkowitej Efektywności Urządzenia, *stacja wzorcownicza*, *kalibracja*, *adiustacja*, *legalizacja*

DOI: 10.4467/2353737XCT.16.129.5740

* Ph.D. Eng. Marta Jagusiak-Kocik, Institute of Production Engineering, Faculty of Management, Czestochowa University of Technology.

1. Introduction

THE Overall Equipment Effectiveness OEE indicator [1–3] is a primary measure used in the Total Productive Maintenance, which is applied to evaluate the current state of technical objects. Any company producing a specific product, in response to customer needs, gives it a certain value. Effective adding value requires an effective use of technical objects, so that they bring the least losses (breakdown, changeover, micro-stoppages, reduced speed, quality defects, startup). The Overall Equipment Effectiveness OEE indicator includes not only the number of products that can be produced by a machine in a specified time frame [3, 4]. Calculation of the machine performance indicator that is the comparison between the actual volume of production and the volume of production planned (among others resulting from the established technology) is one of the elements of the Overall Equipment Effectiveness OEE indicator. Furthermore, this indicator includes the comparison of a potential machine operating time of machine with the time in which the machine is actually used for the production – it calculates the availability indicator of a machine and the quality indicator by comparing the amount of manufactured products and the quantities of products that meet customer's requirements. Multiplying the indicator of performance, availability and quality results in obtaining the Overall Equipment Effectiveness OEE indicator, which is expressed as a percentage [3, 4]. It can be attributed to individual machines, production positions or the whole assembly lines.

2. Characteristics of the research object

Test bench is a device that enables a simultaneous, multiposition calibration, adjustment and verification of single- phase or three- phase electricity meters. Calibration is an action which in certain conditions, firstly determines the relationship between mapped by the standard measurement of values quantity with their measurement uncertainties and the corresponding indications with their uncertainties and, secondly, uses this information to determine the relationship that allows to get results measurement based on the indication. A protocol, calibration function, calibration diagram, calibration curve, or calibration table can be the result of the calibration [5]. The adjustment of a measuring system is a set of activities performed by means of a measuring system to ensure that the values quantity, which they have to be measured, corresponds to the correct indication. The adjustment of a measuring system should not be confused with calibration, which is the prerequisite [5]. Verification is a set of activities involving checking, statement and certifying the proof of verification that the measuring instrument complies with the requirements [6].

Test bench consists of the following components: rack with the quick fixing device system, 3 current sources, 3 voltage sources, reference standard meter (meter used to measure the unit of electricity. It is generally constructed and used in a way to obtain the highest accuracy and stability properties in a controlled laboratory environment [7]), errors calculators and photoelectric scanning heads, separating transformers, computer with control software.

To determine the error of the tested meters, test bench uses the method of reference standard meter. The principle of this method involves a simultaneous measurement of energy by the tested meters and by the reference standard meter. An error of the tested meter is determined by comparing the number of impulses generated by the reference standard meter with the number of impulses which correspond to measured energy from tested meters. Photoelectric scanning head detects the movement of the electromechanical meter disc (identification of black spots on the disc of the meter) or the LED flash of the tested static meter (electronic). During the test, the circuits of the tested meters are serial connected in different phases and operate at the same voltage values and phase shifts. The control software provides automation of the process and prevents interference in the operation of the process.

Figure 1 presents a 6-position test bench with components [10].

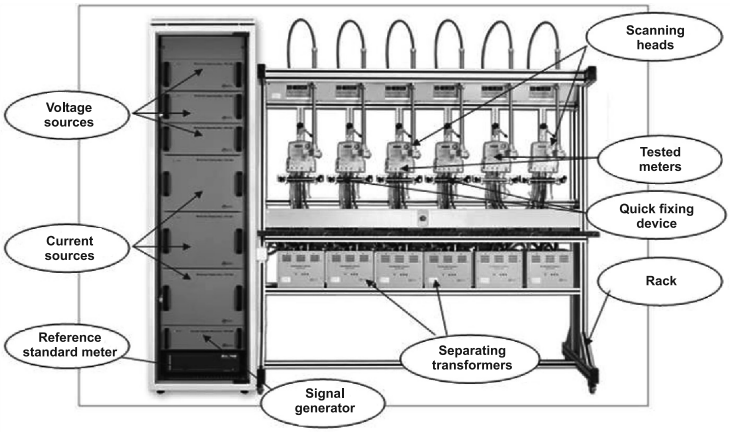

Fig. 1. A 6-position test bench with components [10]

According to the Decree of the Minister of Economy of 7 January 2008 [8] errors of static meters are tested according to the following rules (Table 1).

Table 1

The maximum permissible errors of indications and load points of static meter

Type of meter **and load**	**Load point**		**The maximum permissible errors of meters indications expressed in [%] for accuracy classes**		
	Load current	**Power factor cos φ**	**C**	**B**	**A**
Single phase meters	0.1 I_b	1	± 0.5	± 1.0	± 2.0
	I_b	1	± 0.5	± 1.0	± 2.0
	I_b	0.5(inductive)	± 0.5	± 1.0	± 2.0
	I_{max}	1	± 0.5	± 1.0	± 2.0

Three phase meters loaded symmetrically	0.1 I_b	1	± 0.5	± 1.0	± 2.0
	0.5 I_b	1	± 0.5	± 1.0	± 2.0
	0.5 I_b	0.5(inductive)	± 0.5	± 1.0	± 2.0
	I_b	1	± 0.5	± 1.0	± 2.0
	I_b	0.5(inductive	± 0.5	± 1.0	± 2.0
	I_{max}	1	± 0.5	± 1.0	± 2.0
Three phase meters with a load of only one phase	I_b	1	± 1.0	± 2.0	± 3.0
	I_b	0.5(inductive)	± 1.0	± 2.0	± 3.0

Base current I_b – current value, for which important characteristics of the meter are determined [8], e.g. for transformer meters is rated current.
Maximum current I_{max} – the highest value of current at which a meter error in the reference conditions does not exceed the maximum permissible errors [8].

During the verification of meters of active electricity for alternating current, single-phase and three-phase meters, induction meters and static meters, accuracy class 0.5; 1 and 2, are used according to the requirements corresponding to classes C, B and A [9].

3. Analysis of the effectiveness of test bench by means of OEE indicator

The analysis of effectiveness of the use of test bench time work [1–4, 11–13], by means of the Overall Equipment Effectiveness OEE indicator was carried out during the last 12 weeks of 2015 year.

Table 2 presents the summary of test results of the effectiveness of 24-position test bench, which makes a verification of three- phase meters of C class to indirect measurements (with the meters assembly in a quick fixing device system).

Table 2

Analysis of the effectiveness of the test bench in 12 weeks

Research period [week]	TZ. Shift fund of the working time [h]	Planned time of machine stoppage [h]	Work time [h]	Unplanned stoppage of machine [h]	Time of the net exploitation [h]	WD. Availability indicator [%]	Production [unit]	Ideal time per unit [h\unit]	Actual time per unit [h\unit]	WPD. Speed working indicator [%]	WW. Performance indicator [%]	Number of failures [unit]	WJ. Quality indicator [%]	OEE. Overall Equipment Effectiveness [%]
1	80	0	80	0	80	100.00	480	0.163	0.167	97.80	97.80	0	100.00	97.80
2	80	0	80	0	80	100.00	480	0.163	0.167	97.80	97.80	0	100.00	97.80
3	80	0	80	0	80	100.00	480	0.163	0.167	97.80	97.80	0	100.00	97.80
4	80	0	80	0	80	100.00	480	0.163	0.167	97.80	97.80	0	100.00	97.80

5	64	0	64	0	64	100.00	384	0.163	0.167	97.80	97.80	0	100.00	97.80
6	80	8	72	0	72	100.00	432	0.163	0.170	95.88	97.80	0	100.00	97.80
7	80	0	80	0	80	100.00	480	0.163	0.167	97.80	97.80	0	100.00	97.80
8	80	0	80	0	80	100.00	480	0.163	0.167	97.80	97.80	0	100.00	97.80
9	80	0	80	8	72	90.00	432	0.163	0.170	95.88	97.80	0	100.00	88.02
10	80	0	80	0	80	100.00	480	0.163	0.169	96.45	97.80	0	100.00	97.80
11	48	0	48	0	48	100.00	288	0.163	0.169	96.45	97.80	0	100.00	97.80
12	48	8	40	0	40	100.00	240	0.163	0.169	96.45	97.80	0	100.00	97.80

Graphic interpretation of the selected indicators is showed in Fig. 2.

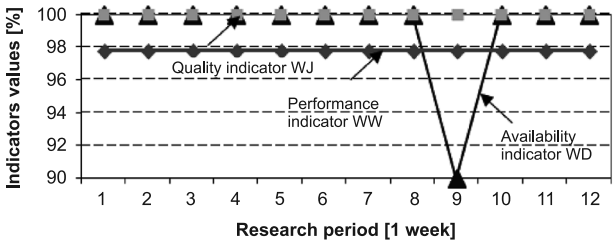

Fig. 2. Graphic interpretation of the availability indicator, performance indicator and quality indicator in the research period for test bench

From the data presented in Table 2 and Fig. 2 it can be concluded that the availability, performance and quality indicators are at a high level, which exceeds 90%. The availability indicator amounts to 100% for all weeks except week 9, where there were unplanned stops of the machine. The performance indicator for all weeks is at the level above 97% and the quality indicator amounts to 100% for all weeks.

Figure 3 presents a graphical interpretation of the Overall Equipment Effectiveness indicator for the test bench in the research period of 12 weeks.

From Fig. 3 it can be concluded that the Overall Equipment Effectiveness indicator is at a very high level, which exceeds 97%, except 9 week, where the OEE decline was caused by the unplanned stops of test bench.

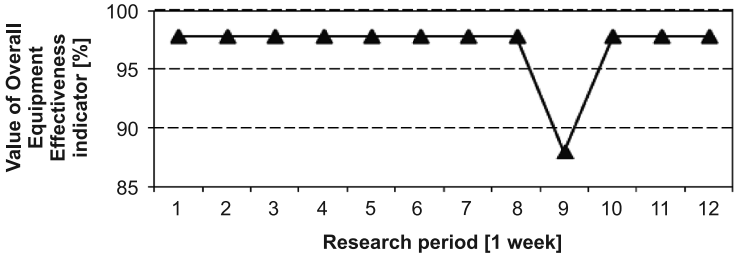

Fig. 3. Graphic interpretation of the Overall Equipment Effectiveness indicator for test bench in the research period

4. Conclusion

To calculate the effectiveness of the use of test bench time work, the Overall Equipment Effectiveness OEE indicator was used. It allowed for evaluating the current state and "condition" of test bench. Thanks to this analysis it can conclude on further activities related to the maintenance of these machines and activities related to the improvement.

The Overall Equipment Effectiveness OEE indicator for test bench is very high and exceeds 97% (except 9 week). The results suggest low losses related to the working time of test bench (only in the ninth analyzed week were was an unplanned machine downtime), the speed of the machine work shows a slight loss of just over 2%. In the analyzed period of 12 weeks there were no losses associated with quality. Such a high indicator of the Overall Equipment Effectiveness for test bench results from, among others, a close cooperation of operators and workers from the maintenance department, training systems and effective supervision by the authorities of legal metrology (Offices of Measures). The reliable and modern design of the test bench, automation of the process and its documentation, application of software with a database of types of meters and passes and control of the course of the verification process are factors which contribute to the high level of the Overall Equipment Effectiveness indicator.

References

[1] Borkowski S., Selejdak J., Salamon Sz., *Efektywność eksploatacji maszyn i urządzeń*, Sekcja Wydawnictw Wydziału Zarządzania Politechniki Częstochowskiej, Częstochowa 2006, 192-195 [in Polish].

[2] Borkowski S., Ulewicz R., *Zarządzania produkcją. Systemy produkcyjne*, Oficyna Wydawnicza „Humanitas", Sosnowiec 2008, 213-216 [in Polish].

[3] The Productivity Press Development Team, *OEE dla operatorów. Całkowita Efektywność Urządzenia*, Wydawnictwo ProdPress, Wrocław 2009, 12-13 [in Polish].

[4] *Wskaźnik OEE – Teoria i praktyka. wydanie II*, http://www.neuron.com.pl/pliki/oee.pdf (date of acc. 15.06.2016).

[5] *Międzynarodowy Słownik Terminów Metrologii Prawnej*, https://www.gum.gov.pl/media/473882/mi_dzynarodowy_s_ownik_termin_w_metrologii_prawnej.pdf (date of acc.: 15.06.2016).

[6] *Prawo o miarach z dnia 11 maja 2001 r.* (Dz.U. Nr 63, poz. 636) [in Polish].

[7] Norma PN-EN 50470-1:2008 Urządzenia do pomiarów energii elektrycznej (prądu przemiennego). Część 1: Wymagania ogólne, badania i warunki badań. Urządzenia do pomiarów (klas A, B i C).

[8] *Rozporządzenie Ministra Gospodarki z dnia 7 stycznia 2008 r. w sprawie wymagań, którym powinny odpowiadać liczniki energii elektrycznej prądu przemiennego, oraz szczegółowego zakresu sprawdzeń wykonywanych podczas prawnej kontroli metrologicznej tych przyrządów pomiarowych* (Dz.U. 2008 nr 11 poz. 63) [in Polish].

[9] MID – Measuring Instruments Directive – Directive 2004/22/EC of the European Parliament and of the Council of 31st March 2004 on measuring instruments.

[10] Materiały Firmy MeterTest Sp. z o.o., http://www.meter-test-equipment.com/ [date of acc. 15.06.2016].

[11] Jagusiak M., Borkowski S., Mielczarek K., *Effectiveness exploitation of autoclave basing on the TPM coefficients*, [in:] Borkowski S., Kročko V. (eds.), *TPM and PAMCO as basis of estimation*

of machines exploitation efficiency, Publishing and Press Association of Universities Russia Saint Petersburg, Saint Petersburg 2008, 101-106.

[12] Krynke M., Knop K., Mielczarek K., *Analysis of the modernity and effectiveness of chosen machines in the processing of high-molecular materials*, Production Engineering Archives, **3** (2), 2014, 18-21.

[13] Zasadzień M., *Wpływ implementacji kart przeglądów na wydajność maszyn w wybranym przedsiębiorstwie produkcyjnym*, Management Systems in Production Engineering, **4** (20), 2015, 225-229.

TECHNICAL TRANSACTIONS | CZASOPISMO TECHNICZNE
MECHANICS | MECHANIKA
3-M/2016

KLAUDIA RADOMSKA*, GRAŻYNA PAWŁOWSKA*,
DOROTA KLIMECKA-TATAR**

THE EFFECT OF CORROSION PROCESS ON THE SURFACE TOPOGRAPHY OF Nd–Fe–B TYPE MAGNETS BONDED WITH BIOPOLIMER

WPŁYW PROCESU KOROZYJNEGO NA TOPOGRAFIĘ POWIERZCHNI MAGNESÓW TYPU Nd–Fe–B WIĄZANYCH BIOPOLIMEREM

Abstract

The article presents the results of surface topography measurements of the Nd–Fe–B type bonded magnetic material before and after the corrosion test in aggressive environments. The roughness of composite materials is closely related to the technological process. The increase in values of surface roughness parameters weakens the corrosion resistance by development of the actual surface and increases the contact surface with corrosive media. The results are a contribution to further work on the selection of appropriate technological parameters – among others enlargement of the bio-polymer content which contributes to the homogenisation of powder composition and thus has a beneficial effect on the resistance of material to an aggressive environment in a long-term use.

Keywords: bonded magnets, *corrosion*, *surface roughness*

Streszczenie

W artykule przedstawiono wyniki badań topografii powierzchni wiązanego materiału magnetycznego Nd–Fe–B przed i po teście korozyjnym w agresywnym środowisku. Chropowatość materiałów kompozytowych tego typu jest ściśle związana z procesem technologicznym. Większa chropowatość powierzchni osłabia odporność korozyjną wskutek zwiększenia rzeczywistej powierzchni styku korodującego elementu z medium korozyjnym. Wyniki są przyczynkiem do dalszych prac nad doborem odpowiednich parametrów technologicznych. M.in. zwiększenie zawartości spoiwa biopolimerowego przyczyniłoby się do zwiększenia homogenizacji kompozycji proszkowej, a tym samym do zwiększenia odporności materiału na działanie agresywnego środowiska przy dłuższej eksploatacji.

Słowa kluczowe: magnesy wiązane, *korozja*, *chropowatość powierzchni*

DOI: 10.4467/2353737XCT.16.130.5741

* M.Sc. Eng. Klaudia Radomska, D.Sc. Ph.D. Eng. Grażyna Pawłowska, Assoc. Prof., Deptartment of Chemistry, Faculty of Production Engineering and Materials Technology, Częstochowa University of Technology.

** Ph.D. Eng. Dorota Klimecka-Tatar, Institute of Production Engineering, Faculty of Management, Częstochowa University of Technology.

1. Introduction

In the era of dynamic development of computers, electronics and automation there has been a steady growth of interest in magnetic materials. The most commonly used materials are hard magnetic materials based on rare earth (RE) and transition metals (M) [1–2]. This group includes, among others, Nd–Fe–B neodymium magnets with unique magnetic properties due to the presence of $Nd_2Fe_{14}B$ ferromagnetic phase. The sintering with liquid phase and the consolidation of high-coercive powders with polymeric binders are among the most commonly used methods of preparing these kind of materials. Sintered materials are characterized by poor resistance to corrosion due to the high content of highly active rare earth element $E^0_{Nd_3+/Nd} = -2,43\ V)$ [3]. These features restrict their use and reduce the life of devices they are part of. Bonded RE-M-B material with lower content of rare earth element obtained in the form of a high-coercive powder [4] is an alternative to sintered materials. These powders, because of the high affinity of oxygen to neodymium, oxidize both in the manufacturing and storage process [5]. The presence of oxide layers on the surface of powder particles may adversely affect the process of consolidation. Insufficiently tight, weakly adhering adhesive coating makes the final material more porous, exhibits inferior magnetic properties and corrosion resistance [6, 7]. In papers [7−9] it has been concluded that loosely connected oxide products can be removed in the process of etching, and then the cover of the surface of powder particles can be coated with a coating and/or bonding material (encapsulation or biencapsulation).

As it has been shown in the studies [7−9] bonding of magnetic powder with the epoxy resin (encapsulation) provides a suitable consistency of the material. However, considering the use of materials in medicine and prosthetics, the epoxy resin is not a suitable binder. The replacement of an epoxy resin with biopolymer does not decrease the magnetic parameters[10]. A suitable binder content can contribute to the increase in homogenization of powder composition, and thus to minimize the occurrence of voids and open pores between metal particles and to smoothen the surface. Surface roughness is recognizable visually or it is mechanically reflected as surface roughness, not due to its shape [11].

The aim of this study was to analyze the surface of a bonded magnetic material (RE-M-B powder consolidated with biopolymer) before and after exposure to aggressive corrosive media.

2. Material preparation

The bonded magnetic materials were prepared from powder $Nd_{12}Fe_{77}Co_5B_6$ (commercial MQP-B, Magnequench). The powder was produced by rapid solidification from the liquid alloy. In the process, the amorphous strip is mechanically ground, and in order to obtain a nanocrystalline structure undergoes heat treatment at the temperature of approximately 600°C. Powder particles surface etching in a 5% aqueous solution of oxalic acid were the preliminary stage of specimens preparation. To protect the etched powder surface against atmospheric agents in the later stages of sample preparation, the encapsulation processes

were used – coating with biopolymer. The composition content was 5% mass. of bio-polymer binder and 95% mass. of magnetic powder.

3. Research methodology

Potentiokinetic polarization curves were performed in 0.5 M sulphate solution (pH = 2). Electrochemical studies were carried out by means of: potential scanning 10 $mV \cdot s^{-1}$ (the potential was changed from the cathode to the anode value (E = –0.8 ÷ 0.8 V vs. SCE), rotation speed of 16 rev s^{-1} (the test samples were in the form of a rotating discs).

The surface roughness analysis was carried out by means of a contact profilometer (Taylor Hobson) and the measurement distance was 4 mm for each sample. During the measurement, the recorded profile which was plotted on the Abbott'a curve indicated a high density altitude on the unit area for sample, participation of surface vertices and distribution of their size as well as the values of stereometric parameter (Rp − maximum peak height, Rv − maximum valley depth, Rz − maximum height of the roughness profile − based on the five highest peaks and lowest valleys over the entire sampling length, Rc − average height of roughness profile elements, Rt − maximum height of the profile, Ra − arithmetic average of absolute values, Rq − Root mean square deviation of the roughness profile).

4. Experimental

Based on the analysis of potentiokinetic curve obtained in the sulphate solution acidified to pH = 2, it can be concluded that the magnetic material of chemical formula $Nd_{12}Fe_{77}Co_5B_6$ undergoes active digestion, and there is not any observed trendof passivation (there is no passive range) and after exceeding the corrosion potential ($E_{corr} \approx$ –0,68 V), the corrosion current continuously increases with the potential increase (Fig. 1).

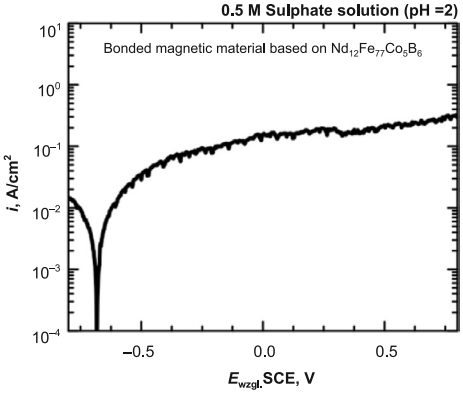

Fig. 1. The potentiokinetic polarization curves for samples obtained from $Nd_{12}Fe_{77}Co_5B_6$ powder encapsulated with biopolymer measured in 0.5 M sulfate solution acidified to pH = 2 (10 $mV \cdot s^{-1}$, 16 $r \cdot s^{-1}$, 20°C) – powder consolidated with biopolymer

The potentiokinetic studies have been complemented by roughness measurements by means of a profilographometer with a pin base and head provided with an inductive transduceras. The measurements were carried out before and after the contact of sample surface with an aggressive environment. The computer system has enabled a complete analysis of the surface of magnetic material. The surface material was measured in 2D and then recorded the operating distance of the profile. Fig. 2 shows an example of the surface profile registered in an electrochemical test.

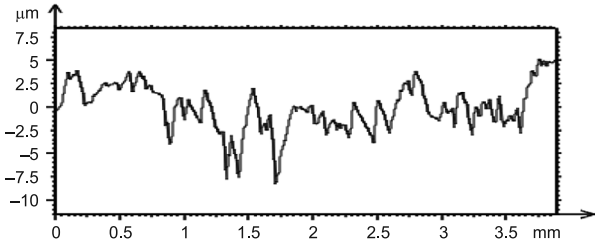

Fig. 2. Profile of operating distance registered for the bonded magnetic material – $Nd_{12}Fe_{77}Co_5B_6$ powder bonded with biopolymer

Roughness parameters from each of the isolated profile were calculated before (sample 1) and after exposition to the sulphate solution acidified to pH = 2 (sample 2) (Tab. 1), statistical analysis was used and the obtained results were compared in Table 3 and Fig. 3.

Table 1

The values of roughness parameters for $Nd_{12}Fe_{77}Co_5B_6$ bonded magnetic material – powder bonded with biopolymer

Symbol	Rp, µm	Rv, µm	Rz, µm	Rc, µm	Rt, µm	Ra, µm	Rq, µm
Sample 1	2.8 ± 0.8	3.3 ± 0.9	6.1 ± 1.6	3.3 ± 0.5	7.9 ± 2.3	1.0 ± 0.2	1.3 ± 0.3
Sample 2	7.9 ± 0.7	10.8 ± 0.6	18.6 ± 1.2	10.1 ± 0.1	22.9 ± 0.6	3.6 ± 0.4	4.4 ± 0.3

The Ra parameter values for the measured surface of magnetic materials based on $Nd_{12}Fe_{77}Co_5B_6$ are Ra = 1.04 (±0.18). and the values of roughness are well tolerated even by

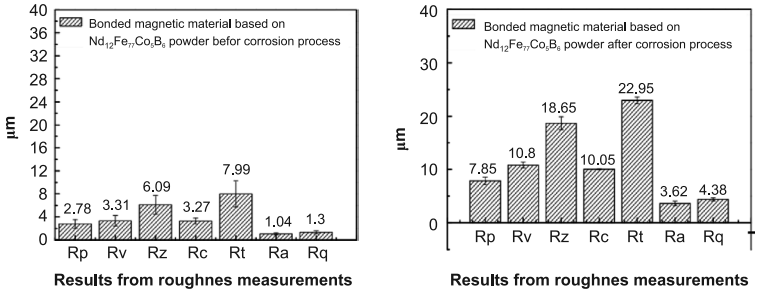

Fig. 3. Selected parameters of the surface profile for $Nd_{12}Fe_{77}Co_5B_6$ bonded magnetic material (powder bonded with biopolymer): a) before corrosion test, b) before corrosion test

cells in the body (Ra < 4 μm [11]). Also other parameters of altitude are relatively low, which is closely correlated with favorable functional properties of the material [12].

The $Nd_{12}Fe_{77}Co_5B_6$ bonded magnetic material (powder bonded with biopolymer) was subjected to a 10-minute (dry contact) exposure to aggressive environments – sulphate acidified to pH = 2 solution (accelerated corrosion test). As it was concluded in work [12], height roughness parameters have the greatest impact on the intensity of corrosive wear surface and for the tested material these parameters increased after the accelerated corrosion test − revealing a significant development of the area. Particular increases were recorded for parameters Rt and Rz (overall and maximum height of roughness profile) (Tab. 3, Fig. 3b).

The increase in other parameters of height Rp (the maximum height profile). Rv (the maximum depth of the Valley) and Rc (the average height of profile elements) also points to the dominance of deeper valleys, which is associated with a progressive deterioration of surface material. Despite relatively low values of roughness parameters of the material, (sample 1) in a structure there may be present discontinuities which in aggressive environmental conditions are associated with an increased susceptibility to corrosion. However, it should be noted that even after corrosion processes, the Ra value is still less than 4 μm.

The elevation distribution of the magnetic material surface and the Abbott curve (unfiltered individual parameters) were also recorded before and after the corrosion test (Fig. 4).

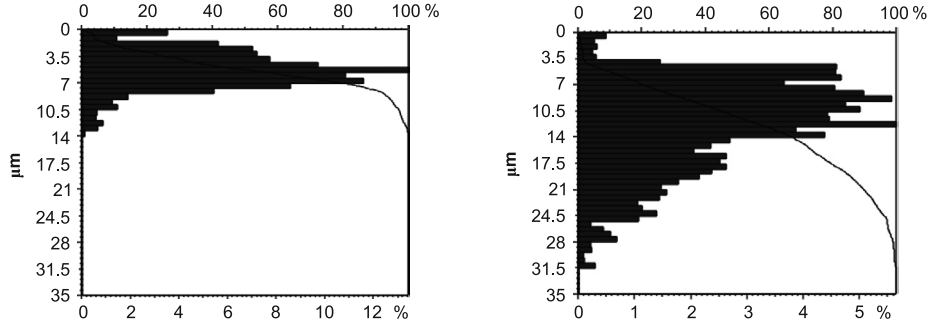

Fig. 4. Abbott curve and distribution of surface elevations for $Nd_{12}Fe_{77}Co_5B_6$ bonded magnetic material (powder bonded with biopolymer): a) before corrosion test, b) before corrosion test

The resulting elevations distribution of tested material surface after the corrosion test (Fig. 4b) testifies to surface development and progressive degradation into the material (to the depth of 30 m).

5. Conclusion

The tested composite – the $Nd_{12}Fe_{77}Co_5B_6$ bonded magnetic material (powder bonded with biopolymer) was actively digested in aggressive corrosive media (acidified to pH = 2 sulfate solution). As a result of this process, the surface of the material degraded as evidenced

by the increase in the height of roughness parameters. The results indicate a further direction of research – a change in process parameters (pressure, binder content, increasing the adhesion of powder particles to the binder) − which would allow for obtaining a material with favorable roughness parameters.

References

[1] Jiles D.C., *Recent advances and future directions in magnetic materials*, Acta Materialia, **51**, 2003, 5907-5939.

[2] Jiles D.C., Lo C.C.H., *The role of new materials in the development of magnetic sensors and actuators*, Sensors and Actuators, A **106**, 2003, 3-7.

[3] Pourbaix M., *Atlas d'equilibres electrochimiques*, Gautier–Villars, Paris 1963.

[4] Pawłowska G., *Procesy korozyjne materiałów magnetycznych typu RE–Fe–B otrzymanych różnymi metodami*, Monografia, nr 10, Politechnika Częstochowska, Częstochowa 2011 [in Polish].

[5] Klimecka-Tatar D., Pawłowska G., Szymura S., *Enkapsulacja jako skuteczny sposób zapobiegania utlenianiu proszków w technologii magnesów wiązanych*, Ochrona przed korozją, **11**, 2010, 585-588 [in Polish].

[6] Klimecka-Tatar D., Bala H., Pawłowska G., *Wpływ modyfikacji powierzchni nanokrystalicznych cząstek proszku $Nd_2(Fe.Co)_{14}B$ na charakterystyki korozyjne magnesów wiązanych*, Ochrona przed korozją, **4–5**, 2010, 43-47 [in Polish].

[7] Klimecka-Tatar D., Bala H., Gęsiarz K., *Wpływ powierzchni nanokrystalicznej proszków na trwałość warstwy pasywnej uzyskanej na materiale MQP-B spajanym żywicą*, Hutnik, **73** (1–2), 2007, 26-29 [in Polish].

[8] Klimecka-Tatar D., Pawłowska G., Szymura S., Radomska K., *Wpływ bienkapsulacji proszków Nd–(Fe.Co)–B powłokami Ni–P na odporność korozyjną magnesów wiązanych w sztucznej ślinie i roztworze Ringera*, Ochrona przed korozją, **11**, 2012, 505508 [in Polish].

[9] Pawłowska G., Klimecka-Tatar D., Mazik A., *Wpływ bienkapsulacji proszków $Nd_{12}Fe_{77}Co_5B_6$ na kinetykę roztwarzania materiałów wiązanych w zakwaszonych roztworach siarczanowych*, Hutnik, Wiadomości Hutnicze, **5**, 2013, 398-403 [in Polish].

[10] Radomska K., Klimecka-Tatar D., Pawłowska G., *Effect of the powder consolidation with biopolymer on the corrosion characteristics of bonded magnets based on Nd–(Fe.Co)–B*, Ochrona przed korozją, **4**, 2016, 128-131.

[11] Tubielewicz K., Krajewska M., Zaborski A., Chmielik I.P., Michalczuk H., *Chropowatość powierzchni implantów stomatologicznych*, Inżynieria Stomatologiczna – Biomateriały, **10** (1), 2013, 37- 44 [in Polish].

[12] Grzesik W., *Możliwości prognozowania właściwości eksploatacyjnych części maszyn na podstawie cech topografii powierzchni*, Mechanik, 8–9/2015, 2015, 775-786 [in Polish].

TECHNICAL TRANSACTIONS | CZASOPISMO TECHNICZNE
MECHANICS | MECHANIKA
3-M/2016

MARTA NICIEJEWSKA*, DOROTA KLIMECKA-TATAR*

EVALUATION OF STATIC LOAD IN DENTISTS' WORK BY MEANS OF OWAS METHOD

OCENA OBCIĄŻENIA STATYCZNEGO W PRACY LEKARZA STOMATOLOGA ZA POMOCĄ METODY OWAS

Abstract

In this study, the work of the dentist and the identification of musculoskeletal disorders have been characterized. The analysis and compatibility with literature on the identification of musculoskeletal disorders resulting from professional work of dentists have been presented. The authors assessed the occupational risks associated with static load on the position of the dentist by means of the OWAS method.

Keywords: risk, *dentist*, *work*, *security*, *OWAS*

Streszczenie

W niniejszym artykule scharakteryzowano pracę lekarza stomatologa oraz dokonano analizy literaturowej dotyczącej identyfikacji dolegliwości mięśniowo-szkieletowych będących skutkiem pracy zawodowej lekarzy stomatologów. Autorzy pracy dokonali oceny ryzyka zawodowego związanego z obciążeniem statycznym na stanowisku lekarza stomatologa z zastosowaniem metody OWAS.

Słowa kluczowe: ryzyko, *lekarz stomatolog*, *praca*, *bezpieczeństwo*, *OWAS*

DOI: 10.4467/2353737XCT.16.131.5742

* M.Sc. Eng. Marta Niciejewska, Ph.D. Eng. Dorota Klimecka-Tatar, Institute of Production Engineering, Faculty of Management, Czestochowa University of Technology.

1. Introduction

Professional work is related to a variety of risks for the employee. One of the most common threats in recent years – both in Poland and other European Union countries – is the exposure to musculoskeletal disorders. This health problem is also – according to the European Agency for Safety & Health at Work (EU-OSHA) – a significant cause of absence from work [1]. Ailments of the musculoskeletal system may occur in various occupational groups. According to studies conducted by the European Foundation for the Improvement of Living and Working Conditions (Eurofound), in the last decade in the European Union, a group of the following professional sectors is most exposed to musculoskeletal disorders: agriculture and fishing, industry, hospitality and civil engineering [2]. In Poland, there is no data that would give the answer to the question of how many people in the workplace are exposed to a risk factor of musculoskeletal disorders. However, it has been estimated that these symptoms occur most often in the industry, agriculture and fishing. Many studies also point to the high prevalence of musculoskeletal disorders among health care professionals, especially nurses, physiotherapists, surgeons and, finally, dentists [3]. The work of the dentist is mainly static – static effort is predominant in relation to dynamic effort. Its inconvenience is caused by monotypic exercise stress directed to the same elements of skeletal system, joints and muscles, which is often forced body position. According to literature [4], the range of dentists' professional activities is quite broad and includes not only dental treatment, but also prevention and rehabilitation of dentistry.

It is possible to see the effect of prevention if the evaluation of musculoskeletal disorders is done correctly, is relatively simple, clear and regards the position of entire body. OWAS is such a method, and it was used in this assessment of musculoskeletal disorders in the dentists' work.

2. Risk assessment of musculoskeletal disorders by means of the OWAS method

The risk evaluation of developing disorders of the musculoskeletal system on the dentist position has been carried out based on the OWAS method (Ovako Working Posture Analysis System). This method is one of the simplest and most commonly used methods for assessing the risk of developing musculoskeletal disorders related primarily to static loads. The OWAS method is particularly useful for assessing various activities at work. The main task of this method is to select all the items as the most important from the point of view of the load. Therefore, the problem of unusual and onerous position at work is the foreground [6]. This method takes into account the position of the body, exerting force, the time to maintain the load and type of body position, whether forced or unforced. The first task in assessing the performance of this method is called: photography of the day, timing of the working day or specifying individual actions performed by the employee (in this case the dentist) during the shift. The estimation is pointed to activities recognized in the timing. Finally, the essence of the analysis is introduction of changes in the work place in accordance with measurement results in the intention of reducing the risk of developing musculoskeletal disorders [6]. The diversity of body position takes into account the position of the torso, arms and legs.

The external load includes the weight below 10 kg, 10 to 20 kg and over 20 kg. The body position must be established by code for each separate action in the timing (e.g. 1 1 2 1). The first three digits in turn are assigned to the torso, arms and legs. The fourth digit of the code is characterized by an external force which directly affects the employee during their work activities. The essence also determines the type of employee's position (forced, unforced) and the total time of breaks [6]. The classification of body position (back) provides indicators from 1 to 4, where the position of the arms is determined by codes from 1 to 3, and the legs are numbered from 1 to 7. External load can be classified with codes from 1 to 3 [7]. Table 1 presents the location codes of body parts (by OWAS category) while Table 2 shows the ranking of an external force which acts during operation – grey marked codes of individual body parts refer to the dentist's work.

Table 1

Codes of the body parts by OWAS category – based on [8]

Torso (back)	Code	Arms	Code	Legs	Code
Upright position	1	**Both elbows below shoulder joint**	**1**	**Sitting position**	**1**
Leaning forward	2	One elbow above the shoulder joint	2	Upright standing position on two legs	2
Sprained positions	3	Both elbows above shoulder joint	3	Upright standing position on one straight leg	3
Leaning forward and sprained	**4**			Upright standing position on two legs bent	4
				Upright standing position on one leg bent	5
				Position on the one or two knees	6
				Walking	7

As a result of the analysis of the dentist's work and photographs of a working day, operating codes were received (concerning various parts of the body during work). It was selected The part of the photo of a working day which takes the most time in the entire process of dentist's work was selected- dental procedures in a sitting position with slightly twisted torso, inclined forward. During the work elbows of the dentist are located below the shoulder joint. Table 2 shows the number of codes of external force acting on the employee in accordance with gender and age. According to the characteristics, dental tools do not exceed 10 kg.

Total code of worker burden connects four labels: the position of the body (back), the position of the arms, legs and the position of the external. According to the scheme for the dentist, the following code has been established. Table 3 indicates categories of static load in the dentist's work. There are individual digits of the code determined in the OWAS matrix.

Table 2

Codes of external forces acting on the employee – by gender and age (based on [7])

Men	Code	Women and juvenile men	Code	Juvenile girls	Code
Up to10 kg	**1**	Up to 5 kg	1	Up to 2 kg	1
From 10 to 20 kg	2	From 5 to 10 kg	2	From 2 to 6 kg	2
More than 20 kg	3	More than 10 kg	3	More than 6 kg	3

Table 3

Assessment categories of static load in the OWAS method – based on [8]

Legs		**1**			2			3			4			5			6			7		
External forces		**1**	2	3	1	2	3	1	2	3	1	2	3	1	2	3	1	2	3	1	2	3
Torso	Arms																					
1	1	1	1	1	1	1	1	1	1	1	2	2	2	2	2	2	1	1	1	1	1	1
	2	1	1	1	1	1	1	1	1	1	2	2	2	2	2	2	1	1	1	1	1	1
	3	1	1	1	1	1	1	1	1	1	2	2	2	2	2	3	1	1	1	1	1	2
2	1	2	2	3	2	2	3	2	2	3	3	3	3	3	3	3	2	2	2	2	3	3
	2	2	2	3	2	2	3	2	2	3	3	4	4	3	4	4	3	3	4	2	3	4
	3	3	3	4	2	2	3	3	3	3	3	4	4	4	4	4	4	4	4	2	3	4
3	1	1	1	1	1	1	1	1	1	2	3	3	3	4	4	4	1	1	1	1	1	1
	2	2	2	3	1	1	1	1	1	2	4	4	4	4	4	4	3	3	3	1	1	1
	3	2	2	3	1	1	1	2	3	3	4	4	4	4	4	4	4	4	4	1	1	1
4	**1**	**2**	3	3	2	2	3	2	2	3	4	4	4	4	4	4	4	4	4	2	3	4
	2	3	3	4	2	3	4	3	3	4	4	4	4	4	4	4	4	4	4	2	3	4
	3	4	4	4	2	3	4	3	3	4	4	4	4	4	4	4	4	4	4	2	3	4

The final result of the evaluation is to determine the static load according to assessment categories. As it results from the matrix, in the dentist's work the load fell into category "2". It is important to assign for each category the total time in which the position is sustained. Table 4 shows the number of such information.

In the analysis of musculoskeletal system load by means of the OWAS method, the time, repeat rate and duration of a particular activity are very important factors. The final risk assessment takes into account the duration of certain OWAS categories. A three-stage evaluation system is carried out on the basis of the data contained in Table 5.

Table 4

Description of categories in the evaluation of static load – based on [6]

Category	Activities for improving the working conditions
1	Positions taken during operation are natural. The load is optimal or acceptable. There is no need to change the position.
2	Position or positions taken during operation may affect the motor system. The load is almost acceptable. There is no need to change the position, but you should take into account the need for such changes in the near future.
3	Position or positions taken during working hours have a negative effect on the motion. The load is large. Changes in the workplace must be carried out as quickly as possible.
4	The position or positions at work have a very negative effect on the motion. The load is very high. Changes in the workplace must be carried out immediately.

Table 5

Classification of static load, taking into account the time of maintaining one position – based on [6]

Load	Body position at work by OWAS category	Time to maintain one position (% of working shift)
Small	Position unforced of category 1	≤ 70
	Position forced of category 1 or unforced category 2	≤ 50
	Position forced of category 2	≤ 30
Average	Position unforced of category 1	> 70
	Position forced of category 1 or unforced category 2	50–70
	Position forced of category 2	30–50
	Position forced of category 3 or 4	≤ 30
High	Position forced of category 1 or unforced category 2	> 70
	Position forced of category 2	> 50
	Position forced of category 3 or 4	> 30

In Table 5 the forced and unforced positions have been highlighted. A forced position is a position which imposes a construction on the workplace or operations type. Unforced position is a position that, in contrast to the forced one, may be amended or modified in accordance with the preferences of the employee [6].

From the characteristics of the dentists' work and photographs of a working day it hasresulted that the time to maintain the characteristic position of body is more than 50% but less than 70%. Due to the fact that the dentist at work leans torso forward and twists it slightly, it can be assumed that the forced position, the "2" category maintains the position for 60% of the time. This gives finally a large load for particular workplace.

3. Conclusion

The OWAS method allows for the full assessment of musculoskeletal disorders risk, which affects the whole body and takes into account the load of upper limbs, lower limbs and back. This method has advantages and disadvantages. The advantages are the following: the opportunity to take different actions at work, both because of the position of the body and the time of exerted forces, as well as the possibility of using the method for each work station. The disadvantage of this method is that it is a qualitative method and fraught with subjectivity of the evaluated person [6]. The risk analysis of musculoskeletal disorders of the dentist by means of the OWAS method is an attempt to draw attention to one of the most common threats, which has been recently closely connected to both doctors and specialists in ergonomics. Musculoskeletal disorders are in fact the most common consequence of non-ergonomic working conditions, inadequate posture when performing work and excessively long time in which this position is dominant. Musculoskeletal disorders are among the most commonly reported symptoms associated with the performance of work.

References

[1] Roman-Liu D., *Narażenie na powstawanie dolegliwości mięśniowo-szkieletowych w krajach Unii Europejskiej*, Bezpieczeństwo Pracy, 11/2008, 2008, 16-20 [in Polish].

[2] *Informacje wprowadzające na temat dolegliwości mięśniowo-szkieletowych związanych z pracą*, Europejska Agencja Bezpieczeństwa i Zdrowia w Pracy, http://www.osha.europa.eu.pl/publications/factsheets/71 [date of acc. 16-08.2016; in Polish].

[3] Bugajska J., Jędryka-Góral A., Gąsik R., Żołnierczyk-Zreda D., *Nabyte zespoły dysfunkcji układu mięśniowo-szkieletowego u pracowników w świetle badań epidemiologicznych*, Medycyna Pracy, **62** (2), 2011, 153-161 [in Polish].

[4] Parent-Thirion A., Fernandez Macias E., Hurley J., Vermeylen G., *Fourth European Working Conditions Survey*, European Foundation for the Improvement of Living and Working Conditions, Dublin 2007.

[5] Lewczuk E., Affelska-Jercha A., Tomczyk J., *Zawodowe zagrożenia zdrowotne w gabinetach stomatologicznych*, Medycyna Pracy, **53** (2), 2002, 161-165 [in Polish].

[6] Jędruszczak J., Słomka-Romanowska I., *Ocena uciążliwości wysiłku fizycznego na stanowisku kelnera metodą chronometrażowo-tabelaryczną Lehmanna oraz OWAS*, Zeszyty Naukowe WSZOP, **1** (7), Katowice 2011 [in Polish].

[7] Górska E., *Metody oceny ryzyka zawodowego*, Wyd. WZ Politechniki Warszawskiej, Warszawa 2010 [in Polish].

[8] Roman-Liu D., *Ocena obciążenia statycznego z zastosowaniem metody OWAS*, Bezpieczeństwo Pracy, nr 7–8/2010, 2010, 28-31 [in Polish].

TECHNICAL TRANSACTIONS | CZASOPISMO TECHNICZNE
MECHANICS | MECHANIKA
3-M/2016

JACEK SELEJDAK*, MACIEJ MAJOR**

HYPERELASTIC ZAHORSKI MATERIAL – NUMERICAL ANALYSIS AND SIMULATION IN ADINA SOFTWARE

HIPERSPRĘŻYSTY MATERIAŁ ZAHORSKIEGO – NUMERYCZNA ANALIZA I SYMULACJA W PROGRAMIE ADINA

A b s t r a c t

The paper discusses and presents a hyperelastic incompressible material described by Zahorski potential. The numerical example comparing effective stresses in a cylinder made of Zahorski and Mooney-Rivlin materials was included. The analysis was made in the ADINA software. Conclusions summarize numerical calculations and demonstrate the differences that suggest the use of Zahorski material for rubber and rubber-like materials subjected to large deformations.

Keywords: hyperelastic Zahorski material, *incompressible material*, *cylinder*, *FEM*, *Adina*

S t r e s z c z e n i e

W artykule omówiono i przedstawiono hipersprężysty nieściśliwy materiał opisany potencjałem Zahorskiego. Zamieszczono przykład numeryczny, w którym porównano naprężenia efektywne w cylindrze wykonanym z materiałów Zahorskiego oraz Mooneya-Rivlina. Analizę wykonano w programie ADINA. We wnioskach podsumowano obliczenia numeryczne i podano różnice, które wskazują na możliwość zastosowania materiału Zahorskiego dla gum i materiałów gumopodobnych poddawanych dużym odkształceniom.

Słowa kluczowe: hipersprężysty materiał Zahorskiego, *materiał nieściśliwy*, *cylinder*, *MES*, *Adina*

DOI: 10.4467/2353737XCT.16.132.5743

* D.Sc. Ph.D. Eng. Jacek Selejdak, Department of Building Structures and Engineering, Faculty of Civil Engineering, Czestochowa University of Technology.

** D.Sc. Ph.D. Eng. Maciej Major, Department of Technical Mechanics, Faculty of Civil Engineering, Czestochowa University of Technology.

1. Introduction

Analysis of non-linear hyperelastic materials can be carried out by means of numerical programs based on the finite element method (FEM). There are many softwares that have used the popular elastic potentials (e.g. ALGOR, ANSYS, ABAQUS, MARC, NASTRAN, ADINA). All of these programs support a group of selected models of materials in their libraries, including the models of non-linear hyperelastic materials. Selection of one of the models of materials allows for performing numerical analysis of the behaviour of elements of construction [1]. However, the above software does not offer possibilities for analysis of the hyperelastic Zahorski material which allows for a more precise determination of the behaviour of rubber and rubber-like materials at significantly higher deformations compared to the commonly used materials such as Mooney-Rivlin or neo-Hookean materials [2]. The proposed solution will translate into a reduction of material consumption and will contribute to a more effective management of the production of rubber products. It can thus reduce the cost of materials, which will have a positive impact on the economics of enterprises which implement orders for many industries [3].

2. Hyperelastic materials - constitutive equations

It can be assumed that constitutive equations that describe the relationships between deformations and energy or between deformations and stresses for hyperelastic materials are obtained based on the equations of mechanical energy balance. In terms of the theory of elasticity and in the widely understood mechanical problems, including continuum mechanics, elastic bodies are considered as continuum of material with or without internal bonds. For the elastic bodies without bonds, the properties of such a medium are given if the function W can be defined. Function W is typically defined as a function of deformation energy and for any deformation d of medium, it determines the corresponding elastic energy $W=W(d)$ accumulated in the unit of volume with respect to the reference configuration $\mathbf{B}_R$.

For uniform isotropic elastic bodies, the constitutive equations can be written as:

$$W = W(I_1, I_2, I_3) \tag{1}$$

where:

I_1, I_2, I_3 – are deformation tensor invariants.

An elastic body with imposed internal bonds cannot be subjected to any deformations. The only acceptable deformations with regard to incompressible bodies are deformations which do not change its volume (isochoric). A condition for acceptable deformations $I_3 = 1$ must be met. This is the cause why I_3 does not occur as an argument of the deformation energy function which, for the incompressible body, represents a function of only two other invariants. This can be re-written in an analogous form to the Eq. 1:

$$W = W(I_1, I_2) \tag{2}$$

The above Eq. 2 define the constitutive relations for incompressible material.

3. Mooney-Rivlin and Zahorski incompressible materials

Non-linear theory of elasticity causes the necessity to renew the definition of constitutive relations so that it matches the problem analysed. With large deformations, each of the rubber-like materials behaves in a specific manner. Therefore, for each individual case of experimental procedure, it is necessary to determine a model of constitutive equation.

3.1. Mooney-Rivlin and neo-Hookean materials

The Mooney-Rivlin and neo-Hookean models are the only popular models used for the description of incompressible rubber and rubber-like materials. It is a peculiar case that results from the general form of elastic energy function defined by Rivlin and Saunders [4] and the empirical form of deformation function proposed by Mooney [5]. The model of Mooney-Rivlin material was defined with the following equation:

$$W = W(I_1, I_2) = \frac{\mu}{2}(f(I_1 - 3) + (1 - f)(I_2 - 3) \tag{3}$$

and represents the most general theoretical model of behaviour of elastic rubber materials.

The neo-Hookean material is a particular case of the Mooney-Rivlin material. The model of neo-Hookean material is defined by the following energy equation:

$$W = W(I_1) = \frac{\mu}{2} f(I_1 - 3) \tag{4}$$

According to the literature [6, 7], the neo-Hookean model defines elastic behaviour of homogeneous rubbers for small and moderate deformations.

3.2. Zahorski material

The model of Zahorski material is described by the equation with non-linear dependency on the invariants of the deformation tensor [8]:

$$W = W(I_1, I_2) = C_1(I_1 - 3) + C_2(I_2 - 3) + C_3(I_1^2 - 9) \tag{5}$$

where:

C_1, C_2, C_3 – are material constants. The values of constants for three types of rubber were given in a study [6].

The above constitutive equation allows for a more comprehensive analysis of the wave phenomena propagating in elastic incompressible materials. A description that suits the behaviour of rubber for the main elongation was obtained even for $\lambda = 3$, whereas for the neo-Hookean and Mooney-Rivlin materials, the acceptable results are observed for $\lambda = 1.4$ [9].

The Eq. 5 models the effects of the dynamic behaviour of materials and is used for the analysis of wave phenomena that concerns propagation of disturbance in the form of shock waves, travelling waves and soliton waves ([10–12] et al.). In the study [13] it was

demonstrated that the constitutive equation with non-linear dependency on the invariants of deformation tensor defines more precisely the behaviour of rubber at much higher deformations than in the case of Mooney-Rivlin or neo-Hookean materials.

4. Comparison of the Mooney-Rivlin and Zahorski materials

Differences in the stress-strain function between the Mooney-Rivlin and Zahorski materials for rubber "A" were shown in the paper [14]. Stress-strain diagrams presented by the authors have clear differences in the shape of curves. The diagrams for Zahorski material were generated from the ADINA software, after modifications introduced into material libraries [2].

Table 1 presents elastic constantsfor rubber "A". The values presented in the table are based on the study [6].

Table 1

Constants C_1, C_2, C_3

Constants	C_1	C_2	C_3
Rubber "A" [Pa]	$6.278 \cdot 10^4$	$8.829 \cdot 10^3$	$6.867 \cdot 10^3$

5. Numerical example

For comparative computation, a cylinder of 12 cm in height and 4 cm in diameter was adopted. Load in the object was obtained by means of a linear displacement of the upper surface of the cylinder applied in the z direction. The size of the displacement was determined by displacement $\lambda = 2$, according to the study [6], assuming 20 steps of time. On the opposite side surface of the cylinder (i.e., on the surface of the base), bonds were added to prevent displacement in x, y and z directions (in accordance with the adopted Cartesian coordinate system).

The aim of numerical calculations by means of FEM was to compare the distribution of stress in the Mooney-Rivlin and Zahorski material at the declared load and boundary conditions. This was obtained through a demonstration of differences in the distribution of effective stress in both materials. In Fig. 1a the distributions of stress in the Mooney--Rivlin material, whereas in Fig. 1b the distributions for Zahorski material are presented. Both materials were obtained for rubber "A". It can be observed that the deformation assumed (including the assumed boundary conditions) yields the expected results.

The comparative analysis of the states of effective stresses for the adopted model revealed differences in the distributions of effective stresses obtained in the Mooney-Rivlin and Zahorski materials (see also [14]).

Fig. 1 illustrates the distributions of stresses in rubber "A" for the cylinder. Substantial difference in the obtained levels of stresses and their distribution on the cylinder can be observed. The maximum value of stress in the Mooney-Rivlin material equals ~540 kPa (Fig. 1a), whereas this value for the Zahorski material amounts to ~780 kPa (Fig. 1b).

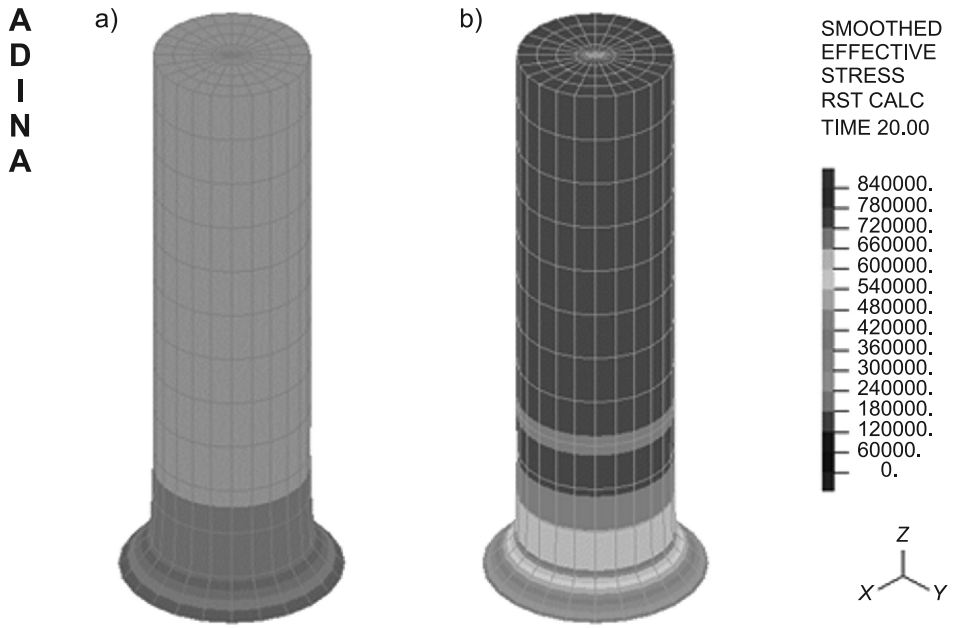

Fig. 1. Distribution of stress [Pa], step 20: a) Mooney-Rivlin material, b) Zahorski material

The comparison of obtained distributions provides information about the differences in the distribution of effective stress.

6. Summary

The study presented and discussed a hyperelastic incompressible material described by Zahorski potential. Distinct differences were obtained for the distribution of effective stresses for the geometrical object modeled with two different hyperelastic materials i.e. the Mooney-Rivlin material and Zahorski material for the 3D model studied. The results obtained from model-based studies show clear qualitative and quantitative differences in the distributions of stresses between the Mooney-Rivlin and Zahorski materials since small differences occur between elastic potentials for both materials.

The method of modification of the material library in order to allow for numerical tests in the ADINA software has considerable values that can be used in technological applications in many scientific fields. With the popularity of hyperelastic incompressible materials (used in different fields of science and technology), the Zahorski potential allows for supplementation of the results of calculations obtained previously for the Mooney-Rivlin material. The non-linear term $C_3(I_I^2 - 9)$ in the Zahorski potential supports a more precise analysis and allows for obtaining other qualitative elements in numerical analyses of rubber and rubber-like materials with respect to non-linear and incompressible hyperelastic materials [15, 16].

References

[1] Major M., Major I., *Przegląd wybranych materiałów hipersprężystych*, [in:] Bobko T., Rajczyk J., Rajczyk M. (eds.), *Tendencje rozwoju budownictwa miejskiego i przemysłowego*, Wyd. Politechniki Częstochowskiej, Czestochowa 2008, 258-263 [in Polish].

[2] Major M., *Modelowanie zjawisk falowych w hipersprężystym materiale Zahorskiego*, Wyd. Politechniki Częstochowskiej, Czestochowa 2013 [in Polish].

[3] Borkowski S., Ulewicz R., Selejdak J., *Materiałoznawstwo dla ekonomistów*, WNT, Warszawa 2005 [in Polish].

[4] Rivlin R.S., Saunders D.W., *Large elastic deformations of isotropic materials*, VII Experiments of the deformation of rubber, Philosophical Transactions of the Royal Society of London, A 243, 1951, 251-288.

[5] Mooney M., *A Theory of Large Elastic Deformation*, Journal of Applied Physics, **11** (9), 1940, 582-592.

[6] Zahorski S., *Doświadczalne badania niektórych własności mechanicznych gumy*, Rozprawy Inżynierskie, **10** (1), 1962, 193-207 [in Polish].

[7] Yeoh O., *Some forms of the strain energy function for rubber*, Rubber Chemistry and Technology, **66** (5), 1993, 754-771.

[8] Zahorski S., *A form of elastic potential for rubber-like materials*, Archives of Mechanics, **5**, 1959, 613-617.

[9] Kosiński S., *Fale sprężyste w gumopodobnych kompozytach warstwowych*, Wydawnictwo Politechniki Łódzkiej, Łódź 2007 [in Polish].

[10] Major M., Major I., *Acceleration wave in a thin segmental hyperelastic rod*, Archives of Civil and Mechanical Engineering, **10** (1), 2010, 59-67.

[11] Major I., *The acceleration wave in a thin two-material and three-segmental rod with slowly changing cross-section made of Murnaghan material*, Communications – Scientific Letters of the University of Žilina, **16** (4), 2014, 48-52.

[12] Major M., *Velocity of Acceleration Wave Propagating in Hyperelastic Zahorski and Mooney – Rivlin Materials*, Journal of Theoretical and Applied Mechanics, **43** (4), 2005, 777-787.

[13] Boyce M.C., Arruda E.M., *Constitutive models of rubber elasticity a review*, Rubber Chemistry and Technology, **73**, 2000, 504-523.

[14] Major I., Major M., *Modeling of Wave Propagation in the ADINA Software for Simple Elastic Structures*, Advanced Materials Research, **1020**, 2014, 171-176.

[15] Major I., Major M., *Traveling Waves in a Thin Layer Composed of Nonlinear HyperelasticZahorski's Material*, Journal of Theoretical and Applied Mechanics, **47** (1), 2009, 109-126.

[16] Osocha P., Ulewicz R., Szataniak P., Pietraszek M., Kołomycki M., Radek N., Pasieczyński Ł., *The empirical assessment of the convergence rate for the bootstrap estimation in design of experiment approach*, Solid State Phenomena, **235**, 2015, 1623.

CONTENTS

Antoszewski B., Krzywicka M., Tofil Sz.: Laser surface texturing of titanium alloys for biomedical applications ... 3
Ulewicz R.: Influence of selected technological factors on fatigue strength ... 9
Szczotok A.: Guidance and advice to image analysis applied in materials science ... 15
Gądek-Moszczak A., Korzekwa J.: Methods of correction of typical defects in the digital images on the example of SEM images of anodic oxide layers ... 23
Kundera Cz., Kozior T.: Influence of printing parameters on the mechanical properties of polyamide in SLS technology ... 31
Lipiński T.: Corrosion analysis of the X2CrNiMoN25-7-4 super duplex stainless steel ... 39
Stasiak-Betlejewska R.: Innovative wooden energy efficient houses constructions ... 47
Kiełbus A., Gawłowski G.: Quality tools of the innovative project in the planning phase analysed on a chosen example ... 53
Radek N., Szczotok A.: Heterogenous surfaces formed by high energy techniques ... 61
Knop K., Mielczarek K.: Significance of visual control types in automotive industry ... 67
Karpisz D.: Design of manufacturing databases ... 73
Radziszewska-Wolińska J.M.: Fire properties of anticorrosion coatings for rolling stock ... 79
Klimecka-Tatar D.: Flow of technical information in the production process of prosthetic restorations ... 87
Osocha P.: The effectiveness of e-learning in engineering education ... 93
Gwoździk M.: Wear of working part of surgical drills ... 99
Wrońska A., Dudek A.: Formation of microstructure and properties of sintered steel through remelting of surface layer ... 105
Jagusiak-Kocik J.: Use of overall equipment effectiveness indicator for analysis of work time of test bench ... 111
Radomska K., Pawłowska G., Klimecka-Tatar D.: The effect of corrosion process on the surface topography of Nd–Fe–B type magnets bonded with biopolimer ... 119
Niciejewska M., Klimecka-Tatar D.: Evaluation of static load in dentists' work by means of OWAS method ... 125
Selejdak J., Major M.: Hyperelastic Zahorski material – numerical analysis and simulation in ADINA software ... 131

TREŚĆ

Antoszewski B., Krzywicka M., Tofil Sz.: Laserowe teksturowanie elementów ze stopów tytanu do zastosowań biomedycznych ... 3
Ulewicz R.: Wpływ wybranych czynników technologicznych na własności zmęczeniowe ... 9
Szczotok A.: Praktyczne wskazówki do analizy obrazu w badaniach materiałów inżynierskich ... 15
Gądek-Moszczak A., Korzekwa J.: Metody korekty typowych wad obrazów cyfrowych na przykładzie orazów SEM anodowych warstw tlenkowych ... 23
Kundera Cz., Kozior T.: Wpływ parametrów technologicznych na właściwości mechaniczne poliamidu w technologii SLS ... 31
Lipiński T.: Analiza korozji stali odpornej na korozję super duplex X2CrNiMoN25-7-4 ... 39
Stasiak-Betlejewska R.: Innowacyjne konstrukcje drewnianych domów energooszczędnych ... 47

Kiełbus A., Gawłowski G.: Narzędzia jakości w fazie planowania innowacyjnego projektu na wybranym przykładzie ... 53
Radek N., Szczotok A.: Powierzchnie niejednorodne kształtowane technologiami wysokoenergetycznymi ... 61
Knop K., Mielczarek K.: Znaczenie rodzajów kontroli wizualnej w branży motoryzacyjnej ... 67
Karpisz D.: Projektowanie przemysłowych baz danych ... 73
Radziszewska-Wolińska J.M.: Właściwości ogniowe antykorozyjnych zabezpieczeń lakierowych taboru szynowego ... 79
Klimecka-Tatar D.: Przepływ informacji technicznych w procesie wytwarzania uzupełnień protetycznych ... 87
Osocha P.: Efektywność e-learningu w edukacji inżynierskiej ... 93
Gwoździk M.: Zużycie części roboczej wierteł chirurgicznych ... 99
Wrońska A., Dudek A.: Kształtowanie mikrostruktury i właściwości stali spiekanych poprzez przetopieniową obróbkę warstwy wierzchniej ... 105
Jagusiak-Kocik J.: Wykorzystanie współczynnika ogólnej efektywności urządzenia do analizy czasu pracy stacji wzorcowniczej ... 111
Radomska K., Pawłowska G., Klimecka-Tatar D.: Wpływ procesu korozyjnego na topografię powierzchni magnesów typu Nd–Fe–B wiązanych biopolimerem ... 119
Niciejewska M., Klimecka-Tatar D.: Ocena obciążenia statycznego w pracy lekarza stomatologa za pomocą metody OWAS ... 125
Selejdak J., Major M.: Hipersprężysty materiał Zahorskiego – numeryczna analiza i symulacja w programie ADINA ... 131